THE UNIVERSITY OF QUEENSLAND

AUSTRALIA

A synoptic climatology of inflow-generating precipitation for the Snowy Mountains, south-eastern Australia

Alison Theobald

Bachelor of Science (Honours)

A thesis submitted for the degree of Doctor of Philosophy at

The University of Queensland in 2016

School of Geography, Planning and Environmental Management

Abstract

Precipitation falling in mountainous areas provides vital water resources for society, agriculture, industry and the environment. The variability, and ocean-atmosphere forcing of precipitation-bearing weather systems is therefore fundamental for regional water availability and management. An increasing body of literature describes synoptic-scale precipitation types for many locations. In the Snowy Mountains region of southeast Australia (SEA), inflows generated from precipitation provide essential resources for hydroelectric power generation, irrigated agriculture and environmental flows throughout the economically-important Murray River system. Interest in the variability of precipitation regimes of the Snowy Mountains has increased due to the significant decline in cool season (April-October) precipitation that occurred during the recent Millennium Drought (1997-2009). To date, cool season synoptic circulation over SEA has been well described, however there is little information regarding year-round synoptic systems. Furthermore, there remains a significant knowledge gap of multi-decadal variability, with most SEA studies concentrating on the past few decades. Given the current focus on climate variability in a warming world, and climate model predictions of changing precipitation regimes, increased understanding of long-term precipitation variability and the influence of large-scale climate drivers ("teleconnections") is critical. This thesis examines the multi-decadal variability of synoptic-scale precipitation-bearing weather systems by developing a climatology of inflow-generating precipitation for the Snowy Mountains. The interaction of teleconnections that underpin precipitation variability, which has yet to be fully described, was assessed by quantifying the relative influence of each driver on synoptic type frequency.

Development of a multi-decadal (1958-2012) synoptic climatology of daily precipitation, triggering a quantifiable increase in stream flow in the headwater catchments of the Snowy Mountains region, formed the first part of this thesis. Using multi-level reanalysis data combined with the novel application of an automated synoptic classification technique, a three-dimensional representation of synoptic circulation was achieved by effectively combining meteorological variables through the depth of the troposphere. Key circulation features and moisture pathways, crucial to the development and steering of synoptic systems that deliver precipitation to the Snowy Mountains were identified. This research demonstrates that synoptic types with the highest precipitation totals are commonly associated with moisture pathways originating from tropical oceans northeast and northwest of Australia. Strong intra-seasonal variability in synoptic types was evident, with frontal and closed low types dominating in winter, and inland heat troughs prevailing in summer. Interaction between tropical and extra-tropical systems, and the advection of tropical moisture however, was evident in all seasons. These findings illustrate that precipitation distribution across the Snowy Mountains catchments varies according to synoptic type and moisture pathway.

Multi-decadal (1958-2012) temporal trends in synoptic type frequency, precipitation and intensity highlighted that annual frequency of precipitation days generating inflows declined by -1.4 days per decade on average, whilst the precipitation they generated increased by +5.7 mm per precipitation day per decade. These results align with climate change projections of fewer, but more intense precipitation events. Whilst the region has historically observed a cool season dominated precipitation regime, changes in annual precipitation distribution were apparent, with an increase in warm season (November-March) precipitation. Results showed declines in precipitation during the autumn and spring transition months, which are particularly important for crop sowing and agricultural production downstream of the Snowy Mountains, and snowmelt and water storage replenishment respectively.

Determination of the proportions of rain and snow for each synoptic type was made using a maximum daily temperature threshold. Results show that the majority of snowfall resulting from precipitation ≥10 mm per day was associated with relatively few synoptic types, all of which originate over the Southern Ocean and bring westerly or north-westerly winds across the Snowy Mountains. A decline in the main snow producing synoptic type, embedded cold fronts, is consistent with declining maximum snow depths, particularly apparent since the 1990s. This is also consistent with a trend towards increasingly positive values of the Southern Annular Mode in recent decades – a pattern which results in a more poleward position of the mid-latitude westerly wind belt and fewer cold fronts crossing southern Australia.

Novel applications of cross-wavelet and regression tree methods over an extended, multi-decadal period (1900-2012) demonstrated the complexity and non-stationarity of large-scale atmospheric forcing of inter-annual and inter-decadal synoptic type frequency over more than 100 years. Importantly, results demonstrate that teleconnections do not act in isolation. In an extension to previous precipitation climatology studies, the relative influence of teleconnections on synoptic type frequency was quantified. The tropical Pacific Ocean was shown to be a key interdecadal driver of synoptic types associated not only with the dominant tropical moisture pathways to the Snowy Mountains, but also with extra-tropical sources. Results indicate that warming tropical sea surface temperatures (SSTs) drive synoptic type frequency and the dominance of synoptic types with tropical moisture sources, most notably since the 1950s.

This thesis makes a substantial new contribution to the understanding of precipitation variability in the economically important region of SEA. This study has successfully demonstrated that multiple parameters can be combined to classify synoptic types based on circulation features throughout the depth of the troposphere, and presents the first study to link three-dimensional atmospheric circulation to regional surface weather conditions in Australia. Combined with quantification of teleconnection influence on synoptic type frequency, this approach has wide ranging applications to

research that seeks more in-depth understanding of the links between change in local weather and climate to large scale synoptic variability.

Declaration by author

This thesis is composed of my original work, and contains no material previously published or written by another person except where due reference has been made in the text. I have clearly stated the contribution by others to jointly-authored works that I have included in my thesis.

I have clearly stated the contribution of others to my thesis as a whole, including statistical assistance, survey design, data analysis, significant technical procedures, professional editorial advice, and any other original research work used or reported in my thesis. The content of my thesis is the result of work I have carried out since the commencement of my research higher degree candidature and does not include a substantial part of work that has been submitted to qualify for the award of any other degree or diploma in any university or other tertiary institution. I have clearly stated which parts of my thesis, if any, have been submitted to qualify for another award.

I acknowledge that an electronic copy of my thesis must be lodged with the University Library and, subject to the policy and procedures of The University of Queensland, the thesis be made available for research and study in accordance with the Copyright Act 1968 unless a period of embargo has been approved by the Dean of the Graduate School.

I acknowledge that copyright of all material contained in my thesis resides with the copyright holder(s) of that material. Where appropriate I have obtained copyright permission from the copyright holder to reproduce material in this thesis.

Publications during candidature

Peer-reviewed papers

Theobald, A., H. McGowan, J. Speirs, and N. Callow, 2015: A synoptic classification of inflow-generating precipitation in the Snowy Mountains, Australia. *Journal of Applied Meteorology and Climatology*, **54**, 1713-1732.

Theobald, A., H. McGowan, and J. Speirs, 2015: Trends in synoptic circulation and precipitation in the Snowy Mountains region, Australia, in the period 1958-2012. *Atmospheric Research*, **169 (2016)**, 434-448.

Theobald, A., and H. McGowan, 2016: Evidence of increased tropical moisture in south-east Australian alpine precipitation during ENSO. *Geophysical Research Letters*, **43**, doi: 10.1002/2016GRL070767.

Conference presentations

Theobald, A., H. McGowan, and J. Speirs, 2014: *A precipitation climatology of the Snowy Mountains.* European Geophysical Union (EGU) General Assembly 2014, 27th April-2nd May 2014, Vienna, Austria.

Theobald, A., H. McGowan, and J. Speirs, 2015: *Trends and variability in precipitation-bearing synoptic circulation, Snowy Mountains, Australia.* Australian Meteorological and Oceanographic Society (AMOS) 21st Annual Conference, 15-17th July 2015, Brisbane, Australia.

Theobald, A., H. McGowan, and J. Speirs, 2015: *Recognising changing seasonality in the precipitation regime of the Snowy Mountains.* GREENHOUSE 2015, 27-30th October 2015, Hobart, Australia.

Theobald, A., H. McGowan, and J. Speirs, 2016: *Influence of large-scale climate drivers on synoptic-scale precipitation variability in the Snowy Mountains, Australia.* American Meteorological Society (AMS) 96th Annual Meeting, 10-14th January 2016, New Orleans, United States.

Publications included in this thesis

Publication 1: Included as Chapter 4.

Theobald, A., H. McGowan, J. Speirs, and N. Callow, 2015: A synoptic classification of inflow-generating precipitation in the Snowy Mountains, Australia. *Journal of Applied Meteorology and Climatology*, **54**, 1713-1732.

Contributor	Statement of contribution
A. Theobald (Candidate)	Research design, implementation (80%) Data analysis (100%) Wrote the paper (100%)
H. McGowan	Research design, implementation (10%) Edited the paper (40%)
J. Speirs	Research design, implementation (10%) Edited the paper (40%)
N. Callow	Advice on determination of precipitation threshold Edited the paper (20%)

Publication 2: Included as Chapter 5.

Theobald, A., H. McGowan, and J. Speirs, 2015: Trends in synoptic circulation and precipitation in the Snowy Mountains region, Australia, in the period 1958-2012. *Atmospheric Research*, **169 (2016)**, 434-448.

Contributor	Statement of contribution
A. Theobald (Candidate)	Research design, implementation (80%) Data analysis (100%) Wrote the paper (100%)
H. McGowan	Research design, implementation (10%) Edited the paper (50%)
J. Speirs	Research design, implementation (10%) Edited the paper (50%)

Contributions by others to the thesis

The supervision team Hamish McGowan and Johanna Speirs made standard contributions to the thesis. This included experimental design, revision and editing of this thesis. Nik Callow provided hydrological advice and made contributions to a manuscript as outlined above. Michael Hewson ran the WRF model as described in Chapter 4 and produced the animated sequences that are provided in the supplementary materials.

Statement of parts of the thesis submitted to qualify for the award of another degree

None.

Acknowledgements

I would firstly like to thank my principal supervisor, Professor Hamish McGowan, for the guidance, enthusiasm, and encouragement during my candidature. I am very grateful to you for the opportunity to have carried out this research. To my co-supervisor Dr Johanna Speirs, whose editing skills and keen eye for grammatical typos are second to none, your support has been very much appreciated.

This research was, in part, funded by Snowy Hydro, and I would like to thank them for their financial support. Thanks must also go to the staff of the Scientific Services and Hydrography departments for providing data and for sharing their knowledge along the way. To Nik Callow, part of our research team at UWA, thank you for your hydrological insights and showing me round the mountains.

I would like to acknowledge the contribution of Michael Hewson for the WRF modelling included in this thesis. Your animations of the synoptic type case studies have given a whole new dimension to visualising moisture transport, and never fail to impress! Also to Joshua Soderholm for his assistance with software issues throughout my PhD, and Andrew Lowry for introducing me to wavelet analysis and invaluable help interpreting results.

Many thanks must go to the professional staff at GPEM for their tireless work and constant good humour, and the department for the opportunity to travel widely over the course of my candidature.

Finally, I wish to thank my friends and family for your support and positivity during this academic journey. A special thanks must go to Dr Harry Leach at the University of Liverpool, who saw potential in me and encouraged me at every step of my undergraduate degree to go on to bigger and better things. Most of all to my partner and best friend, Rob. I could not have done this without your constant support, encouragement and belief in me. Thank you for your kind words and always making me laugh through what has been a very challenging but rewarding time.

Keywords

synoptic climatology, precipitation, atmospheric circulation, teleconnections, alpine, water resources.

Australian and New Zealand Standard Research Classifications (ANZSRC)

040105 Climatology (excl. Climate Change Processes) (40%)

040102 Atmospheric Dynamics (40%)

040104 Climate Change Processes (20%)

Fields of Research (FoR) Classification

0401 Atmospheric sciences (100%)

Table of contents

List of Figures and Tables

Figures

Chapter 1. Introduction

Chapter 3. Physical Setting

Chapter 4. A synoptic classification of inflow-generating precipitation in the Snowy Mountains, Australia

Chapter 5. Trends in synoptic circulation and precipitation 1958-2012

Chapter 6. Determination of the proportion of rain versus snow for synoptic types

Chapter 7. Teleconnection forcing of precipitation-bearing synoptic types

Chapter 5. Trends in synoptic circulation and precipitation 1958-2012

Chapter 6. Determination of the proportion of rain versus snow for synoptic types

Chapter 7. Teleconnection forcing of precipitation-bearing synoptic types

Appendix.

List of abbreviations used in the thesis

SEA	south-east Australia
SST	sea surface temperature
IPCC	Intergovernmental panel on climate change
MSLP	mean sea level pressure
PCA	principal component analysis
SOM	self-organising map
ENSO	El Nino Southern Oscillation
SOI	Southern Oscillation Index
PDO	Pacific Decadal Oscillation
IOD	Indian Ocean Dipole
SAM	Southern Annular Mode
IPO	Interdecadal Pacific Oscillation
NWCB	north-west cloud band
NWWA	north-west Western Australia
EAC	East Australia Current
ECMWF	European Centre for Medium Range Weather Forecasts
STR	subtropical ridge
ECL	east coast low
DFIR	double fence intercomparison reference
WMO	World Meteorological Organisation
GDR	Great Dividing Range
MDB	Murray Darling Basin
MDBA	Murray Darling Basin Authority
CSIRO	Commonwealth Scientific and Industrial Research Organisation
SHL	Snowy Hydro Limited
SILO	Scientific Information for Land Owners
BoM	Bureau of Meteorology
DJF	December-January-February
MAM	March-April-May
JJA	June-July-August
SON	September-October-November
ECMWF	European Centre for Medium Range Weather Forecasting
WRF	Weather Research and Forecasting model
NCEP	National Centres for Environmental Protection

POD	probability of detection
MAE	mean absolute error
NOAA	National Oceanographic and Atmospheric Administration
PW	precipitable water
CVA	cyclonic vorticity advection
WAA	warm air advection
SPJ	subpolar jet stream
STJ	subtropical jet stream
CAA	cold air advection
PMF	penalised maximal *F* test
ONI	Oceanic Niño Index
DMI	Dipole Mode Index
PPD	patched point data
JISAO	Joint Institute for the Study of the Atmosphere and Ocean
TSI	Tasman Sea Index
NE	north-east synoptic group
NW	north-west synoptic group
SO	Southern Ocean synoptic group
BRT	boosted regression trees
lr	learning rate
tc	tree complexity
cv	cross validation deviance
se	standard error
COI	cone of influence
ITF	Indonesian Through Flow
JJAS	June-July-August-September
GRACE	Gravity Recovery And Climate Experiment

Chapter 1. Introduction

This thesis presents a climatology of synoptic-scale weather patterns that deliver precipitation to the Snowy Mountains, southeast Australia, their multi-decadal variability and the influence of large-scale ocean-atmosphere drivers of variability on their frequency of occurrence.

1.1 Importance and vulnerability of precipitation in temperate mountainous regions

Precipitation falling in alpine regions provides important water resources for society, industry, agriculture and the environment (Christensen et al 2007). Alpine areas are particularly vulnerable to climate change and its impact on their hydroclimate (Demiroglu et al 2016; Beniston 2003). The complex nature of their alpine terrain results in rapid changes in climate over short distances meaning that mountainous regions may not follow the larger-scale trends in climate change (Viviroli et al 2011; Beniston 2003). Naturally variable precipitation in marginal alpine areas such as the Australian Alps can result in increased pressure on water resources that rely on snow melt. The snowpack in these settings is often close to melting and as such is very susceptible to minor changes in temperature. Consistent with ambient lapse rates, projections show that the snowline rises by 150m for every 1°C of warming (Christensen et al 2007; Beniston 2003), hence climate change results in additional stresses for marginal alpine environments. In the Australian Alps low mountain heights limit the migration of the snowline, thus altitudinal and warming effects could have dramatic consequences for seasonal snowmelt and runoff (Viviroli et al 2011; Beniston 2003).

Evidence exists that changes to precipitation patterns are occurring worldwide (e.g. IPCC 2014; Gillies et al 2012), with fewer, more intense precipitation events a common projection of climate change modelling since the early 1990s (IPCC 1995). Changes to the distribution and timing (i.e. seasonality) of precipitation may also eventuate as global warming alters patterns of atmospheric circulation (Whan et al 2014; Timbal and Fawcett 2013; Post et al 2012). Furthermore, variations in the spatial distribution of precipitation associated with synoptic types can have important implications for catchment management, as small variations in atmospheric circulation and precipitation distribution can result in large changes in runoff and water availability (Newton et al 2014a, b). In the headwater catchments of the Snowy Mountains, where precipitation provides a nationally important economic resource, such changes have implications for water storage replenishment, irrigated agriculture, and environmental flows. Accordingly, it is crucial to gain understanding of precipitation variability and its association with changing weather patterns, in order to make better-informed water resource decisions (Viviroli et al 2011).

1.2 The state of knowledge and key knowledge gaps in precipitation climatology

Synoptic-scale weather systems associated with a particular surface variable (e.g. precipitation, heat waves, ozone concentration) can be defined using synoptic climatology, a method for relating surface climate to the overlying atmosphere which results in a classification of weather types (Yarnal 1993).

In many previous studies, precipitation climatologies have been represented by a limited range of meteorological variables, often based on mean sea level pressure (MSLP). Accordingly, the association of surface atmospheric circulation with precipitation is well understood (e.g. Hope 2006; Kidson 2000). Other studies have classified synoptic types based on mid or upper level variables, in particular geopotential height (e.g. Newton et al 2014a, b; Bettolli et al 2010). Due to complexities involved in combining data from multiple levels, it is less well understood how circulation patterns throughout the depth of the troposphere interact to influence precipitation (Kidson 2000). This presents a significant challenge in understanding the full three-dimensional aspect of synoptic circulation that plays a vital role in the weather experienced at the surface, and which is masked by surface-only or single-variable studies (Stahl et al 2006; Pook et al 2006). Whilst several studies have carried out three-dimensional analyses (e.g. Milrad et al 2014; Moore et al 2013), these were conducted using manual classification techniques. Accordingly, to the author's knowledge there remains no objective three-dimensional synoptic-typing technique, and a lack of three-dimensional analysis for the Australian region. In addition, climatologies constructed using manual typing methods, with the exception of Pook et al (2014), have historically been limited to short time frames due to their time-consuming nature, and the requirement of satellite data to pinpoint surface features such as fronts.

An increasing body of literature has focussed on automated typing methods (e.g. Newton et al 2014; Bettolli et al 2010; Verdon-Kidd and Kiem 2009; Stahl et al 2006; Hope 2006), which allows longer periods to be analysed due to reduced computation times. However, these have also typically considered just one atmospheric variable (often MSLP). Therefore, there is a significant knowledge gap in considering multiple atmospheric variables at multiple levels through the troposphere when classifying synoptic systems. The majority of precipitation studies in SEA have been largely limited to the cool season (April-October). Climatologies that consider all seasons however, can shed light on changes in the seasonality of precipitation by assessing trends in synoptic types that result in precipitation at particular times of year (Newton et al 2014a, b).

There is widespread agreement that global warming has led to an increase in heavier precipitation events, due to the ability of a warmer atmosphere to hold more moisture, with associated greater

risks of flooding (Kirkman et al 2013; Chiew et al 2011; Meehl et al 2005). This trend is projected to continue for mid-latitude and tropical regions, with heavier precipitation becoming more intense and more frequent (IPCC 2014). Whilst regional precipitation projections remain uncertain (Whetton et al 2012), Post et al (2012) show that catchments within the Snowy Mountains will likely experience drier conditions on average, but with an exacerbation of the wettest and driest events, over the coming decades. Consequences of such trends e.g. drought, flooding, surface runoff and erosion are already apparent in areas of the Mediterranean (Vallebona et al 2014; Hoy et al 2014; Alpert et al 2002). Furthermore, snow depths in the Australian alpine region are reported to have already declined by 40% (Christensen et al 2007; Nicholls 2005) since the 1960s, a trend which is projected to continue (Hendrikx et al 2013; Hennessy et al 2003, 2008). Changes in the timing of precipitation has consequences for snow accumulation and snowmelt (Gillies et al 2012), alpine tourism, water storage replenishment (Verdon-Kidd et al 2013), and agriculture (Lobell et al 2011; Pook et al 2006, 2009). Elucidation of the timing of any changes in the delivery of precipitation is therefore crucial.

Since the multi-year drought ('the Millennium drought') that persisted for much of the 1990s and 2000s across SEA, there has been a strong focus on cool-season precipitation, which experienced a significant decline during that period. Prior to the drought however, several studies identified increases in annual rainfall over much of eastern Australia, linked to positive rainfall trends during the warm season (November-March; Suppiah and Hennessey 1998; Nicholls and Lavery 1992). Projected seasonal changes in precipitation as a result of climate change (Whan et al 2014; Timbal and Fawcett 2013; Post et al 2012), warrant an investigation of precipitation in all seasons, over timescales long enough to reveal climatic trends. Furthermore, analysis of precipitation-bearing synoptic types in all seasons can shed light on trends in particular weather types and therefore trends in the larger-scale atmospheric circulation (Newton et al 2014a, b). The lack of understanding of causes of interannual and interdecadal variability in seasonal precipitation in SEA remains a key knowledge gap.

Analysis of synoptic circulation through synoptic typing can shed light on sources of precipitation and moisture pathways through the atmosphere, increasing understanding of the physical mechanisms that underpin weather and climate variability. The effects of individual climate drivers ("teleconnections") on precipitation variability are well established (e.g. Pepler et al 2015; Newton et al 2014a, b; Lorenzo et al 2008; Stahl et al 2006). Importantly however, teleconnections do not act in isolation, and to date, the combined influence of teleconnections on precipitation variability is not well understood (Risbey et al 2009b). This knowledge is important for a number of reasons: to elucidate teleconnection interactions that underpin synoptic type variability; facilitate better

understanding of the ocean-atmosphere processes that lead to precipitation variability; improving precipitation forecasts, and informing climate model projections. Therefore, a key knowledge gap exists regarding the quantification of the relative influence of teleconnections on the variability of precipitation-bearing synoptic types. Furthermore, studies have demonstrated that the modulation of precipitation by teleconnections exhibits non-stationarity, with periods of enhanced and diminished modulation (e.g. Speer et al 2011). It is therefore necessary to investigate the relationships between synoptic type frequency and teleconnections over a period long enough to capture several cycles of each teleconnection.

Emergent trends in large-scale climate drivers have the potential to fundamentally alter atmospheric circulation patterns (Cai et al 2005, 2013, 2014; Marshall 2003), including the frequency of precipitation-bearing synoptic types (Newton et al 2014; Risbey et al 2009; Stahl et al 2006), by enhancing or impeding precipitation mechanisms in and along moisture source regions and pathways. In addition, increasing tropical sea surface temperatures (SSTs) enhance evaporation to the overlying atmosphere (Cravatte et al 2009; Godfrey 1996; Graham 1995), thereby affecting subsequent advection of humid air away from tropical source regions to the mid-latitudes (Gillies et al 2012; Meehl et al 2005).

Therefore, understanding the origins of precipitation-bearing synoptic types, their moisture pathways throughout the troposphere, and the influence of teleconnections on atmospheric circulation in source regions is important for more accurately assessing regional responses to precipitation variability, including droughts, floods, and water availability (Kiem and Verdon-Kidd 2011). Accordingly, a more detailed understanding of precipitation variability, including changes associated with a warming climate, provides critical information for weather and climate forecasting as well as water management.

In summary, this thesis will address the following fundamental gaps in knowledge which inform the research objectives in Section 1.3:

1) The substantial gap in knowledge and understanding of the climatological characteristics of the three-dimensional properties of precipitation-bearing synoptic types, and the resulting spatial and temporal variability of precipitation from intra-annual to inter-decadal time scales across SEA.

2) The deficiency in understanding of synoptic and teleconnection forcing of non-cool season precipitation across SEA.

3) The limited understanding of the role of teleconnections in the variability of precipitation bearing synoptic weather systems that affect SEA.

1.3 Research Aim and Objectives

The primary research aim of this thesis is to develop a synoptic climatology of weather systems delivering inflow-generating precipitation to the Snowy Mountains headwater catchments in the Australian Alps. The specific objectives of this thesis are to:

1. *Develop a synoptic classification of inflow-generating precipitation events for the Snowy Mountains 1900-2012:*
    - Use ECMWF reanalysis data as input for a cluster analysis to produce an objective synoptic-types classification for precipitation events.
    - Validate the synoptic classification against manual synoptic analyses and satellite imagery.
    - Use the Weather Research Forecasting (WRF) model to produce high spatial resolution, mean sea level pressure charts for case studies of each synoptic type.
    - Develop a climatological database of the dominant synoptic systems.

2. *Understand the synoptic influences on precipitation that produces inflow in the Snowy Mountains.*
    - Use gridded precipitation data to understand spatial variability of precipitation associated with each synoptic type.
    - Determine the contributions of precipitation (rain and snow) from each synoptic type to generating an inflow response in the streams and rivers of the Snowy Mountains hydroelectric scheme.

3. *Investigate the variability and trends in synoptic types that influence the Snowy Mountains.*
    - Describe and quantify the temporal variability and trends of synoptic types between 1958-2012.
    - Identify any long-term trends in synoptic types, their precipitation, frequency and intensity (1958-2012).
    - Explore statistical techniques to investigate the combined effects of multiple climate drivers on synoptic type frequency.
    - Quantify the influence of climate drivers on the frequency of synoptic types, and the resulting effects on precipitation (1900-2012).
    - Determine the lead and lagged effects of the climate drivers on the frequency of precipitation-bearing synoptic weather types (1900-2012).

This study will ultimately inform regional water management strategies, inflow forecasting, and contribute to climate change adaptation and mitigation measures through improved understanding of precipitation trends and variability.

1.4 Thesis structure

This thesis comprises a literature review (Chapter 2) and description of the physical setting for the study (Chapter 3), followed by a series of published (Chapters 4 and 5), unpublished (Chapter 6) and in review manuscripts (Chapter 7). A synthesis and summary of the key research outcomes, and directions for future research are presented in Chapter 8.

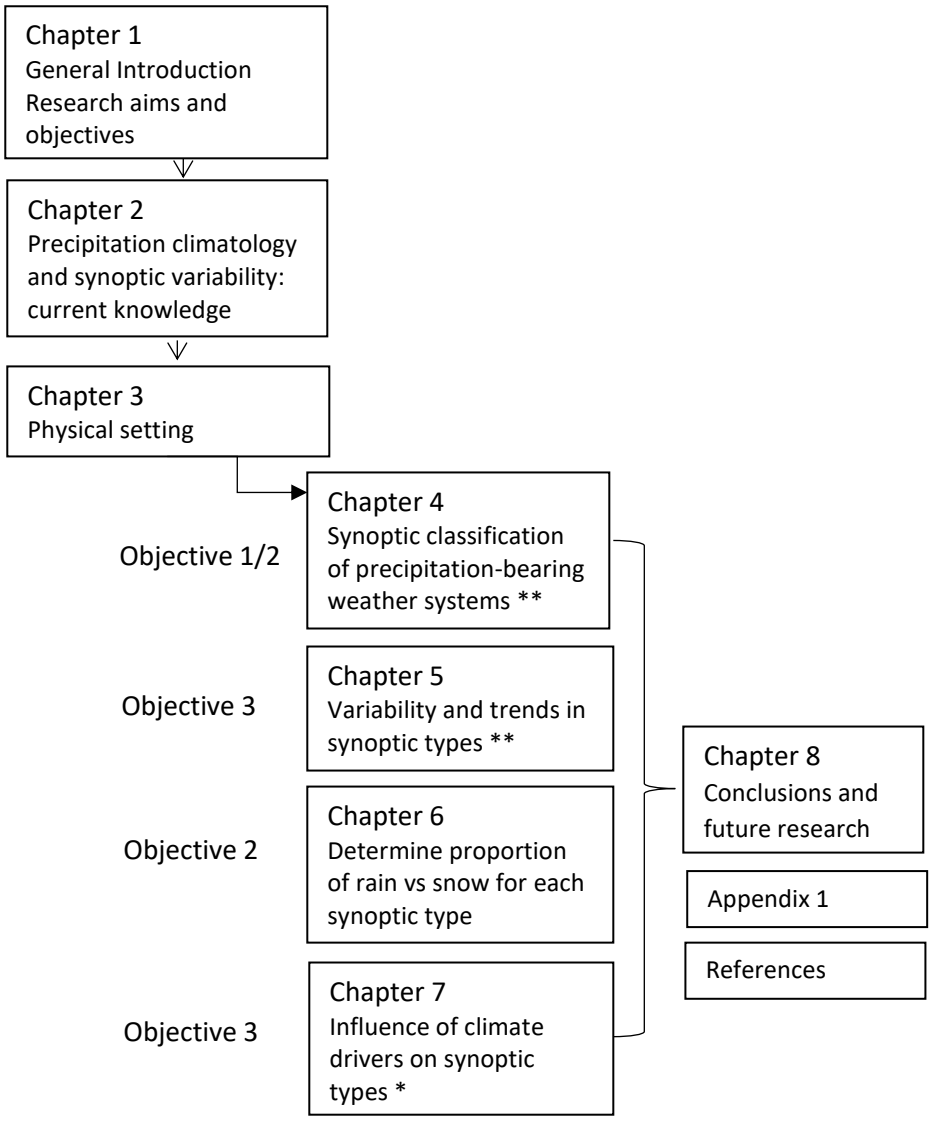

*Figure 1.1 Thesis structure. ** denotes published manuscript, * denotes manuscript in review.*

Chapter 2. Precipitation climatology: background, current status and knowledge gaps

This chapter provides background information and a summary of the existing literature pertaining to synoptic-scale climatology, and more specifically precipitation climatology. It identifies the methods by which climatologies are constructed, and other fundamental concepts for this study. Key knowledge gaps from this literature review are summarised at the end of the chapter (Section 2.5).

2.1 Synoptic climatology

Synoptic climatology, by definition, seeks to establish relationships between small-scale regional surface climate and the overlying large-scale atmospheric circulation (Yarnal 1993). In terms of meteorology, synoptic climatology is an effective tool to determine modes (or 'types') of atmospheric circulation related to specific weather events of interest. 'Synoptic typing' groups circulation patterns based on similarities of atmospheric properties. In doing so, the dynamics of the atmosphere and coupled response of the surface environment are integrated (Yarnal 1993).

There are two fundamental approaches to synoptic typing: 1) *circulation-to-environment* which first constructs the classification and later relates the synoptic types to the environment, for example, classification of weather types for all days within the study period followed by assignment of rain-days to particular types (e.g. Bettolli et al 2010; Verdon-Kidd and Kiem 2009a); 2) *environment-to-circulation* which classifies the atmospheric circulation based on environmental criteria, for example, days on which surface ozone exceeded a critical threshold (Hart et al 2006; Yarnal 1993).

Synoptic typing includes manual and automated techniques, both of which have advantages and disadvantages discussed further in the following sections (2.1.1 and 2.1.2).

2.1.1 Manual typing

Manual typing assigns weather patterns to a synoptic type based on visual inspection of weather charts, satellite imagery and the researcher's experience of the region's weather patterns.

Advantages:

- Allows for expert input from experienced forecasters;
- Permits incorporation of satellite imagery to confirm the position of fronts, cloudbands (e.g. Chubb et al 2011; Pook et al 2006), and identify (and follow through) interacting systems (Wright 1989).

Disadvantages:

- Subjective classification: two analysists may not classify a particular event in the same way (difficult to reproduce);
- Time-consuming and labour intensive;
- Necessitates the availability of satellite imagery, limiting analyses to post-satellite era (post 1979);
- Coarse-resolution reanalysis data unable to identify key surface features.

This combination of factors means that manual classification methods lack the ability to conduct long-term and consistent synoptic typing, which is considered essential to determine the effect of longer period climate variability on synoptic circulation.

2.1.2 Automated typing

In recent decades automated classification schemes have become common due to advances in computing technology and availability of long-term reanalysis datasets (Jiang et al 2012). These methods include principal component analysis (PCA), clustering and self-organising maps (SOMs). Automated methods rely on a computer program to determine the weather types.

Advantages:

- Objective classification;
- Repeatable;
- Allows a longer time period to be analysed due to quicker computation time.

Disadvantages:

- Some subjective decisions remain, for example determination of the final number of types;
- Has not yet incorporated satellite imagery;
- Similar to manual methods, coarser resolution reanalysis data is not sufficient to detect important surface atmospheric features, such as frontal and trough positions, especially at regional scales.

In order to extract synoptic types using PCA, it is necessary to follow the PCA with a clustering method, of which a number are available. Two of the most widely used in the literature are average-linkage and *k*-means, both of which have proved successful in several previous studies (e.g. Kidson 2000; Ye et al 1993). The *k*-means method in particular produces weather types that are best separated (Jiang et al 2012). Although clustering has often been used in addition to PCA, the use of clustering alone produces essentially the same synoptic types and allows the retention of all data,

for example all atmospheric variables conducive to precipitation generation and distribution (Romero et al 1999).

In general, automated schemes produce a greater number of synoptic types than manual methods, often with less well-defined boundaries between types, and more of a continuum between types (Hewitson and Crane 2002). This can offer greater insight into the evolution of synoptic circulation, as systems traverse a region, as well as important subtle differences between types. The advantages of automated typing have seen their popularity increase over manual methods. Previous studies however, have lacked the classification of weather systems based on data throughout the troposphere, and have typically concentrated on surface, or single-level, features.

2.2 Tropospheric data

Previous synoptic classifications of precipitation-bearing weather systems both worldwide and in Australia focus mainly on surface pressure fields with limited analyses of mid and upper level atmospheric properties. The lack of climatology studies using multi-level meteorological data is attributed to difficulties inherent in combining such data into a classification, and the larger number of possible combinations that result (Kidson 2000). Although several studies have produced three-dimensional typing, these have been constructed using manual techniques (e.g. Milrad et al 2014; Moore et al 2013). Studies that have applied automated techniques have been based on a single atmospheric variable, usually MSLP (Jiang 2011; Renwick 2011; Kidson 2000; Whetton 1988). These approaches, as noted by Stahl et al (2006), conceal the complex three-dimensional nature and internal variability of synoptic types. Consequently, causes of variability in seasonal rainfall which depend not only on the annual cycle of surface pressure, but also on patterns of atmospheric circulation in the mid- and upper-troposphere (Pook et al 2006), may not be identified.

Whilst some manual typing studies have included limited mid-level data (e.g. Landvogt et al 2008; Pook et al 2006), automated schemes that consider upper level data have tended to classify each level separately, combining the results of each in their interpretation of results (Bettolli et al 2010), or using data reduction techniques such as PCA (e.g. Moron et al 2008; Coleman and Rogers 2007; Stahl et al 2006). This approach does not therefore produce synoptic types based on combined similarities at multiple levels. At the time of writing, no examples were found to exist in the literature of multiple levels being combined within the SOM technique. The potential for combining multi-level data for a point-location was demonstrated by Stone (1989) and Hart et al (2006) using PCA followed by clustering. Similarly, Wilson et al (2013) showed that this was possible using clustering alone to describe the relationship between rainfall and weather regimes in south-east

Queensland. Their study used upper air data such as wind vectors, and moisture flux as input to a k-means cluster analysis.

2.3 Precipitation climatologies

The classification of weather types responsible for delivering precipitation often stems from a need to better understand atmospheric circulation patterns that affect regional water resources (e.g. Newton et al 2014a, b; Bettolli et al 2010; Kiem and Verdon-Kidd 2009a). Frei and Schar (1998) highlighted that accurate knowledge of spatial and seasonal variations in precipitation and its causes is a necessity for industry, agriculture and land management. In general, precipitation climatologies find that specific circulation patterns are associated with enhanced or diminished precipitation characteristics. In western Canada, areas of complex terrain and a reliance on winter storms for water resources means that knowledge of precipitation-bearing weather systems is critical for understanding river flows and development of well-informed regional water management policy. Separate studies to assess catchment-scale hydroclimate variability classifying either MSLP or 500 hPa geopotential height found a greater frequency of wet days were associated with low pressure troughs over western North America, than with anticyclonic or ridging patterns, using PCA/clustering and SOM techniques (Newton et al 2014a, b; Cassano and Cassano 2010; Stahl et al 2006). Bettolli et al (2010) classified 1000 hPa and 500 hPa geopotential height anomalies in order to assess weather types responsible for rainfall in an important crop-producing region of Argentina, where irrigation is rarely used. Upper-level instability, a cyclonic anomaly to the east of the continent and enhanced east-southeasterly airflow were all found to be critical factors for rainfall generation.

In Europe, weather type classification has a relatively long history, beginning with the Lamb classification for the British Isles (Lamb 1950), and later the Groβwetterlagen (Hess and Brezowsky 1969) describing circulation patterns over central Europe. More recently, climatologies produced for specific regions have demonstrated that precipitation climatology methods can shed light on larger-scale atmospheric processes that result in regional-scale synoptic variability. For example, using a combination of airflow strength, direction and vorticity, atmospheric circulation patterns resulting in strong, cyclonic flow were associated with greater frequency of precipitation over the Czech Republic (Plavcova et al 2014). Furthermore, observed changes in precipitation variability can be associated with synoptic type frequencies, offering insight into potential hydroclimate changes associated with larger-scale atmospheric circulation variability. Declines in winter rainfall over Greece between 1958 and 2000 were attributed to an increase in blocking circulation types and fewer cyclonic types (Maheras et al 2004). Similarly, widespread decline in the winter snowpack in Utah was attributed to a reduction in the frequency of cyclones and greater rate of decline in snow-

producing synoptic systems over western North America, with associated implications for regional water policy (Gillies et al 2012).

Kidson (2000), Jiang (2011) and Renwick (2011) all described a set of 12 daily weather types for New Zealand using an automated (PCA and clustering) circulation-to-environment approach. Several types were associated with precipitation: trough regimes resulted in above average precipitation to the entire country, whilst blocking regimes were associated with higher precipitation in the northeast during summer and autumn due to onshore winds. Significant declines in the frequency of weather patterns related to flood occurrence have been linked to exceptionally dry conditions for river catchments on the east coast of New Zealand's South Island (McKerchar et al 2010). Renwick (2011) noted that ongoing research would seek to further explore the climatic differences associated with the synoptic types and their expression in terms of weather impacts (e.g. floods) and frequency of extreme events. This is demonstrated by Gibson et al (2016) who provide evidence of increased (decreased) anticyclonic (cyclonic) circulation across New Zealand over the course of the 21st century. Such changes suggest a decline in rain-bearing synoptic systems, with implications for water resource management and meteorological drought.

2.4 Synoptic circulation over south-east Australia

Existing manual precipitation climatologies for south-east Australia (SEA) have, in general, been restricted to analyses of MSLP, with limited inclusion of upper level data, such as mid-level height, atmospheric thickness, as well as satellite records of cloud cover (e.g. Chubb et al 2011; Risbey et al 2009a; Pook et al 2006). Automated classifications (e.g. SOMs) have focussed on MSLP alone (e.g. Verdon-Kidd and Kiem 2009a) and do not concentrate solely on precipitation events, but all weather events in a climate-to-environment approach.

Cool-season synoptic circulation over various regions of SEA has been well described (e.g. Gallant et al 2012; Risbey et al 2009a; Landvogt et al 2008; Pook et al 2006; Wright 1989), since it is historically the season during which the majority of precipitation across the region is received (e.g. Chubb et al 2011; Ummenhofer et al 2009a; Pook et al 2006). Conversely however, precipitation occurs year-round and seasonal means were found to be similar throughout the year in SEA (e.g. Schnur and Lettenmaier 1998; Simmonds and Hope 1997). Consideration of precipitation-bearing synoptic types in all seasons is therefore warranted. With the exception of Pook et al (2014), the predominantly manual classifications have typically concentrated on describing the atmospheric circulation over the recent few decades only. In particular their focus has been the period of extended drought that persisted for much of the 1990s and 2000s (Millennium Drought) in an

attempt to understand the significant precipitation decline that occurred during this period (e.g. Risbey et al 2013).

Typically, between three and five synoptic types were identified for the cool season in SEA (Risbey et al 2013; Chubb et al 2011; Landvogt et al 2008; Pook et al 2006; Wright 1989), based on manual typing methods. Overwhelmingly, the cool-season classifications concentrate on two synoptic types: cold fronts and cutoff lows, both of which are dependent on the mid-latitude westerly storm track for their formation. Cutoff lows have been found to account for as much as 50% of total cool-season precipitation in previous studies (Pook et al 2006), and can bring precipitation totals in excess of 25 mm per day (Gallant et al 2012). They are a major source of precipitation in the region, and together with cold fronts can occur year-round (Wright 1989). Other synoptic types such as warm lows and inland troughs are considered more frequent during the warmer months (Landvogt et al 2008) when the subtropical ridge is in its most southerly position, enhancing airflow and moisture transport from tropical latitudes (Speer et al 2011). This consideration of warm-season systems however, is based only on a five year period from 2000 to 2005 for an elevated region of northeast Victoria, and demonstrates the need to fully describe the year-round precipitation-bearing systems over a multi-decadal period.

Accordingly, there is a key knowledge gap regarding the long-term trends and temporal variability of precipitation-bearing synoptic systems in all seasons, and in the amount and spatial distribution of precipitation generated. Variability and seasonal predictions of precipitation-bearing systems were identified by Pook et al (2006) as an area needing improvement.

2.5 Influence of teleconnections on synoptic circulation

The need to understand how synoptic type frequencies vary in response to large-scale climate drivers ("teleconnections"), and in turn how changes in the synoptic-scale atmospheric circulation manifest into changes in regional climate is an area that needs to be better understood (Sheridan and Lee 2012; Stahl et al 2006).

A fundamental factor in the propagation of climate anomalies from the tropics is the El Niño Southern Oscillation (ENSO) phenomenon: a leading cause of interannual climate variability, with impacts known to disrupt weather patterns worldwide through global teleconnections (Cai et al 2014a; Trenberth 1998). ENSO can be defined either by SST anomalies across the tropical Pacific Ocean or by its atmospheric component, the Southern Oscillation Index (SOI). The SOI is a measure of the surface pressure difference between Darwin and Tahiti, close to the western Pacific warm pool and central Pacific respectively and therefore the main centres of convection (Trenberth

1997). Operating on timescales of 2-7 years, sustained positive (negative) values of the SOI indicate La Niña (El Niño) episodes.

The Pacific Decadal Oscillation (PDO) is the leading mode of low frequency Pacific climate variability, expressed as spatial and temporal characteristics of SST anomalies over the North Pacific Ocean (Christensen et al 2007; Mantua and Hare 2002). Warm phases of the PDO result from cool SST anomalies in the central North Pacific and above (below) average MSLP in the tropical regions of the western (eastern) Pacific. Whilst ENSO-like in its pattern, the PDO persists on much longer multi-decadal time scales, with phases typically lasting 20-30 years (Mantua and Hare 2002).

The Indian Ocean Dipole (IOD) is an ocean-atmosphere coupled climate mode that occurs on interannual timescales across the tropical Indian Ocean (Saji et al 1999). During positive IOD events, persistent high pressure over Australia induces anomalous easterly winds over the eastern Indian Ocean with associated upwelling and cooler SSTs, with above average SSTs in the western tropical Indian Ocean. Conversely, negative IOD events result in warmer (cooler) SSTs in the eastern (western) Indian Ocean region (Ummenhofer et al 2009a). Indian Ocean Dipole events usually begin around May or June and are at their peak between August and October, after which they tend to rapidly decay (Bureau of Meteorology 2013; Saji et al 1999). The IOD affects rainfall patterns across the Indian Ocean Basin, including in Africa, Indonesia and Australia (Murphy and Timbal 2008; Saji and Yamagata 2003).

The Southern Annular Mode (SAM) is the leading mode of extra-tropical variability for the Southern Hemisphere, including Australia (Chiew et al 2011; Murphy and Timbal 2008). It is defined as the difference in zonal MSLP between latitudes 40°S and 65°S (Gong and Wang 1999). Positive (negative) SAM values indicate anomalously high (low) pressure in the mid-latitudes, and an associated southwards (northwards) shift in the mid-latitude westerly storm track (Ho et al 2012). The SAM is a high frequency mode of variability, which operates on timescales of weeks to a few months between positive and negative phases (Bureau of Meteorology 2008b).

Several of the precipitation climatologies discussed in Section 2.3 analysed the response of synoptic types to teleconnections. Significant differences in synoptic type frequency over western Canada exist during positive and negative phases of teleconnections including the Southern Oscillation Index (SOI) and Pacific Decadal Oscillation (PDO) (Newton et al 2014a, b; Stahl et al 2006). Furthermore, precipitation amounts also varied between different phases of the SOI and PDO, with subsequent effects on catchment hydrology and regional water availability (Newton et al 2014a, b). In a similar way, a ‘southeastern low’ synoptic type, associated with a strong subtropical jet, over

the central United States was found to be significantly more frequent during strong El Niño events (Coleman and Rogers 2007). Furthermore, Sheridan (2003) and Knight et al (2008) show statistically significant changes in the frequency of polar weather types over eastern parts of North America associated with warmer temperatures experienced during positive phases of the North Atlantic Oscillation. Kidson (2000), Jiang (2011) and Renwick (2011) all performed correlations between the frequency of New Zealand weather types and the annual mean SOI. Whilst Kidson (2000) found only a weak relationship to the SOI, both Jiang (2011) and Renwick (2011) reported that weather types with prevailing southwesterly-westerly (zonal) winds were more prominent during El Niño phases of the SOI and negative SAM, whereas anticyclonic/blocking circulation was more prominent during La Niña episodes and positive SAM.

2.5.1 Teleconnection influence on precipitation in south-east Australia

Precipitation characteristics in SEA are influenced by tropical and extra-tropical large-scale teleconnections. The state of the oceans surrounding Australia and subsequent transport of humid air across SEA is particularly important. Sea surface temperatures (SSTs) in the tropical Pacific and Indian Oceans (including the Timor Sea to the north of Australia) are inextricably linked to rainfall patterns across Australia.

Effects of individual teleconnections on Australian rainfall are well documented. ENSO is commonly recognised as having a significant impact on Australian climate, and as a leading driver of precipitation variability in SEA (Alexander and Arblaster 2009; Murphy and Timbal 2008). During La Niña (El Niño) events the Walker circulation and tropical convection shifts towards (away from) the Australian region with above (below) average rainfall for eastern Australia (Murphy and Timbal 2008). Relationships between regional SEA precipitation and the SOI vary. Whetton (1988) showed year round positive correlations with the SOI for precipitation in northern Victoria, whereas Simmonds and Hope (1997) found that SEA precipitation correlates most significantly with the SOI in winter and spring. More recently, Kiem and Verdon-Kidd (2009) reported that ENSO significantly impacted rainfall in northern and eastern Victoria but was less influential in the south or west of the state. Accordingly, the relationship between precipitation and ENSO is site-specific, linked to the dominant synoptic systems of a region.

Warm phases of the PDO result in anomalously warm and dry weather for eastern Australia. The cool phase of the PDO exhibits opposite characteristics, with wetter than average conditions for eastern Australia (Mantua and Hare 2002). Whilst not shown to directly affect the synoptic-scale circulation (Kiem et al 2003), the PDO influences Australian precipitation variability via modulation of the ENSO cycle (Gallant et al 2007, 2012; McGowan et al 2009; Garreaud and

Battisti 1999; Trenberth and Hoar 1996). For example, La Niña events are enhanced during a cool PDO phase and diminished during a warm phase (Gallant et al 2012; Power et al 1999). The Interdecadal Pacific Oscillation (IPO) is the Pacific-wide expression of the PDO (Folland 2008; Christensen et al 2007) and operates on similar timescales (Christensen et al 2007). While source regions for the IPO and the PDO are different, they are referred to interchangeably in the literature. The PDO phase has previously been shown to have significant impacts on inflow in the Snowy Mountains region of SEA (McGowan et al 2009).

Precipitation in SEA fluctuates in response to SSTs in the eastern pole of the IOD. Above average precipitation can be generated from northwest cloud bands (NWCBs), that form more readily over the warmer surface waters northwest of Australia during negative IOD events (Verdon-Kidd et al 2013; Gallant et al 2012; Ummenhofer et 2009b), and their interaction with frontal systems (Wright 1989). Murphy and Timbal (2008) demonstrated that precipitation anomalies have usually already begun to manifest prior to the May onset of IOD events and so cannot be said to be caused solely by the IOD, but more likely by the presence of, and in combination with, other drivers.

The effects of SAM phases on SEA precipitation are seasonally dependent. Positive SAM phases during the Austral winter result in a retraction of the westerly wind circulation (and its associated cold fronts and low pressure systems) towards Antarctica, with subsequent reduction in precipitation over southern Australia. In spring and summer however, a positive phase sees southern Australia positioned under the northerly half of a high pressure cell with increased moisture over north-west Western Australia (NWWA; O'Donnell et al 2015) and moist onshore winds from the Tasman Sea, which can result in increased warm season rain over southeast Australia (Bureau of Meteorology 2008b; Murphy and Timbal 2008; Shi et al 2008; Meneghini et al 2007). In addition to these large-scale drivers of variability, more localised effects such as SST anomalies in the adjacent Tasman Sea also influence precipitation in SEA, particularly in summer when above average SSTs can drive moist onshore easterlies and result in enhanced precipitation (Risbey et al 2009b; Shi et al 2008; Murphy and Timbal 2008).

Importantly, the teleconnections described above do not act in isolation (Gallant et al 2012; Kiem and Verdon-Kidd 2011). Previous studies have identified that individually, each typically accounts for less than 20% of precipitation variability in the Murray-Darling Basin (Gallant 2012; Risbey 2009b), of which the Snowy Mountains form a part. A noted feedback from an increasingly positive trend in the SAM phase since the 1970s is the strengthening of the East Australia Current (EAC), leading to warming in the Tasman Sea and an increase in summer precipitation in SEA (Gallant et al 2012; Shi et al 2008; Cai et al 2005), demonstrating the importance of teleconnection interaction. Accordingly, while a proportion of precipitation variability can be accounted for by individual,

large-scale teleconnections (Gallant et al 2012; Risbey et al 2009b), enhanced understanding of precipitation variability can only be gained from study of the interaction between all relevant climate drivers (Kiem and Verdon-Kidd 2011).

2.5.2 Trends in teleconnections

Changes in the strength and characteristics of teleconnections, are likely to have consequences for the hydro-climate of SEA, including the Snowy Mountains. Increasingly positive trends in the IOD and SAM have occurred since the 1950s and 1970s respectively (Cai et al 2013; Murphy and Timbal 2008; Marshall 2003) and are likely to be associated with continued cool-season precipitation declines. More extreme ENSO cycles, with a bias towards longer, more extreme El Niño's, interspersed with intense flooding La Niña events, are suggested as a consequence of climate change (Cai et al 2014a; Alexander and Arblaster 2009). Furthermore, the subtropical ridge (STR), the strength and position of which influences areas of convection and subsidence and is inextricably linked to SAM, has expanded by 0.5° latitude per decade since 1979, with continued intensification and more southward position predicted in future (Whan et al 2014; Timbal and Fawcett 2013; Post et al 2012).

During the Millennium Drought no negative IOD events were recorded (Ummenhofer et al 2009b; Murphy and Timbal 2008). At the same time positive PDO and El Niño conditions persisted for much of the period in the Pacific, all of which lead to dryer conditions over SEA (McGowan et al 2009). It was for this period that many synoptic climatology studies of the SEA region were conducted. Analysis of the recent breaking of the drought and shift towards wetter conditions (until 2013/2014) dominated by La Niña, negative IOD and negative PDO phases, as well as the combined influence of teleconnections before the onset of the Millennium Drought, is therefore required to provide further understanding of the long-term variability of the hydroclimatology of the Snowy Mountains region.

2.6 Precipitation trends

Variability of precipitation has wide-ranging impacts for the natural environment, agriculture, and water management. Studies from North America and Europe have shown that hydroclimate changes associated with warmer temperatures and increasing precipitation intensity have ongoing implications for water policy and society (Hoy et al 2014; Gillies et al 2012). Upward trends in extreme rainfall intensity in the Mediterranean are already adversely affecting soil erosion with associated risks for flash flooding (Vallebona et al 2014), whilst changes in precipitation regimes can affect the timing and success of crop production (Stocker et al 2013; Pook et al 2009).

Global climate models project a likely decline in overall precipitation events, yet it is widely reported that heavy precipitation events, precipitation intensity and extreme events will increase in a warming climate (Kirtman et al 2013; Chiew et al 2011; Meehl et al 2005) in both Northern (e.g. Newton et al 2014a, b; Zappa et al 2013; Champion et al 2011) and Southern Hemispheres (e.g. Delworth and Zeng 2014; Grieger et al 2014; Sturman and Tapper 2006). Increased water vapour associated with positive tropical SST anomalies produces increased precipitation over tropical land areas, and increased precipitation intensity in the mid-latitudes due to transport along moisture pathways (Meehl et al 2005). Both Gillies et al (2012) and Knight et al (2008) show increasingly higher frequencies of warmer, more humid weather types since approximately 1950 across parts of the United States. Similar findings are described for Europe (Champion et al 2011) and Southern Hemisphere Pacific regions (Grieger et al 2014). These studies support projections of increasingly intense precipitation events in an atmosphere with higher greenhouse gas concentrations (Kirtman et al 2013).

In Australia, a trend towards more extreme precipitation events has already occurred over the 20th Century (Alexander and Arblaster 2009 and references therein). Highly variable rainfall, with droughts and flooding rains, is a natural part of the Australian climate. An overall drying trend has been detected in SEA with a maximum decline over the alpine regions (Risbey et al 2013), particularly marked since the 1990s. Several other studies report similar cool-season declines across both SEA (e.g. Gallant et al 2012; Chubb et al 2011; Nicholls 2010) and south-western Australia (Bates et al 2008; Hope 2006). Whilst not unprecedented in magnitude or extent (Verdon-Kidd and Kiem 2009b), the Millennium Drought saw autumn and early-winter precipitation and associated inflows drop to historically low levels (Cai and Cowan 2008), a time of year critical for wetting catchments across SEA before the onset of winter rains (Kiem and Verdon-Kidd 2009b) and replenishment of water storages (Verdon-Kidd et al 2013), as well as crop sowing (Pook et al 2014, 2009).

Furthermore, snow depths in the Australian alpine region are reported to have declined by 40% (Christensen et al 2007; Nicholls 2005) since the 1960s. Modelling of the snow-depth under climate change by Hennessy et al (2003, 2008) and Hendrikx et al (2013) have shown that significant declines, in association with rising alpine temperatures and a decrease in wintertime precipitation are likely to continue in the future. Climate models predict that both rainfall and runoff will decrease over Australia in coming years, whilst demand for water and energy are forecast to increase into the future (Christensen et al 2007).

The upward trends in the IOD and SAM are likely to have contributed to the recent and ongoing precipitation trends in SEA. Whilst there has been no significant trend in ENSO, stronger ENSO

cycles may influence greater extremes of precipitation in SEA, as well as further afield (Cai et al 2014a; Alexander and Arblaster 2009). Significantly increasing SSTs in the Tasman Sea (Oliver et al 2015) are also likely to contribute to changing precipitation patterns over SEA, particularly in summer.

2.7 Existing research from the Snowy Mountains

Although cool-season synoptic circulation over various regions of SEA has been well studied (e.g. Gallant et al 2012; Risbey et al 2009a; Landvogt et al 2008; Pook et al 2006; Wright 1989), few studies relate specifically to the Snowy Mountains area (Fiddes et al 2014; Chubb et al 2011; Colquhoun 1978), all of which focus only on the cool season. Chubb et al (2011) describe two precipitation-bearing synoptic categories for the Snowy Mountains in wintertime – cutoff lows and embedded lows (those lows that migrate within the westerly wind belt). Fiddes et al (2014) extended this classification to four synoptic types that resulted in precipitation > 95th percentile, with the addition of easterly dips and east coast lows (ECLs). Both of these studies cover only relatively short timeframes: 1990-2009 and 1980-2011 respectively, and report overall cool season declines in precipitation, consistent with studies from the wider SEA area. The decline is particularly apparent on the western side of the range, whereas easterly elevations are the only part of the alpine region reported to have experienced an increase in precipitation (Fiddes et al 2014). Since these studies were conducted for a period which largely falls within the Millennium Drought, and during a warm PDO period, the reported trends may in part reflect changes in atmospheric circulation at that time, and may not be representative of the longer term natural variability of the region.

Colquhoun (1978) describes synoptic situations most conducive to snowfall, namely a cold NW-WNW airstream ahead of a cold front and the westerly airstream associated with the passage of cold fronts. These results are rein-forced by Fiddes et al (2014) who showed that snowfall in the Australian Alps (Victorian snow resorts) is largely produced by cutoff lows and embedded lows. Of the synoptic systems that bring precipitation > 95th percentile to the eastern elevations (easterly dips and ECLs) very few of these were reported to deliver snowfall (Fiddes et al 2014), consistent with the western and high elevations receiving greatest snowfall (Colquhoun 1978). It is acknowledged that measurement of solid precipitation is particularly challenging. Systematic errors can result from under-catch (losses due to wind), wetting losses, and capping (Rasmussen et al 2012). These issues can be ameliorated by the use of heated and fenced gauges. A comparison of fenced and unfenced precipitation gauges in the Snowy Mountains, with a view to correcting undercatch losses, showed that naturally protected gauges and those below 1400 m required very little adjustment. For those gauges above 1400 m, losses averaged between 6% and 15% over winter. It was also shown that

half-DFIR fences, such as those used at 75% of precipitation gauges > 1400 m in the Snowy Mountains, provided a similar level of protection from wind losses as the World Meteorological Organisation (WMO) standard DFIR (Chubb et al 2015). An alternative measure of snow is snow depth. Use of snow depth can negate some of the challenges discussed above, however does itself vary in response to precipitation amount, wind speed and in particular wind direction (Green and Pickering 2009). Observations can be affected by wind-blown snow which redistributes snow, and temporal variability of snow can be high (Rasmussen et al 2012).

An anticipated effect of climate change may result in changes to the seasonality of precipitation as weather systems shift in response to changes in atmospheric circulation (Christensen et al 2013). Synoptic weather patterns also respond to phase changes in the teleconnections ENSO, IOD, SAM and PDO. Although these relationships are not fully described specifically for the Snowy Mountains, the number of extreme rainfall days (>95th percentile) in western and high elevations was found to have significant negative (positive) correlations with the IOD (SOI) (Fiddes et al 2014). Furthermore, Pepler et al (2015) identified a strong decline in snow cover in the Snowy Mountains during periods of El Niño, and positive SAM. The widely reported fundamental changes in some of these teleconnections (Section 2.5.2) are likely to have profound consequences for regional water availability. For instance, the highest 7-day accumulated rainfall total in the Snowy Mountains region fell between 27 February and 4 March 2012, in conjunction with a strong La Niña event, resulting in > 400 mm of rain, and causing widespread flooding (Bureau of Meteorology, 2012). In addition, the frequency of important wintertime synoptic systems, in particular embedded cold fronts, is likely to undergo further significant decline in conjunction with continued positive trends in SAM (Marshall 2003).

2.8 Summary and key research gaps

Synoptic climatology provides a platform by which to assess patterns of atmospheric circulation such as those conducive to precipitation. Both manual and automated climatologies have proved robust in defining precipitation-bearing synoptic types in regions geographically close to the Snowy Mountains. Climatologies confined to the cool-season and shorter periods however, may not be fully representative of synoptic circulation over a multi-decadal period, or reveal fundamental and changing relationships between teleconnections and synoptic types. Accordingly, there is a need to extend the present understanding of synoptic circulation beyond the last few decades and encompass year-round synoptic systems.

This thesis will address the lack of multi-level and multi-variable synoptic climatologies by integrating a large variety of data simultaneously throughout the depth of the troposphere. This is

particularly important given that precipitation in the study region is typically generated from the 700hPa level (McIntosh et al 2007), and winds in the upper and mid-levels all have a guiding influence on low level systems (Pook et al 2006). Whilst strong links between precipitation and airflow direction have been found in Australia for the cool-season precipitation types cold fronts and cutoff lows (Chubb et al 2011; McIntosh et al 2007), there remains a lack of knowledge regarding the comprehensive analysis of moisture source regions and pathways, flow strength and direction for year-round synoptic types.

Accordingly, this thesis seeks to address this gap by mapping atmospheric moisture, wind strength and direction associated with synoptic types at different tropospheric levels. In addition to the lack of multi-level studies, many past precipitation climatologies have used coarse resolution (2.5° latitude x 2.5° longitude) reanalysis data to represent atmospheric circulation. It is noted that this resolution is insufficient to identify local climate phenomena (Verdon-Kidd et al 2013) or to resolve surface features such as cold fronts and troughs (Eichler and Gottschalck 2013). By using a finer resolution dataset (0.75° x 0.75°) this thesis demonstrates that the issues associated with coarser resolution data, and the need to incorporate satellite data to identify synoptic features can be overcome, offering an automated typing approach that both identifies and accurately locates features associated with synoptic types.

Significant changes in precipitation regimes are expected to occur globally as a result of climate change. Fewer but more intense precipitation events are predicted due to a warmer, more humid, and more energetic atmosphere. For SEA, dramatic declines in cool season precipitation have occurred since the 1990s, however there is a lack of knowledge regarding rainfall trends during warmer months and over timescales longer than a few decades. Despite the reported declines in precipitation, runoff and snow depth over the Australian alpine region, there remains a fundamental knowledge gap on the long-term variability of precipitation-bearing synoptic circulation affecting the Snowy Mountains (Chubb et al 2011). Previous studies of the Snowy Mountains are few and focus only on describing precipitation-bearing synoptic patterns during the cool season (April to November). Furthermore, these studies were largely limited to periods encompassing the Millennium Drought and their results may not therefore be representative of longer term climate variability, including periods during which record floods and above average rainfall were recorded. Accordingly, this thesis aims to assess the dominance and variability of all synoptic systems during each season over a multi-decadal period, and their response to teleconnection drivers. Synoptic types respond differently to teleconnections, trends in which are already seemingly affecting precipitation patterns. Furthermore, these relationships are not necessarily stationary through time (Ashcroft et al 2016). Whilst it is known how individual teleconnections affect cool-season

precipitation described for SEA, an understanding of how teleconnections combine to influence precipitation variability is a key aim of this research. Importantly, there has been no quantification of the relative influence of teleconnections on precipitation-bearing synoptic type frequency and the link to variability in precipitation type and intensity.

Chapter 3. Physical setting

Aerial view of the Snowy Mountains, looking west

This chapter describes the physical setting of the Snowy Mountains and the importance of precipitation falling in the region is discussed in the context of this thesis.

3.1 The Snowy Mountains region

Located in SEA between latitudes 35°S and 37°S, and longitudes 147.5°E and 149°E (Figure. 3.1a, b), the Snowy Mountains are one of only two alpine regions in Australia. They form the highest part of the Great Dividing Range (GDR) and include Australia's highest peak, Mt Kosciuszko, at 2228 m. The landscape of the Snowy Mountains has been shaped by long periods of crustal stability, followed by uplift, extensive fracturing and faulting of rocks, and subsequent erosion to form deep valleys such as that of the upper Snowy River. Glacial processes resulted in features such as the cirques, moraines and lakes seen today (Costin et al 2000). In contrast to younger mountain ranges such as the European Alps, the topography is not as steep, rugged or high in elevation. However the range rises sharply in the west near Khancoban to the highest elevations along the ridge-line before declining more gradually to the undulating tablelands that dominate the east (Figure. 3.1c).

The Snowy Mountains comprise of the headwater catchments of several of Australia's major rivers including the Murray, Murrumbidgee which flow west into the Murray-Darling Basin (MDB), and Snowy River which flows east. The MDB is Australia's most important agricultural region and contains 65% of Australia's irrigated farmland. Irrigation uses more than 80% of the MDB's water resources (Murray Darling Basin Authority (MDBA) 2016), and is, in part, dependent on

precipitation and river flows originating in the Snowy Mountains. The Snowy Mountains are largely incorporated within National Parks, and are an important area for alpine tourism as well as hydro-electric power generation.

3.1.1 The Snowy Hydro-electric Scheme

In response to a series of severe droughts recorded in the region since European settlement, construction began on the Snowy Mountains Hydro-Electric Scheme ("Scheme") in 1949, and was completed in 1974. The Scheme consists of a complex network of dams, hydro-electric power stations, tunnels, aqueducts and pipelines, which divert eastward flowing rivers under the mountain range inland to the Murray and Murrumbidgee Rivers. The Scheme's hydroelectric power generation meets the peak power demand for much of Eastern Australia, and currently provides 32% of all renewable annual energy production in Australia (Snowy Hydro Limited, unpublished data, 2014, available from http://www.snowyhydro.com.au/energy/hydro/snowy-mountains-scheme). The Scheme provides an average of 2360 gigalitres of water per year for irrigation, underwriting more than $6 billion of agricultural production in the MDB (accurate as of 2012/13; MDBA 2016). Furthermore, the water provides environmental flows along major rivers, offering a degree of flow regulation and drought security to Australia's dry inland (MDBA 2014; Ghassemi and White 2007; Snowy Hydro Limited 2003).

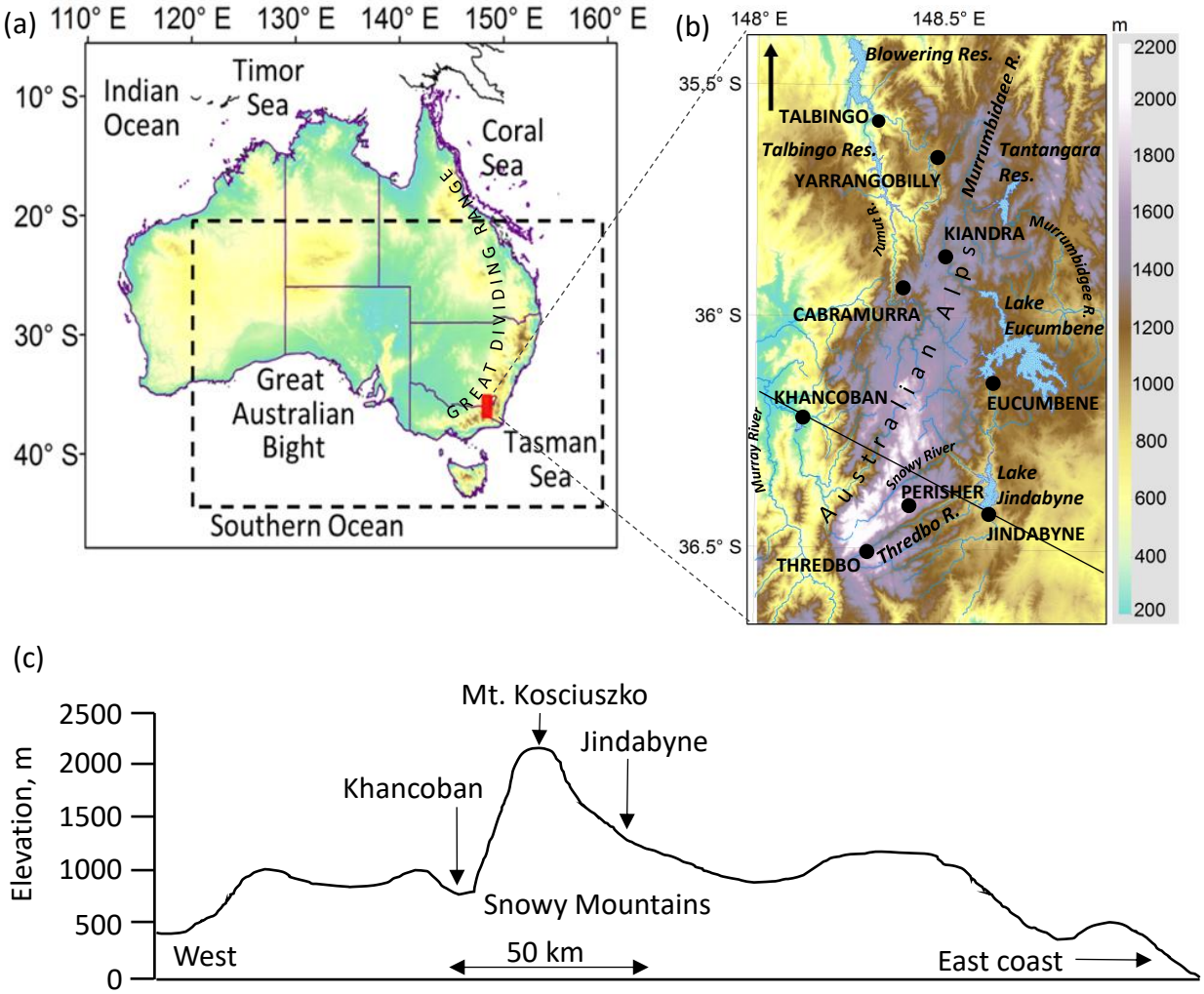

Figure 3.1 (a) Location of the Snowy Mountains region within Australia (red box) and the synoptic analysis region (dashed line) used throughout this thesis, (b) Snowy Mountains region showing towns, rivers and reservoirs, black line indicates the location of the orographic profile in (c), (c) Profile of the Snowy Mountains from west to east (adapted from Sturman and Tapper 2006 their figure 4.38).

3.2 Climate of the Snowy Mountains

The Snowy Mountains are near the boundary between the mid-latitudes and sub-tropics, and their climate is therefore influenced by both mid-latitude and tropical atmospheric circulation. The region lies towards the northern limits of the influence of the mid-latitude westerly wind belt, where interaction between tropical and extra-tropical weather systems is an important factor in the generation of precipitation (Wright 1989). Accordingly, the region is sensitive to changes in the annual cycle of the subtropical ridge, and shifts in the mid-latitude westerly storm tracks (Verdon-Kidd et al 2013; Timbal and Drosdowsky 2013; Murphy & Timbal 2008; Drosdowsky 2005). The region is also influenced by changes in the hydrological cycle in response to an anthropogenically warming climate and effects on seasonal precipitation and runoff (Viviroli et al 2011; Beniston

2003). Although typically one of Australia's wettest regions, precipitation in the Snowy Mountains is highly variable. Between 1900 and 2012 annual precipitation across the highest elevations of the Snowy Mountains ranged between 760 mm and 2800 mm (Figure 3.2), and high variability is also found for western and eastern elevations. Similarly, snow accumulation exhibits strong inter-annual variance (Figure 3.3). For example, low snow depths in 2006 coincided with the lowest inflows on record to reservoirs of the Snowy hydro-electric scheme, whereas strong La Niña events in 2010-2012 broke the Millennium drought and saw a return to wetter conditions. Furthermore, precipitation variability exists on intra and inter-annual timescales in response to ENSO, the IOD, SAM and PDO as well as SST anomalies in the adjoining Tasman Sea, the strength and position of the subtropical ridge and subtropical jet.

Precipitation in winter and spring is heavily influenced by the prevailing mid-latitude westerly winds in conjunction with orographic enhancement, and these are commonly considered to be the wettest seasons (Chubb et al 2011; Ummenhofer et al 2009a; Cai and Cowan 2008; Pook et al 2006; Snowy Hydro Limited 2003). High intensity and warm spring rains falling onto the snowpack are a major source of inflows (McGowan et al 2009), generating as much as 50% of the total annual inflows to the hydroelectric catchments (Snowy Hydro Limited 2003). Although the warmer months have historically been drier, heavy rainfall can result from trajectories of warm, moist air from tropical latitudes and small-scale convective events that generate thunderstorms (Snowy Hydro Limited 2003; Basist et al 1994; Barry 1992).

Widely reported impacts of climate change include fewer, more intense precipitation events, and changes in the seasonality of precipitation due to altered atmospheric circulation patterns (IPCC 2014; Shi et al 2008). Changes to the temporal distribution of precipitation may impact the timing of reservoir replenishment, with subsequent effects for water managers in downstream regions. In a similar way, changes to the proportion of rain and snow in a warming climate is likely to affect timing and volume of inflows. Furthermore, the relationships described between teleconnections and Australian snow depths (Pepler et al 2015), and trends in those teleconnections (discussed in Chapter 2.5.2) are likely to have detrimental effects on snow depths in the Snowy Mountains. Hence, climate change presents a challenge for the Scheme as demand for electricity generation, irrigation and environmental flows becomes greater, yet water resources to provide these services may become altered and stressed if precipitation patterns change.

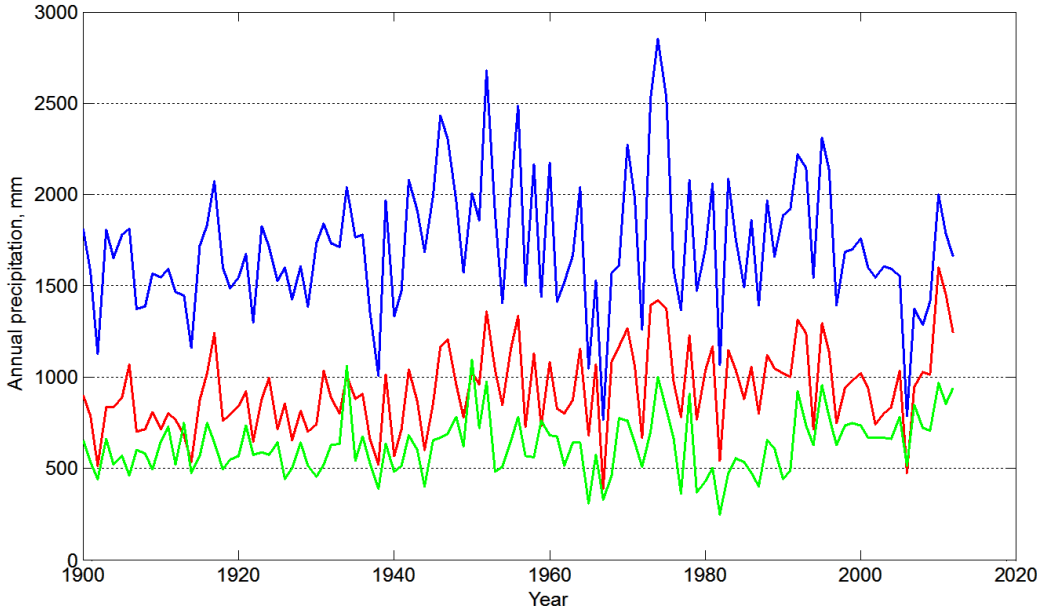

Figure 3.2 Annual precipitation, mm for the western (red), high (blue) and eastern (green) elevations of the Snowy Mountains between 1900 and 2012.

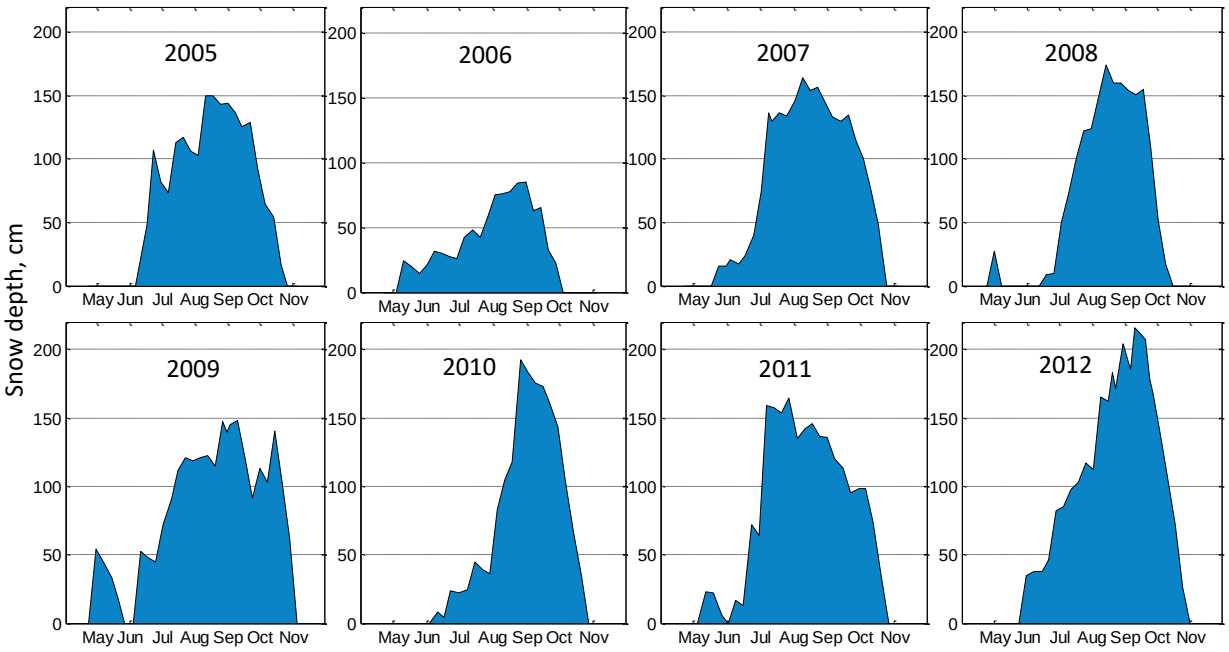

Figure 3.3 Snow accumulation (cm) at Spencers Creek snow course 2005-2012, demonstrating the high inter-annual temporal variability in snow depth.

3.3 Orographic effects

Topography plays an important role in the distribution of precipitation across mountain ranges. Basist et al (1994) found that the most significant factors explaining the variance of mean annual total precipitation in New South Wales were slope and a combination of elevation and exposure to prevailing westerlies (winter) and easterly (summer) airflow. Although orographic effects in the region vary seasonally, statistical relationships between topography and precipitation distribution found exposure to prevailing winds to be one of the most important factors year-round (Basist et al 1994). The complex terrain, and approximately north-south alignment, of the Snowy Mountains result in considerable orographic influence on precipitation distribution (Chubb et al 2011), particularly across western and high elevations. Data from precipitation gauges across the Snowy Mountains show mean annual precipitation for the western, high and eastern elevations is 1006 mm, 1724 mm and 643 mm respectively, over the period 1958-2012. In summer, convective cloud forms dominate (Basist et al 1994), influenced by differential surface heating between sunny and shaded slopes (Barry 1992). Known transport corridors for atmospheric moisture and resultant heavy winter precipitation include from the north and north-west towards the Australian Alps (Chubb et al 2011; McIntosh et al 2007). There is a lack of similar information for synoptic systems occurring outside of winter.

3.4 Summary

The geological history of the Snowy Mountains has resulted in complex terrain. Deep river valleys on the western elevations give way to undulating tablelands on the eastern side of the range. Winter and spring have historically been the wettest seasons as a result of prevailing westerly winds, leading to greater amounts of precipitation across western and high elevations. However, climate change modelling, along with trends in key teleconnections indicate potential changes to the seasonality and characteristics of precipitation. Climate change in mountainous regions cannot though be presumed to follow large-scale trends due to orographic effects and rapid changes in climate parameters over small distances (Christensen et al 2013). The snowpack, which provides up to half of the annual inflows to the Snowy Hydro Scheme reservoirs, may respond rapidly to increasing temperatures associated with climate change, given the marginal nature of the alpine area.

Chapter 4. A synoptic classification of inflow-generating precipitation in the Snowy Mountains, Australia


Precipitation gauges, Guthega Pondage

This chapter is based on the manuscript *Theobald, A., H. McGowan, and J. Speirs, 2015: A synoptic classification of inflow-generating precipitation in the Snowy Mountains, Australia, Journal of Applied Meteorology and Climatology, 54, pp 1713-1732.*

Following the description of the motivation for this study discussed in chapter 1, an automated methodology for classifying synoptic-scale weather systems associated with days on which inflow-generating precipitation was observed, is presented here. The dominant synoptic systems for each season are outlined for a multi-decadal period extending from 1958-2012. This classification was later extended to cover the period 1900-2012, following the release of the ERA-20C reanalysis dataset from the European Centre for Medium Range Weather Forecasts (Poli et al 2013). The extended period is used for the study in chapter 7.

4.1 Introduction

Synoptic typing offers insight into the weather systems responsible for regional precipitation variability (e.g. Newton et al 2014a, b; Gillies et al 2012; Stahl et al 2006), which typically respond to atmospheric circulation and available moisture, as well as large-scale climate drivers. It is widely acknowledged that precipitation falling in mountainous areas provides a vital water resource for society, agriculture, industry and the environment (Viviroli et al 2011). In Australia, a country with

relatively flat terrain, the importance of precipitation falling in the Snowy Mountains headwater catchments is critical: inflows generated from precipitation provide water resources for irrigation and environmental flows in the agriculturally important and ecologically diverse Murray-Darling Basin, as well as fuel for hydroelectric power generation as detailed in chapter 2. The high inter-annual variability of both precipitation and inflows in this region is projected to amplify in a warming climate, providing challenges for regional water management (CSIRO 2012; Chiew et al 2011).

Despite the importance of inflow-generating precipitation in the Snowy Mountains, there remains a knowledge gap regarding the long-term, historic climatological behaviour of the synoptic weather systems that deliver precipitation to the region. For SEA, it is widely reported that cool-season precipitation is dominated by cold fronts and embedded lows associated with the mid-latitude westerly wind belt (Chubb et al 2011; Risbey et al 2009a; Pook et al 2006), and a recent study described two further synoptic types (easterly dips and east coast lows) that contribute to cool season precipitation extremes (Fiddes et al 2014). By comparison, little is known of precipitation-bearing synoptic types outside of the cool-season, save for a 5-year period in the 2000s (Landvogt et al 2008) and with no direct reference to the Snowy Mountains specifically. Furthermore, there is a lack of precipitation classifications extending well beyond the recent Millennium Drought, and a lack of inclusion of upper air variables that are important for the development, intensity and steering of synoptic systems.

Factors such as the strengthening of the EAC, and associated Tasman Sea warming due to climate change suggest increasing summer precipitation in SEA (Gallant et al 2012; Shi et al 2008; Cai et al 2005), with potential to alter the historic winter-dominant seasonality of precipitation in the region (Risbey et al 2009b; Shi et al 2008). Accordingly, there is a need to extend understanding of synoptic circulation by describing year-round synoptic systems beyond the last few decades. This study presents a seasonal, 55 year (1958–2012) synoptic climatology of inflow-generating precipitation days for the Snowy Mountains region. Importantly, it provides the first multi-decadal assessment of dominant precipitation-bearing synoptic systems in each season. A novel application of an objective classification method is developed which describes synoptic types on the basis of a suite of 21 meteorological variables throughout the depth of the troposphere. Use of reanalysis data and an automated approach allows a multi-decade time period to be investigated and removes much of the subjectivity of manual classifications (Yarnal 1993). Importantly, this approach allows robust conclusions to be drawn regarding patterns of synoptic circulation responsible for inflow-generating precipitation, enabling investigation of trends in synoptic circulation variability and their significance for local to regional hydroclimate.

A description of the data and methods used is outlined in section 4.2. Results of the climatology and the variability of the synoptic weather types are presented in section 4.3. A discussion and summary are presented in sections 4.4 and 4.5 respectively.

4.2 Data and Methods

4.2.1 Data

Snowy Hydro Limited (SHL) operates an extensive network of tipping- and weighing-bucket gauges. Records in the SHL dataset began in the 1950s during the construction phase of the Scheme, however much of the early data (pre-1975) is discontinuous. A substantial increase in the SHL precipitation gauge network size to assess the effectiveness of a snow seeding program after 2004 improved data quality. The challenges in collecting precipitation data from a mountainous environment have been addressed somewhat by the installation of newer heated and weighing gauges at higher elevations, 75% of which have wind shields, to more accurately record snowfall. There are currently 57 active precipitation gauges within the Snowy Mountains, 21 of which operate only during the cool season. Of those 21 gauges, 81% are fitted with half-DFIR wind fences. It is therefore believed that these gauges offer the best available measurement of both solid and liquid precipitation. The locations of these gauges are shown in Figure 4.1a: the majority are located across the high elevation areas, with 5 and 6 in the western and eastern elevations respectively.

The Queensland Government developed the Scientific Information for Land Owners (SILO) "Patch Point dataset" ("SILO"; https://www.longpaddock.qld.gov.au/silo/ppd/ index.php?reset=reset, accessed January 2014; Jeffrey et al 2001) using data from the Australian Bureau of Meteorology (BoM) recording stations. The SILO dataset consists of observations from BoM gauges, filled in with interpolated values where observations are unavailable. Rainfall is interpolated using the geostatistical method of ordinary kriging (Jeffrey et al 2001). An interpolated surface (0.05° x 0.05° grid resolution) is produced for each day, from which missing data values for point locations are extracted from the nearest grid cell. The provision of daily data for individual stations rather than a gridded product allows direct insertion of data (Pook et al 2010) into discontinuities in the SHL record. For any point location, the nearest 30 stations and all within 100 km are used for the interpolation, whichever is greater. It has been shown that normalised precipitation removes the component of precipitation variability due to topographic influences, and can be reliably interpolated at timescales of hourly to monthly (Jeffrey et al 2001). Topographic effects are subsequently accounted for by de-normalising (i.e. reversing the normalisation process for each grid

cell individually) the interpolated surface to derive the final rainfall surface. The SILO dataset is available for the period from 1889 to present.

In total, records from 56 active SHL gauges have been used for this study, which covers the period 1958-2012. Data are recorded instantaneously and were aggregated to daily totals to 0900 local time (in line with the BoM convention for daily precipitation observations). SHL data from two inflow recording stations, Yarrangobilly River at Ravine and the Snowy River above Guthega stations (Figure 4.1a) were also aggregated to daily totals. Data from 10 gauges within the Snowy Mountains were selected from the SILO dataset (Figure 4.1a) and used to ensure a continuous daily precipitation record. Precipitation data from all seasons were considered. The standard climatological seasons have been used throughout this study: December-February (DJF), March-May (MAM), June-August (JJA), and September-November (SON).

For the purpose of producing a synoptic climatology, the European Centre for Medium Range Weather Forecasting (ECMWF) ERA-Interim and ERA-40 Reanalysis products (Dee et al 2011) were used as input to a clustering algorithm, and to construct composite maps of the synoptic atmospheric circulation associated with precipitation days. ERA-Interim spans the period 1979 to near real-time and is available at a default 0.75° latitude x 0.75° longitude grid resolution. ERA-40 spans the period 1958-2002 and has a default resolution of 2.5° x 2.5°, but a 0.75° x 0.75° resolution can also be obtained and is used here. The two datasets were concatenated across 1978-1979.

Reanalysis products at coarser scales have been shown in previous studies to be unsuitable for regional climate assessments (Eichler and Gottschalck 2013) and to have difficulty accurately detecting features such as surface fronts and troughs. As a result, past synoptic studies have needed to supplement coarse-resolution reanalysis data with satellite imagery and manual-analysis charts (e.g. Pook et al 2006). Furthermore, ECMWF reanalyses have improved representation of Southern Hemisphere high-latitude atmospheric circulation when compared to other reanalysis products (Marshall 2003).

ERA-Interim represented the latest reanalysis product (at the time of writing this study) from ECMWF and has addressed several data-assimilation issues that were encountered in ERA-40 (Dee et al 2011). Comparison of clustering results from the two products for an overlapping 22 year period (1979-2001) demonstrated agreement on > 80% of days. This is in agreement with Hoskins and Hodge (2005) who evaluated the impact of changes to observing systems in their analysis of Southern Hemisphere storm tracks. They concluded that their climatology remained robust between different reanalyses and pre- and post-satellite era.

Daily mean values of the following variables were used in this study: MSLP; 500 hPa geopotential height; wind vectors at the surface, 850, 700, 500 and 250 hPa; relative humidity and temperature at 850, 700, 500 and 250 hPa; and (the computed) 1000-500 hPa atmospheric thickness. The subtropical jet stream, the strength and position of which over Australia is known to influence steering and development of synoptic systems, was calculated as the magnitude of the wind vector at 250 hPa (Risbey et al 2009a). For the purposes of this study, temperature and humidity profiles are standard airmass indicators of atmospheric stability and available moisture respectively (Davis and Kalkstein 1990). Wind vectors provide critical information on direction of moisture transport and steering of synoptic systems (Pook et al 2006). Mean sea level pressure provides an indicator of the large-scale current atmospheric state (Eder et al 1994), whilst thickness provides information on advection and frontal position (e.g. Pook et al 2006). Variables were obtained for the synoptic analysis area bounded by latitudes 20°S - 46°S, and longitudes 120°E - 160°E (Figure 3.1a). This region is considered to be extensive enough to capture all synoptic weather systems affecting the Snowy Mountains, including those originating in, and interacting with, tropical latitudes.

The Australian daily gridded rainfall dataset from the Australian Bureau of Meteorology (http://www.bom.gov.au/climate/how/newproducts/IDCdrgrids.shtml) was used to assess the spatial characteristics of precipitation associated with each synoptic type, and to produce composite maps of each type for the Snowy Mountains catchments. This data is available at daily resolution on a 5 km x 5 km grid for the Australian continent for the period 1900 onwards. Data were extracted for each classified precipitation day in the period 2005-2012 (a period representative of different precipitation and teleconnection conditions), composited for each type and plotted as contour maps.

Furthermore, to support these static representations of spatial variability, the Weather Research and Forecasting (WRF, version 3.5) model was used to generate MSLP and 30 m above ground level water vapour mixing ratio (specific humidity) for one case study of each synoptic type. The WRF model was setup in accordance with a physics scheme configuration found suitable for Australia (Evans et al 2012). The model was initialised with NCEP reanalysis data at 2.5° grid resolution, and used a 1:5 ratio two nested domain design, with a 30 km resolution for the outer Australian region domain (80°E-180°E, 10°N-60°S), and a 6 km resolution for the inner SEA domain (130°E-160°E, 23°S-47°S). WRF was configured to allow the feedback of parametrization back into the outer domain as each time step calculation progressed. The model atmospheric depth was divided into 30 terrain-following, sigma coordinate levels determined by the default nonlinear WRF scheme for determining distances between each level. Each WRF run included a 7 day prior spin-up time to equalise model dynamics. A model run time step of 180 seconds was utilised. Taken together, these model configuration specifications were an optimal trade off of WRF spatial and temporal accuracy

against computing processing resources available to the study (M. Hewson, personal communication). Hourly plots of MSLP and water vapour mixing ratio were compiled into animated sequences, allowing moisture source regions and movement of moisture along transport pathways to be visualised.

4.2.2 Methods:

4.2.2.1 Quality control

For the purposes of this study, all data were subject to quality control and any data flagged as unsuitable for climatology purposes were automatically removed. Precipitation data were checked on a gauge-by-gauge basis for anomalous values by calculating the maximum, minimum and range. Furthermore, any data with a quality flag indicating potentially unsuitable data were subject to additional quality control, and in a few cases were removed due to anomalously high half-hourly values. In addition, SHL data coded as 'good' but with a zero amount where the corresponding SILO dataset showed a value greater than zero were disregarded when calculating the daily mean values.

4.2.2.2 Precipitation threshold

This study investigates days on which precipitation generates inflow to reservoirs within the Scheme's water catchments (Figure 4.1a). To define a threshold amount for a precipitation day, a Lyne and Hollick filter was applied to separate quickflow (surface runoff) from baseflow in the inflow dataset (Nathan and McMahon 1990) at the Snowy River and Yarrangobilly River gauging stations (Figure 4.1a). As alpine and sub-alpine sites (1630 m and 590 m elevation) respectively, these two stations provide indicative conditions across the region, including the high elevation area of the scheme catchments affected by significant winter snowfall. Precipitation from the most relevant gauges to the inflow gauging stations was then correlated with quickflow at a lag time of +1 day (based on prior knowledge of the behaviour of precipitation and runoff in these catchments). The application of the Lyne and Hollick filter to inflow data resulted in a threshold precipitation amount of 10 mm, above which quickflow and therefore inflow was enhanced (Appendix 1 Figure A1).

Only precipitation during the period from December to April was considered for the determination of this threshold. During the cool-season, precipitation can be stored as snowpack or enhance inflow during spring snowmelt and, particularly during this period, a static precipitation-runoff threshold does not apply. It is acknowledged that such a precipitation-runoff threshold is typically

dynamic and depends upon numerous catchment conditions, however is necessary for the purpose of synoptic classification of inflow-generating precipitation days in this study.

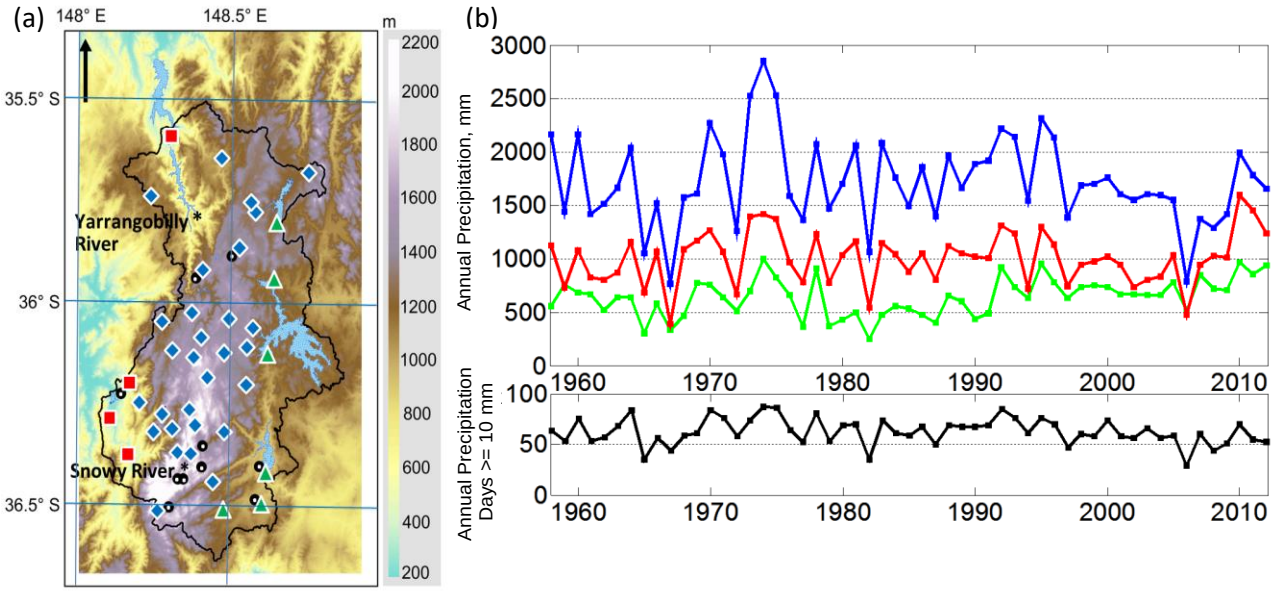

Figure 4.1 (a) Snowy Mountains region showing the water catchment (solid black line) and precipitation gauges used in this study (red squares indicate gauges on the western elevations, blue diamonds indicate gauges on the high elevations, green triangles indicate gauges on the eastern slopes. Black dots indicate SILO gauges). Inflow gauges at Snowy River and Yarrangobilly River are marked with asterisks. (b) Annual precipitation across the western (red), high (blue) and eastern (green) elevations (upper panel), and annual number of precipitation days ≥ 10 mm (lower panel) for the period 1958–2012.

4.2.2.3 Data groupings

Different precipitation regimes are experienced across the Snowy Mountains region, in part because of topographic interaction with the prevailing flow (Fiddes et al 2014; Chubb et al 2011). Following Chubb et al (2011), the 56 SHL gauges were divided into western, high and eastern elevation groups (Figure 4.1a) on the basis of the similarity of the statistics shown in Table 4.1. Although the high elevation group contains a greater number of gauges, most of these began operating after 2004. Prior to 2004 the number of gauges was more similar across all groups (Table 4.1). Such regionalisation of data has been used successfully in previous studies in a variety of locations worldwide, helping to reduce noise and spatial autocorrelation in the data (Plavcova et al 2013; Chubb et al 2011; Kidson 2000; Widmann and Schär 1997; Whetton 1988). In addition, spatial autocorrelation in areas of complex topography like the Snowy Mountains has only a short range (Tozer et al 2012; Jeffrey et al 2001) and is therefore not considered further in this study after grouping the gauges.

A continuous daily precipitation record back to 1958 was not possible using only the SHL data; therefore comparisons between the SHL and SILO datasets were carried out to determine the suitability, and associated uncertainty, in combining the two datasets. Correlations, contingency tables and their associated skill-score statistics [bias, probability of detection (POD), and mean absolute error (MAE)] were calculated (Tozer et al 2012; Beesley et al 2009; Wilks 1996). Data from all 10 SILO gauges within the catchment boundary provided the best comparison with the most recent SHL data (which include high-resolution, heated and fenced gauges), suggesting that using all gauges in the SILO dataset back to 1958 provides the most robust estimate of precipitation.

Table 4.1 Statistics of grouped precipitation gauges.

Group	Average elevation, m	Average annual precipitation, mm	Correlation between gauges	No. gauges prior to 2004	No. gauges after 2004
Western	391	1246	> 0.78	2	5
High	1484	1602	> 0.74	8	45
Eastern	1107	857	> 0.70	3	6

Contingency table statistics were better overall for gauges within the high elevation group, with POD scores indicating that at least 78%-84% of precipitation days over 10 mm are accurately detected by SILO. The MAE between the SILO and SHL datasets varies between 0.03 mm (high elevations) and 3.66 mm (eastern elevations) in good agreement with Jeffrey et al (2001) for the study region. SILO estimates of precipitation do not demonstrate a forecast bias for the high elevations, but there is a tendency to under-forecast (over-forecast) precipitation days after (before) 2006 in the western and eastern elevations. Lower skill scores in the western and eastern elevations are likely due to fewer gauges in these areas. Particularly in the east, the only two gauges in the SILO dataset are located in the southern part of the catchment. Lack of representation in the northern catchment may explain the lower skill there. Despite the lower skill scores for the eastern and western elevations, only 4.5%–4.9% of precipitation days are detected solely in these groups.

A daily precipitation amount for each group was calculated as the mean daily precipitation from each gauge within the group (Fiddes et al 2014; Dai et al 2013; Chubb et al 2011). Following WMO guidelines and Chubb et al (2011), a minimum of four data values were used to calculate a mean (WMO 2011). When this was unachievable using only SHL data, the SILO data were included in the calculation. The change in the number of SHL gauges, particularly within the high elevation group, was shown to have minimal effect on the calculation of the mean, with an average difference of 0.11 mm between mean values. Prior to the commencement of data recording in the western

(eastern) elevations by the Snowy Hydro Scheme in 1961 (1960), daily precipitation totals were calculated solely from the SILO dataset.

Each day with a precipitation total greater than the threshold amount of 10 mm was extracted from the daily record. The corresponding ECMWF reanalysis variables at each grid point for each of those days were collated into a data matrix, which consisted of each of the grid point values included as one column, for each variable. The data matrix was standardised on a monthly basis (over the full study period) using z-scores, to account for the inconsistent units (Gao et al 2014; Wilson et al 2013; Hart et al 2006; Yarnal 1993). Standardising climate data has been demonstrated to have the additional benefit of removing seasonal variations in intensity of synoptic systems, allowing comparison between data with different variabilities and means (Gao et al 2014; Jiang 2011; Wilks 2006; Kidson 2000; Yarnal 1993). The strong influence of the seasonal cycle of the STR on weather patterns in SEA means clustering applied to standardised data better reflects the daily changes in atmospheric circulation (Yarnal 1993). For example, Pook et al (2006, their Figure 3) show the variability in monthly mean MSLP across the cool-season. In this study, the monthly standardised MSLP data reveal that precipitation days are always associated with negative anomalies, which become stronger during the cooler months and are at a maximum in May. Similar month-to-month variations are apparent in the other variables used in this study. The standardised data matrix was used as input into the cluster analysis.

4.2.2.4 Cluster analysis

To generate synoptic types for the period 1958-2012, cluster analysis was applied to the standardised meteorological variables for each day when the precipitation total exceeded the threshold amount of 10 mm. The cluster analysis was performed across all seasons simultaneously, given the prior removal of the seasonal cycle by data standardisation. Equal weighting was given to each variable, given the importance of each in influencing the synoptic circulation and precipitation received, as outlined in section 4.2.1. Hierarchical average-linkage clustering gave an initial indication of the number of groups contained in the data (Trauth 2007; Wilks 2006; Hart et al 2006).

The k-means clustering method of Wilson et al (2013), with a city block distance measure, was then applied to the standardised variables to assign each precipitation day to a synoptic type (Wilson et al 2013; Hart et al 2006). The iterative nature of the k-means technique refines the clusters by reclassifying days until the smallest within-cluster solution is found, and days with similar meteorological characteristics are classified in the same cluster (Hart et al 2006). The algorithm was tested for a range of clusters between 2 and 20. Examining a plot of the distance measure against

number of clusters for the point at which the line flattens out, and after which distance increases again, commonly gives an indication of the optimum number of clusters (Wilson et al 2013; Wilks 2006; Tan et al 2006). This was used in conjunction with physical interpretation of composite maps (generated from the mean value of all days assigned to each cluster; Kalkstein et al 1987). The k-means algorithm was initialised several times using random subsets of the data as cluster seed values. The iteration for which the sum of distances was smallest was then used as the cluster seeds for the full dataset.

Comparison of clustering results between the ERA-Interim and ERA-40 reanalyses for an overlapping 22 year period produced no significant differences in the resulting synoptic types, with a hit rate of > 80% in the assignment of individual days to the same synoptic type. This is in agreement with Hoskins and Hodges (2005) whose comprehensive comparison of synoptic climatologies remained robust between different reanalyses products, and pre- and post-satellite era.

The automated clustering procedure was validated by comparison with a manual classification for a 5 year period (2008–2012) and non-parametric hypothesis testing of the precipitation assigned to each cluster. Surface and 500 hPa height charts, readily available from BoM (www.bom.gov.au/australia/charts/archive/), and NOAA satellite imagery (www.ncdc.noaa.gov/gibbs/year) were used to classify each day based on identification of key surface and upper air features (Yarnal 1993; Davis & Kalkstein 1990), and presence of cloudbands.

Classification on the basis of these variables revealed several days that could have been placed into more than one cluster. Further inspection of additional reanalysis-generated variables (temperature, humidity and wind vectors) showed that most days could belong to only one particular cluster. Overall, only 8% of days were moved into a different cluster based on the manual analysis, from that generated by the k-means algorithm.

4.3 Results

4.3.1 Synoptic classification of precipitation-bearing systems

The application of the threshold precipitation amount to daily precipitation for the period 1958–2012 resulted in 3443 days being identified with inflow-generating precipitation and requiring synoptic classification. A day was classified if at least 10 mm of precipitation was recorded in either the western, high or eastern elevation group. These specific days account for almost 40% of all precipitation days, that is, those where precipitation ≥ 1 mm is recorded. It is acknowledged that this definition of a precipitation day does not account for multi-day precipitation events, where a series of synoptic types may traverse the region as a precipitation-bearing weather system evolves

through time. Instead, each individual day is assigned to a specific synoptic type, following Pook et al (2006) and Risbey et al (2009). Figure 4.1b shows the annual precipitation across the different elevations (upper panel) and the annual number of precipitation days of at least 10 mm (lower panel) between 1958 and 2012, demonstrating the high degree of inter-annual variability in the precipitation of the Snowy Mountains region. A statistically significant trend in precipitation of +38 mm per decade in the eastern elevations is apparent, but western and high elevations and annual precipitation days exhibit non-significant decreases.

A two-sided Wilcoxon-Mann-Whitney test demonstrated that the median rainfall amount in corresponding clusters of the manual and automated classification was equal at a 95% confidence level ($p < 0.05$). Furthermore, the manual classification confirmed that the automated scheme was capable of detecting expected synoptic patterns. The types were not as clearly defined as in previous manual classification studies (e.g. Chubb et al 2011; Pook et al 2006) however, likely because of the greater number of variables considered and thus the greater possible combinations of variables as well as the multi-type nature of some synoptic systems.

The k-means clustering method, applied to the daily, standardised reanalysis data for a range of cluster numbers *k*, suggested the optimum number of clusters to be 10 or 11 (Figure 4.2). Comparison of composite maps for each of these solutions further suggested that 11 synoptic types better represented known synoptic systems and reinforced initial hierarchical clustering results. A Wilcoxon-Mann-Whitney test determined that median precipitation between types was significantly different, rejecting the null hypothesis that all medians were equal ($p < 0.05$), for 80% of all possible combinations (considering precipitation across all areas of the catchment). Given that only those days experiencing precipitation ≥ 10 mm have been classified, rather than rain versus no-rain days, and the natural variability in precipitation amount from individual occurrences of the same type (Gallant et al 2012), it is more likely that the null hypothesis will not be rejected in all cases. This result, along with physical interpretation of composite maps for each reanalysis parameter (Kalkstein et al 1987; Wilson et al 2013), demonstrates that each of the 11 clusters represents a specific synoptic type.

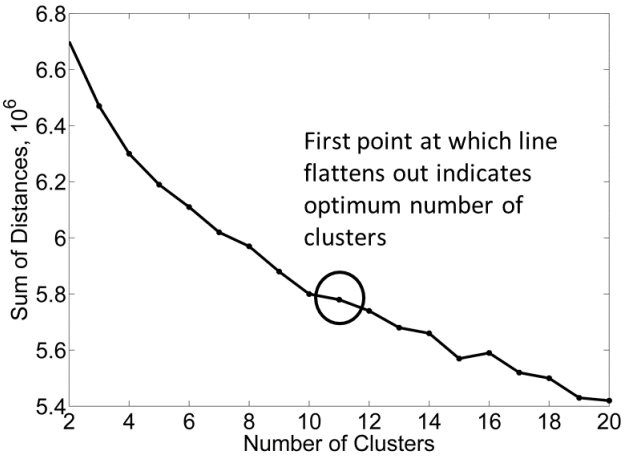

Figure 4.2 Within-cluster sum of distances. Similar to a scree plot, the point at which the plot flattens out (shown by the circled area) indicates that there are 11 clusters in the data.

Composite charts showing average meteorological conditions for a number of key parameters for each of the 11 synoptic types are presented in Figures 4.3-4.8. In addition to the clustering parameters, an analysis of columnar precipitable water (PW) and relative vorticity for each synoptic type was conducted, and is shown in Figure 4.9. These additional parameters give further information on available moisture and system development, respectively. Some between-type similarities exist in individual variables for a given level (e.g., MSLP), but when all variables are considered together, each type has distinct characteristics and distinguishing features. Table 4.2 summarises the three-dimensional characteristics, ascent mechanisms and moisture pathways for each synoptic type. The frequency of occurrence of each synoptic type and the resulting precipitation contributions in each elevation group are presented in Table 4.3.

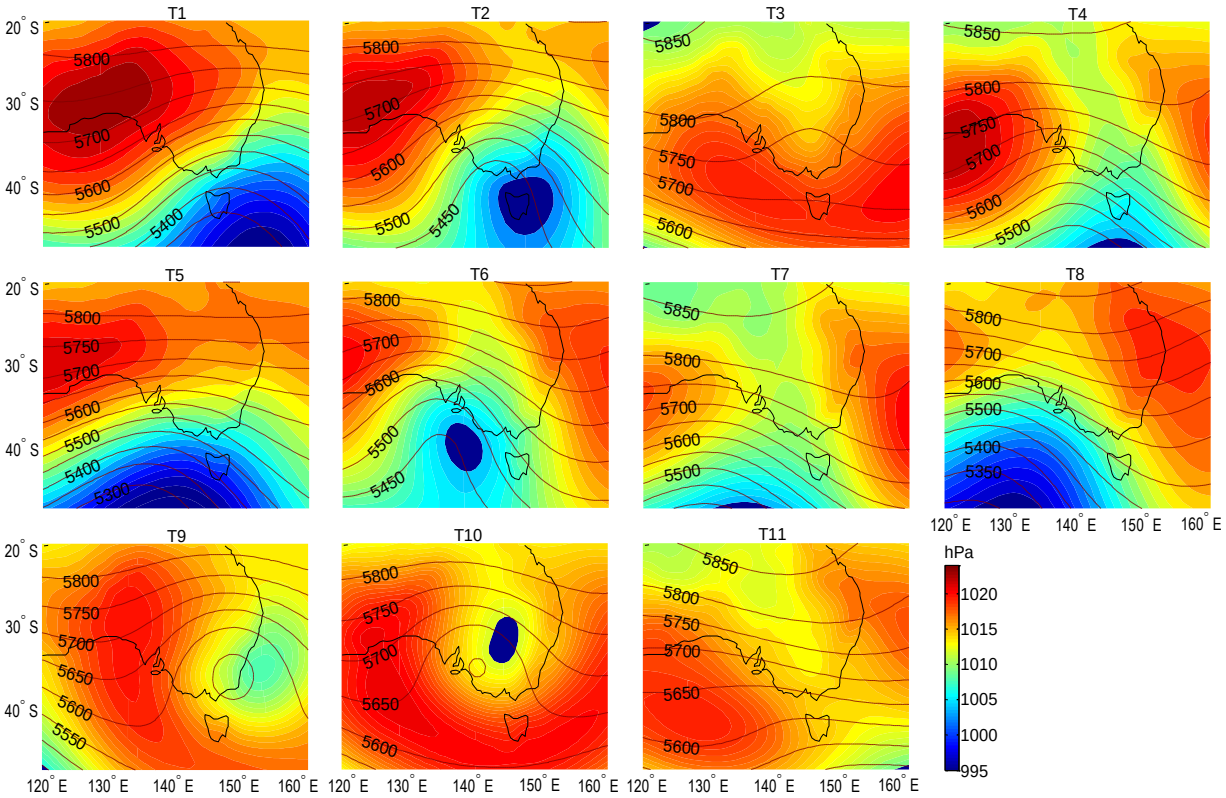

Figure 4.3 Composite maps for each synoptic type showing MSLP (coloured contours, hPa) and 500 hPa height (contour lines, units are metres). Longitude and latitude are displayed on the x and y axes respectively. The area represented in these composite maps is the synoptic analysis region as shown in Figure 3.1a.

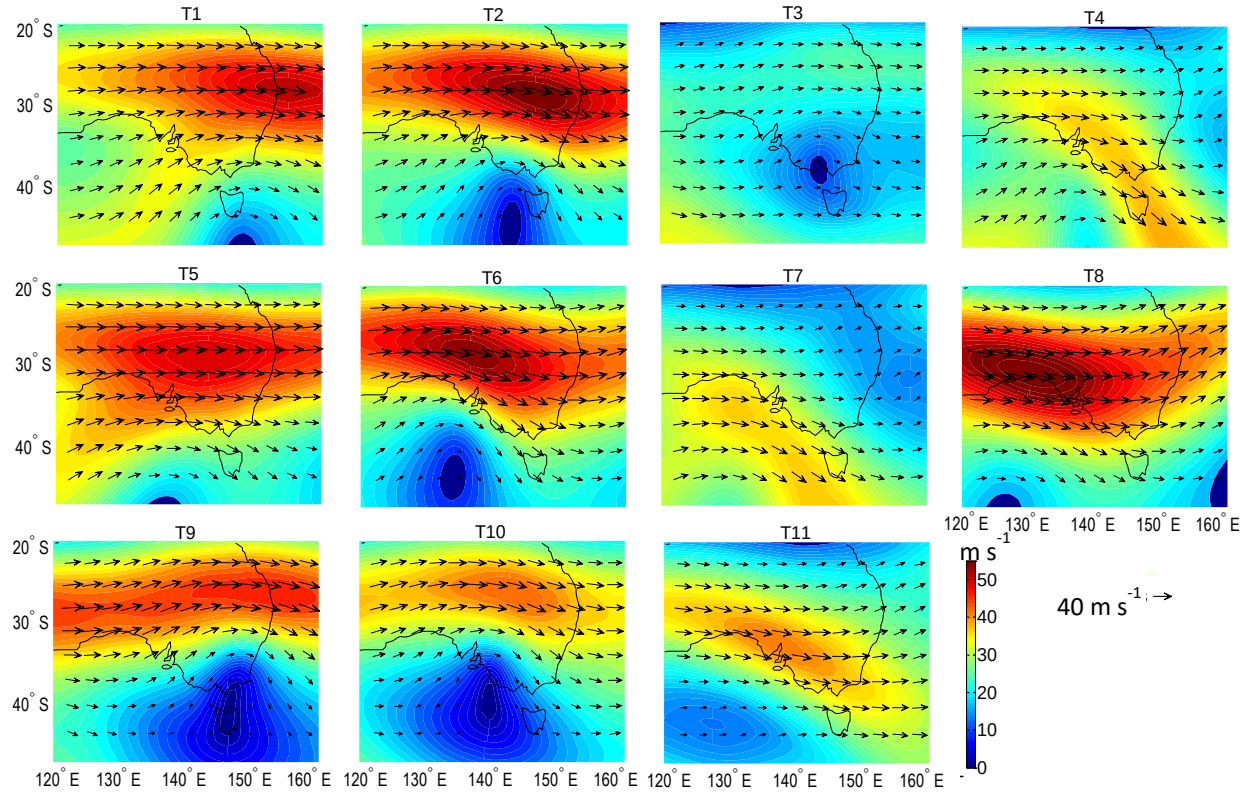

Figure 4.4 As in Figure 4.3 but showing the 250 hPa level wind speed (coloured contours, m s^{-1}) and vectors (black arrows).

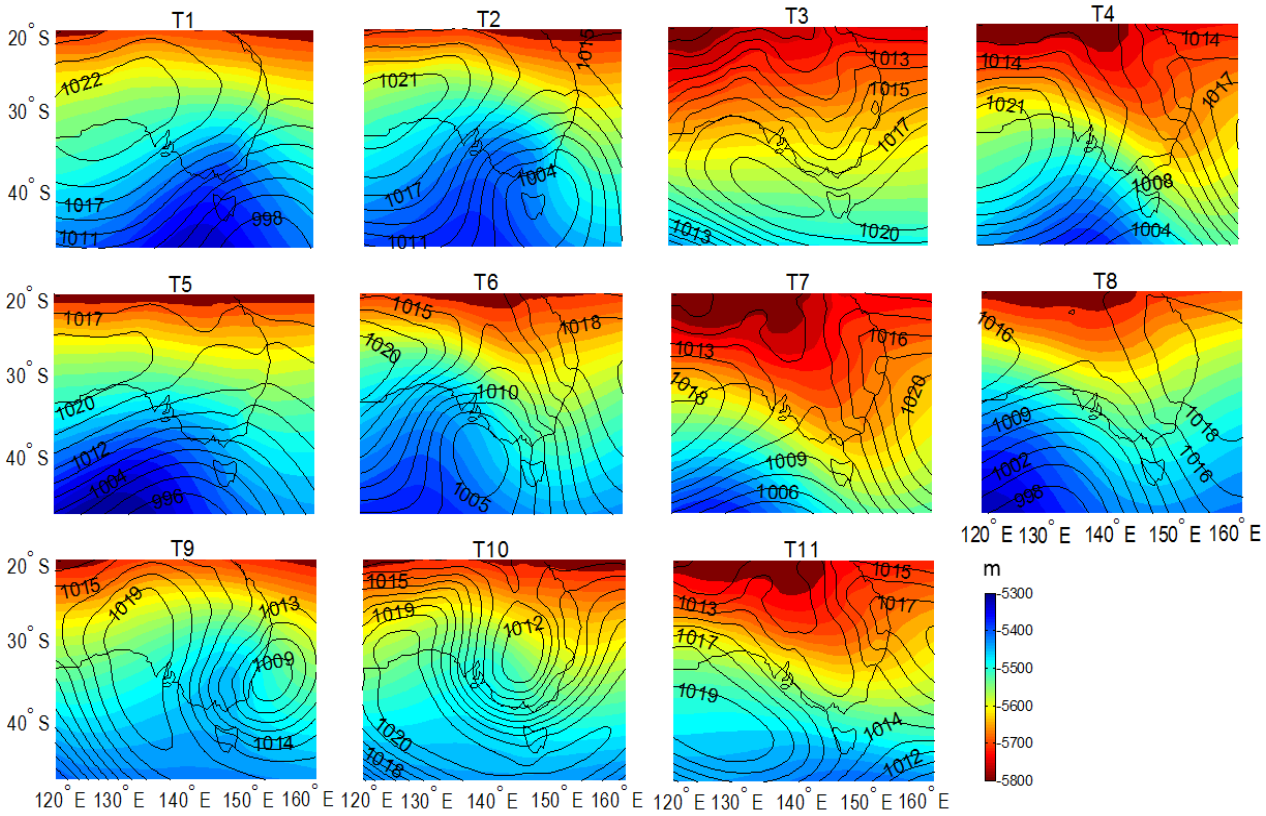

Figure 4.5 As Figure 4.3 but showing 1000-500 hPa thickness (coloured contours, m) and MSLP (line contours, hPa).

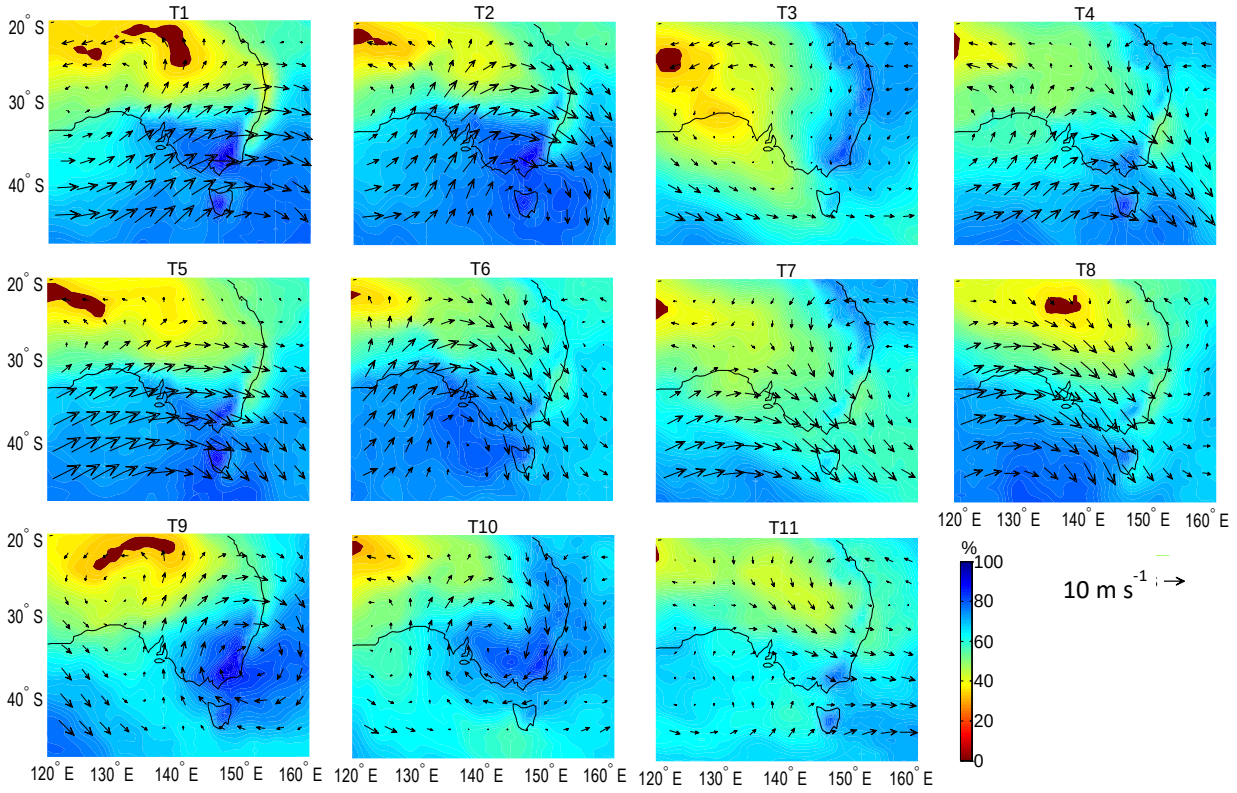

Figure 4.6 As Figure 4.3 but for relative humidity (coloured contours, %) and wind vectors (black arrows, m s^{-1}) at 850 hPa.

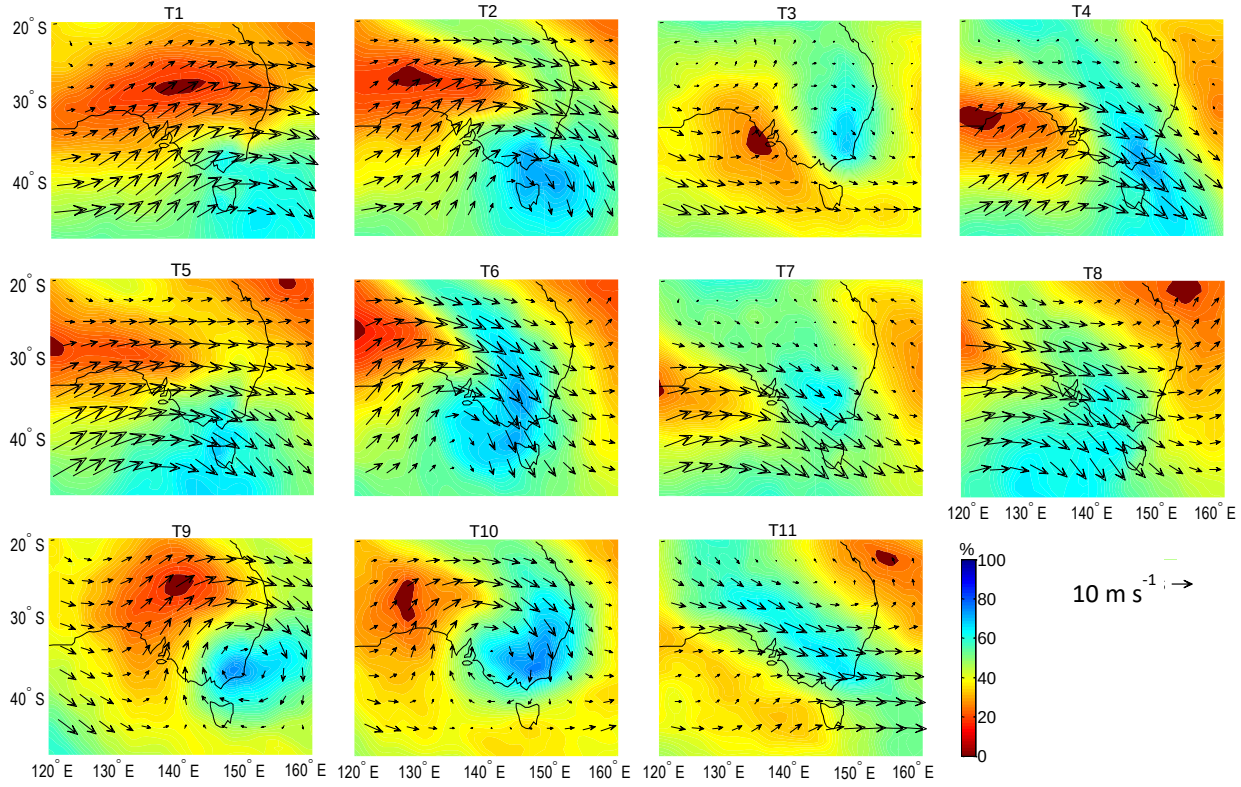

Figure 4.7 As Figure 4.6 but for 700 hPa.

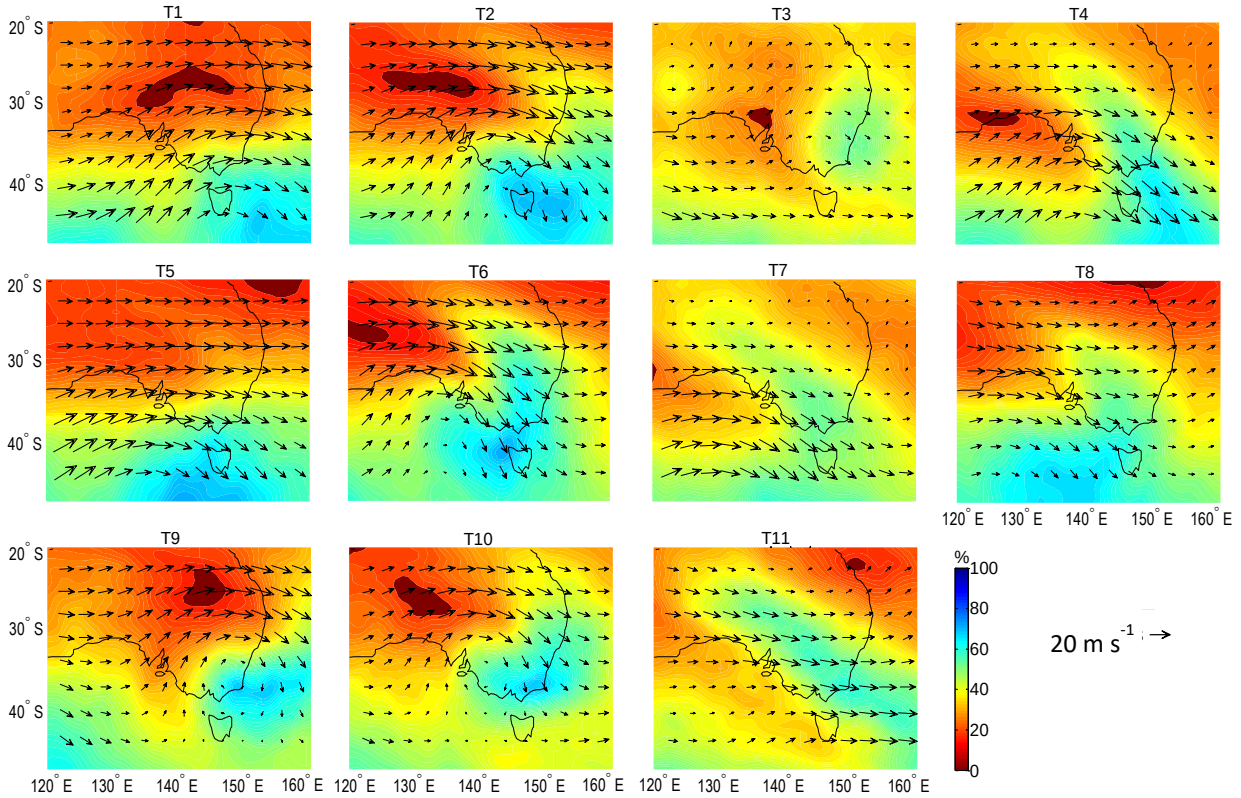

Figure 4.8 As Figure 4.6 but for 500 hPa.

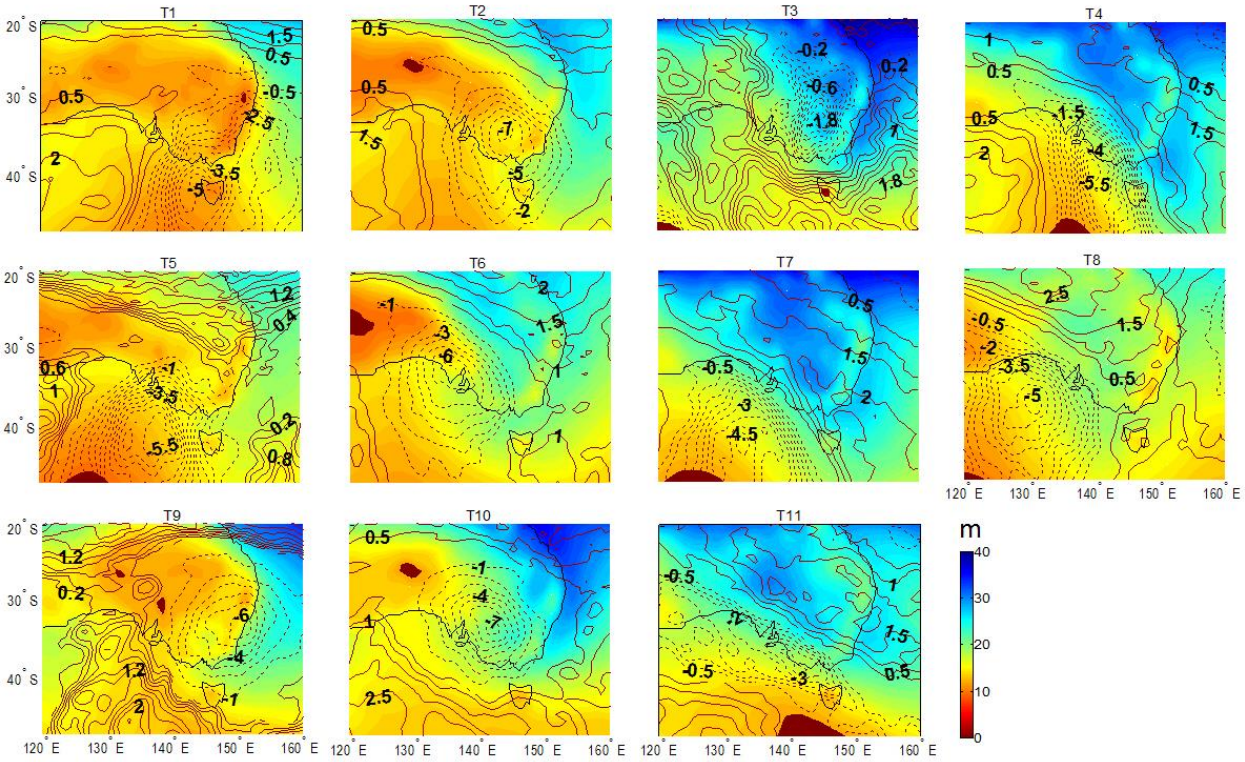

Figure 4.9 As Figure 4.3 but for columnar precipitable water (coloured contours), mm and relative vorticity at 500 hPa, x10^{-5} s^{-1}. Solid vorticity contours indicate positive (anticyclonic) vorticity and dotted contours indicate negative (cyclonic) vorticity.

Table 4.2 Description of key characteristics for each synoptic type. Directional information is referred to by the standard compass point notation – north (N), west (W), south (S), east (E) and corresponding points in-between.

Synoptic Type	Synoptic Summary	Ascent Mechanism	Moisture Pathway
T1 Embedded cold fronts.	• Cold fronts over or rapidly approaching region. • Cold core. • Mid-level trough. • No connection to tropics.	• Frontal lift. • CVA. • Convergence of SPJ and STJ over Tasmania. • Weak downstream divergence in poleward exit quadrant of jet streak.	• Southern Ocean. • No tropical moisture connection at any tropospheric level.
T2 Closed lows.	• Closed lows, including cut-off lows centred over Tasmania. • Cold core. • Weak downstream ridge. • Strong trough at 500 hPa, with cut off circulation on ~ 50% of occasions.	• WAA over Coral Sea enhanced by downstream ridge. • CVA. • Divergence in poleward exit quadrant of STJ jetstreak over Snowy Mountains region.	• Southern Ocean 850 hPa. • NW tropical 700 hPa.
T3 Inland heat troughs.	• Heat troughs extend equatorwards from low pressure centre in northwest Queensland. • Warm core. • Downstream anticyclone. • Mid-level trough.	• Convergent airflow at 850 hPa. • Winds back strongly. • Strong WAA, enhanced by downstream ridging. • Weak divergence in poleward exit quadrant of STJ.	• NE tropical 850 - 500 hPa. • High precipitable water (PW) content (~40 mm) along NE pathway.
T4 Narrow, interacting, inland heat troughs.	• Narrow inland heat troughs aligned NW-SE, interacting with cold core low. • Strong downstream anticyclone. • Upstream mid- level trough. • NWCBs on ~10% of occasions.	• Convergent airflow at 850 hPa. • WAA into divergent poleward exit quadrant of STJ.	• Southern Ocean and NE tropical 850 hPa. • NW tropical 700 - 500 hPa. • High (~40 mm) PW along NE and NW pathways.

T5 Pre-frontal troughs; upstream cold fronts.	• Pre-frontal troughs and approaching cold fronts (west of Snowy Mountains). • Cold core. • Upstream mid- level trough.	• CVA. • Divergence in poleward exit quadrant of jet streak, south of Snowy Mountains region.	• Southern Ocean. • No tropical moisture connection.
T6 Upstream closed lows.	• Approaching closed lows, including cut off lows over Bight. • Cold-core. • Downstream anticyclone. • Upstream, strong mid-level trough, with cut off circulation on ~45% of occasions.	• Downstream anticyclone enhances WAA into area of divergent poleward exit quadrant of jet streak. • CVA. • Winds back strongly.	• Southern Ocean 850 hPa. • NW 700 - 500 hPa. • Moderate PW (~25 mm) along NW pathway.
T7 Broad, interacting inland heat troughs.	• Broad inland heat troughs west of study region, aligned N-S. • Interaction with low pressure system SW of region. • Strong downstream anticyclone.	• Convergent airflow at 850 hPa. • WAA enhanced by downstream anticyclone. • Divergence in poleward exit quadrant of STJ SW of Snowy Mountains.	• NE tropical 850 hPa. • NW tropical 700 - 500 hPa. • Extensive area of high PW (~40 mm) along NE and NW pathways.
T8 Upstream pre-frontal troughs and cold fronts. NWCBs.	• Approaching cold fronts and pre-frontal troughs aligned NW-SE. • Warm core. • Strong downstream anticyclone. • NWCBs on ~40% of occasions.	• WAA, enhanced by downstream anticyclone. • Divergence in poleward exit quadrant of jet streak upstream of Snowy Mountains. • CVA. • Winds back strongly.	• Southern Ocean 850 hPa. • NW tropical 700 - 500 hPa. • Moderate (~20 mm) PW along NW pathway.

T9 Offshore low pressure systems.	• Offshore low pressure centres and troughs. • Includes East coast lows (ECLs). • Cold core. • Mid-level closed circulation. • No interaction with tropics.	• WAA on poleward side of cyclonic circulation. • CVA.	• Tasman Sea. • No tropical moisture connection at any level. • Moderate PW (~25 mm) over Tasman Sea.
T10 Easterly dips.	• Closed low pressure centres and troughs aligned N-S, N or NW of Snowy Mountains and extending to tropics. • Cold core. • Mid-level closed circulation.	• Convergent airflow at 850 hPa. • Downstream ridging and associated WAA. • Divergence in poleward exit quadrant of STJ.	• NE tropical 850 - 500 hPa. • High (>30 mm) PW along NE pathway.
T11 Non-interacting inland heat troughs.	• Inland troughs. • Warm-core lows over central Australia. • Lack of upstream trough. • NWCBs on ~35% of occasions.	• Convergent airflow at 850 hPa. • Downstream anticyclone enhances WAA. • Winds back strongly.	• NW tropical 850 - 500 hPa. • High (~30 mm) along NW pathway.

Table 4.3 Percentage occurrence of each synoptic type across all elevation groups (upper portion of table) and percentage of total precipitation ≥ 10 mm received from each synoptic type across each elevation group (lower portion of table), for the period 1958–2012.

All elevations	T1	T2	T3	T4	T5	T6	T7	T8	T9	T10	T11
% occurrence	10.4	11.3	8.6	9.7	10.5	9.6	10.3	10.8	7.3	6.2	5.3
% precipitation											
West	6.8	10.6	6.0	10.9	9.2	15.2	12.6	12.4	4.4	6.8	5.1
High	8.8	10.9	6.0	10.4	10.9	12.4	11.0	12.1	6.1	6.1	5.3
East	4.1	6.7	13.9	9.6	7.1	9.0	11.4	8.5	10.0	12.3	7.3
All elevations	7.3	10.0	7.5	10.4	9.7	12.6	11.6	11.5	6.3	7.5	5.6

The synoptic classification reveals that 8 of the 11 types (all except T1, T5 and T9) represent atmospheric circulation patterns with a direct connection to tropical latitudes, in particular where a north or north-westerly airflow (specifically between 700 and 500 hPa, Figures 4.7–4.8) advects a conveyor of warm, moist air originating from the warm oceans surrounding tropical Australia towards the Snowy Mountains (Figures 4.5-4.8). These tropical connected systems deliver over 70% of total precipitation greater than 10 mm across the whole catchment (Table 4.3). Three of the tropical connected synoptic types: T8, T11 and T4, display synoptic circulation conducive to NWCBs. For T4, however, NWCBS are detected on only ~10% of occurrences, when conditions match those in Wright (1989, their figure 3). North-west cloud bands form over the warm surface waters to the northwest of Australia, where deep convection feeds moisture from the tropical Indian Ocean along the cloud band to southeast Australia (Sturman and Tapper 2006; Tapp and Barrell 1984). This circulation, evident in Figures 4.3 and 4.4 for T8 (and to a lesser extent T4 and 11), features moisture aligned with the core of the STJ and its region of maximum intensity [as shown in Tapp and Barrell (1984)]. Together these three synoptic types account for 26% of all days over 10 mm. In a similar way, and as confirmed by the manual classification, T10-classified synoptic types have circulation that is conducive to cloud bands extending northwards along the east coast, commonly seen as an easterly dip and cloud-band pattern (Fiddes et al 2014; Gallant et al 2012). Downstream anticyclones and ridging, apparent for T3, T4, T6, T7, T8, T10 and T11, contribute to tropical moisture transport and enhancement of warm air advection (WAA; Figure 4.5), which, combined with an anticlockwise rotation of winds with height ("backing") signifies forced ascent (Figures 4.6–4.8). With the exception of T11, all tropical-connected systems demonstrate upper level divergence in the exit quadrant of the STJ (Figure 4.4). All synoptic types exhibit airflow directions conducive to orographic enhancement of precipitation (Chubb et al 2011; McIntosh et al 2007).

Synoptic types T1, T2, T5, T6 and T8 can be grouped as cold-cored frontal-type days [including contributions from closed and cutoff lows (T2 and T6) and pre-frontal troughs (T5 and T8)], and together account for 53% of all classified precipitation days (Table 4.3). Cutoff lows here follow the definition in the SEA studies of Pook et al (2006), Risbey et al (2009a) and Chubb et al (2011) amongst others, in which closed circulation can be apparent at the surface or mid-levels with a trough above or below, respectively. The manual analysis showed that T2 fulfils the traditional criteria of cutoff lows on approximately 60% (50%) of occurrences and T6 fulfils them on 72% (44%) of occurrences when considering MSLP (500 hPa geopotential height). In addition, closed-low types have associated fronts on 75% (T2) and 45% (T6) of occurrences.

Cold-frontal types have in common differential cyclonic vorticity advection (CVA) at 500 hPa as an ascent mechanism (Figure 4.9), but closed-low types demonstrate stronger cyclonic vorticity maxima than embedded cold fronts and pre-frontal types. The types T4 and T7 show the signature of heat lows and troughs interacting with cold-cored extra-tropical fronts to the south of Australia (Gallant et al 2012; Sturman & Tapper 2006). Localised acceleration of the STJ core along the enhanced thickness gradient, jet-stream divergence in the poleward exit quadrant and strong WAA (associated with strong downstream anticyclones) are consistent with enhanced system development and higher precipitation totals (Risbey et al 2009a).

Embedded cold fronts (T1) occur at a frequency that is similar to those of other frontal types, although they deliver smaller amounts of precipitation across all elevations, consistent with lower humidity and precipitable water. Because strong cold-air advection (CAA), clockwise rotation of winds with height, and jet-streak divergence occur downstream of the front, ascent is provided primarily by frontal lift. Development of closed and cut-off lows is associated with a localisation and concentration of the STJ, often forming on the poleward side of the jet. This relationship is represented in Figure 4.4 which shows a strong jet core located to the north of the closed low for types 2 and 6. Similarly, for classifications that include the passage of a cold front (T1 and to some extent T5), meridional excursions of the polar jet that cause it to merge with the subtropical jet near the location of the front are a known feature (Risbey et al 2009a; Sturman and Tapper 2006). Furthermore, Risbey et al (2009a) associate cyclonic curvature of the jet-stream core, the exit region of which is divergent, with the largest amounts of precipitation (> 5 mm and, in particular, for synoptic systems that produce ≥ 15 mm of precipitation) from frontal systems - evident here in Figure 4.4 for frontal type days over 10 mm.

Synoptic type T3 is representative of inland heat troughs extending from a low pressure centre in northern Australia known locally as the Cloncurry Low (Gallant et al 2012; Sturman and Tapper

2006). Strong WAA, into the divergent region of the jetstream is apparent in the vicinity of the trough (Figure 4.5).

Topographic interaction of the prevailing airflow in each synoptic type creates differences in precipitation contributions between elevation areas. Synoptic types generating the greatest precipitation totals across westerly elevations are the result of upstream cold fronts or troughs, closed-lows and troughs that extend towards northwest Western Australia (T2, T4, T6, T7, and T8, and 11; Table 4.3). A noticeable decrease in precipitation (rain-shadow) is apparent in the eastern part of the catchment for these types (Figure 4.10a, b). This is similar for the high elevations, where NWCBs associated with days that are classified as T8 and upstream closed-lows (T6) bring the highest percentage of precipitation totals per day. Days classified as T6 in particular stand out for delivering high amounts of precipitation to northern parts of the Snowy Mountains catchment (Figure 4.10b). A common feature in each of these types (T2, T4, T6, T7 and T8) is a downstream anticyclone, with WAA and relatively high PW to the northeast and northwest of the study region (Figures 4.5 and 4.9), along with divergence in the poleward exit quadrant of the jet-stream (Figure 4.4) and orographic enhancement. As a result, thermal wind is enhanced and directed south-eastward along the thickness gradient, causing acceleration of the STJ (Figure 4.4), apparent here for those synoptic systems classified as T2, T6 and T8. Classifications that include closed lows alone account for approximately 20% of precipitation days and contribute 26%, 23% and 16% of total precipitation to the western, high and eastern groups respectively.

The contribution of precipitation from frontal systems and the mid-latitude westerly airflow is reduced in eastern elevations, in the lee of the mountain range (Figure 4.10a). Instead, onshore easterlies in the subtropics associated with downstream anticyclones or ridging that advect warm, humid air from a moisture corridor along the east coast via inland, meridional troughs (T3 and T10), and offshore lows (T9), are the major sources of precipitation (Table 4.3, Figure 4.10c, d). Precipitation from offshore lows is greatest in the southern half of the catchment (Figure 4.10d), while there is a clear increase in precipitation across eastern elevations for T3 and T10 (Figure 4.10c). WAA is a common ascent mechanism for these types. Differences in the spatial distribution of precipitation between synoptic types shown here are consistent with investigations by Chubb et al (2011) and Fiddes et al (2014).

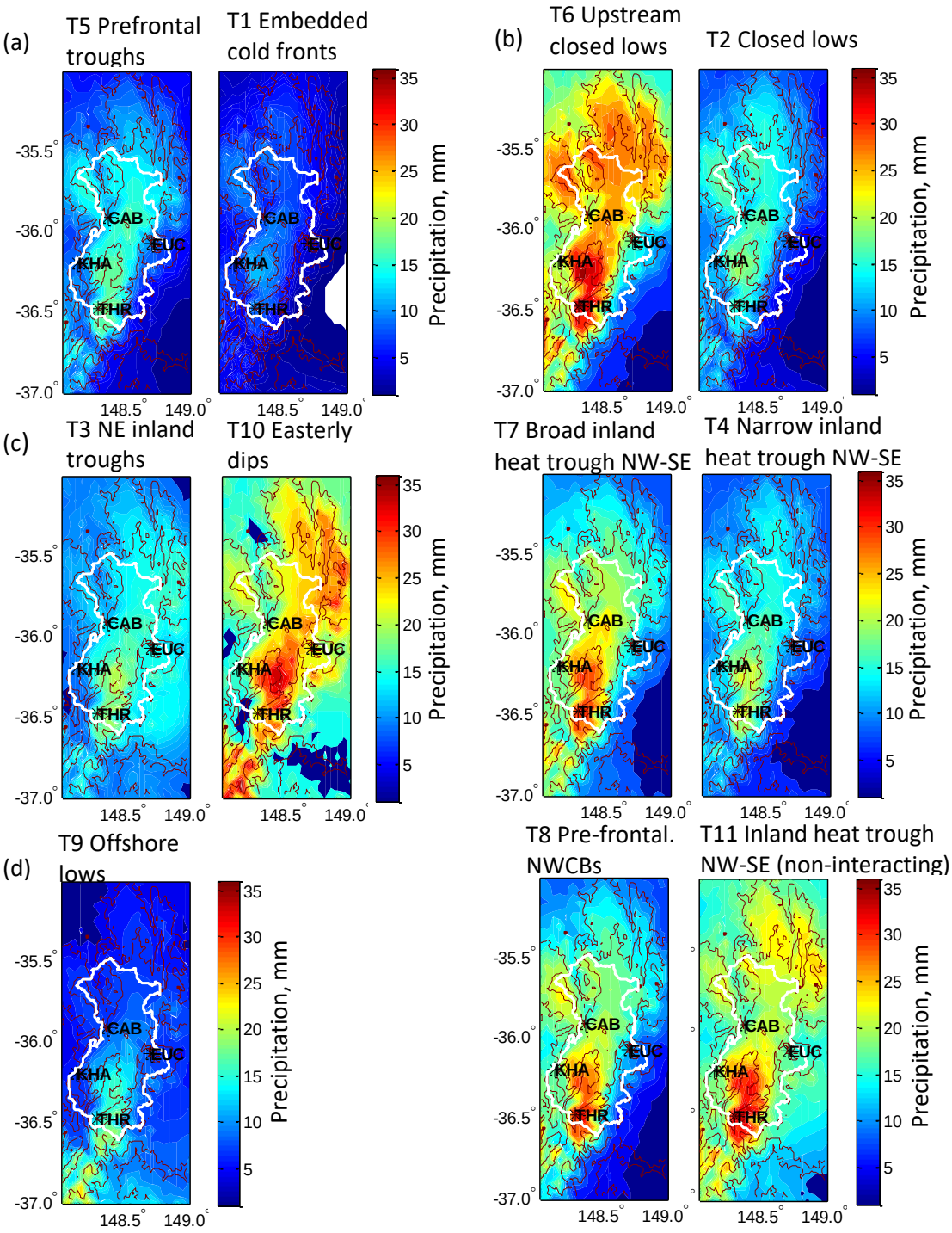

Figure 4.10 Composite maps showing spatial representation of precipitation (coloured contours, mm) across the Snowy Mountains catchment (white line) for all occurrences of each synoptic type between 2005 and 2012, grouped by predominant moisture pathway at 700 hPa (see Figure 4.7): (a) Southern Ocean, (b) north-west, (c) north-east and (d) Tasman Sea. Towns across the western (KHA, Khancoban), high (CAB, Cabramurra; THR, Thredbo) and eastern elevations (EUC, Eucumbene) are marked, and black contours indicate topography of the region.

Results of the WRF modelling for the SEA domain are presented in Appendix 1, alongside BoM surface analysis charts for the same day. Overall, WRF captures well the synoptic circulation, position of fronts, troughs, and high and low pressure centres, demonstrating that it can accurately model the passage of synoptic systems at a regional scale. The location and intensity of surface features are well represented, and there is some evidence of frontal distortion in the lee of the range for T1 (Appendix 1 Table A1). Orographic enhancement of precipitation over the range is not always apparent within the SEA domain (130°-160°E, 23°-47°S), however the boundaries between moist tropical and drier extra-tropical air (ahead and behind trough lines) are clearly delineated. The importance of downstream anticyclones in transporting tropical moisture towards the Snowy Mountains region is apparent for types T2, T3, T4, T6, T7, T8, T10 and T11 (Table A1). Perhaps the most interesting result with regards to these modelling results is the animation of atmospheric moisture content for four days leading up to an event (Supplementary material). For those types with some degree of tropical connection, higher specific humidity can clearly be seen moving towards the Snowy Mountains along either the northeast or northwest pathways shown in Figures 4.6-4.8. Similarly, for embedded cold fronts and prefrontal troughs the lack of this tropical moisture influx is also apparent.

4.3.2 Seasonality of synoptic types

Clear seasonality in the frequency of synoptic types is evident in Figure 4.11, which reflects seasonal movement of the STR. The mean contribution of each type to seasonal precipitation accumulations (Figure 4.12) demonstrates the high degree of intra-annual variability. The greatest between-type variability, in terms of both frequency and precipitation, occurs in winter and summer. Orographic enhancement of precipitation for all types is evident with highest elevations consistently receiving the largest precipitation totals in all seasons (Figure 4.12), consistent with the spatial maps shown in Figure 4.10.

The majority of types can produce seasonal precipitation accumulations beyond the 95th percentile ($> 2\ \sigma$) and could be considered extreme (Pook et al 2012). Notable large falls of precipitation, exceeding 300 mm in the western and high elevations, have resulted from the dominant summer types T4 and T7 (not shown). As noted in Section 4.3.1, these types display properties that are consistent with enhanced system development, strong WAA and higher precipitation totals.

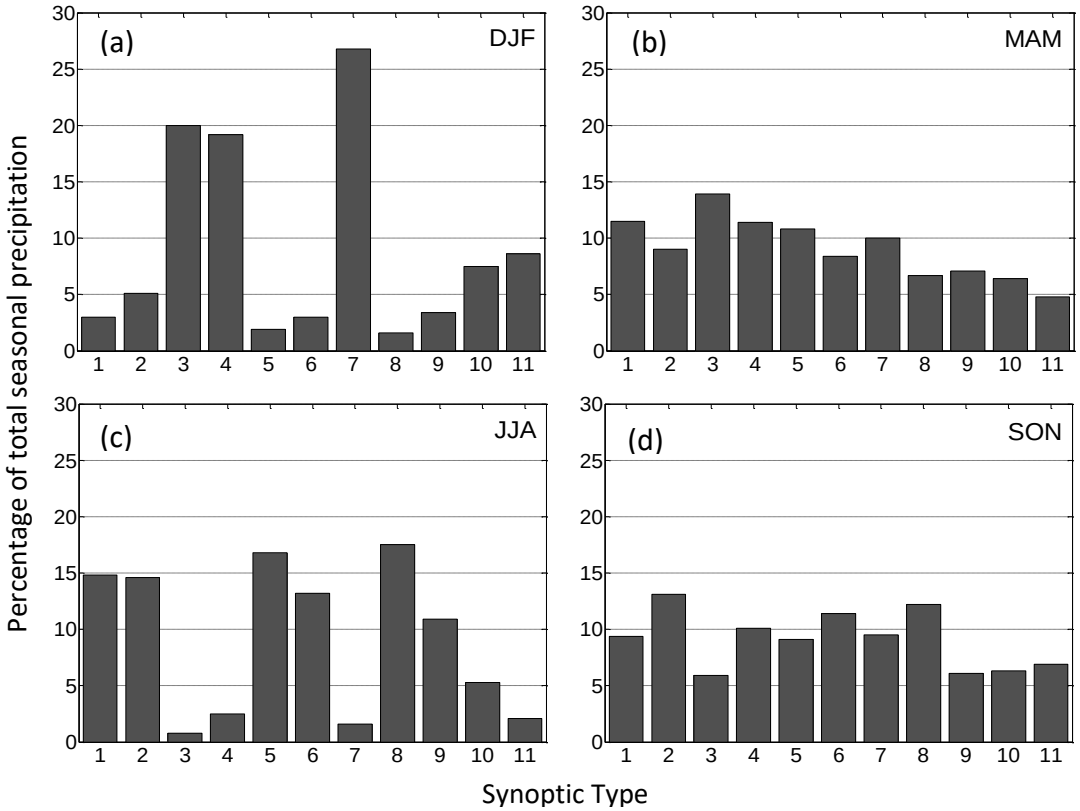

Figure 4.11 Intra-annual variability and relative contributions of each synoptic type to the total number of seasonal precipitation days ≥ 10 mm, for (a) DJF, (b) MAM, (c) JJA and (d) SON.

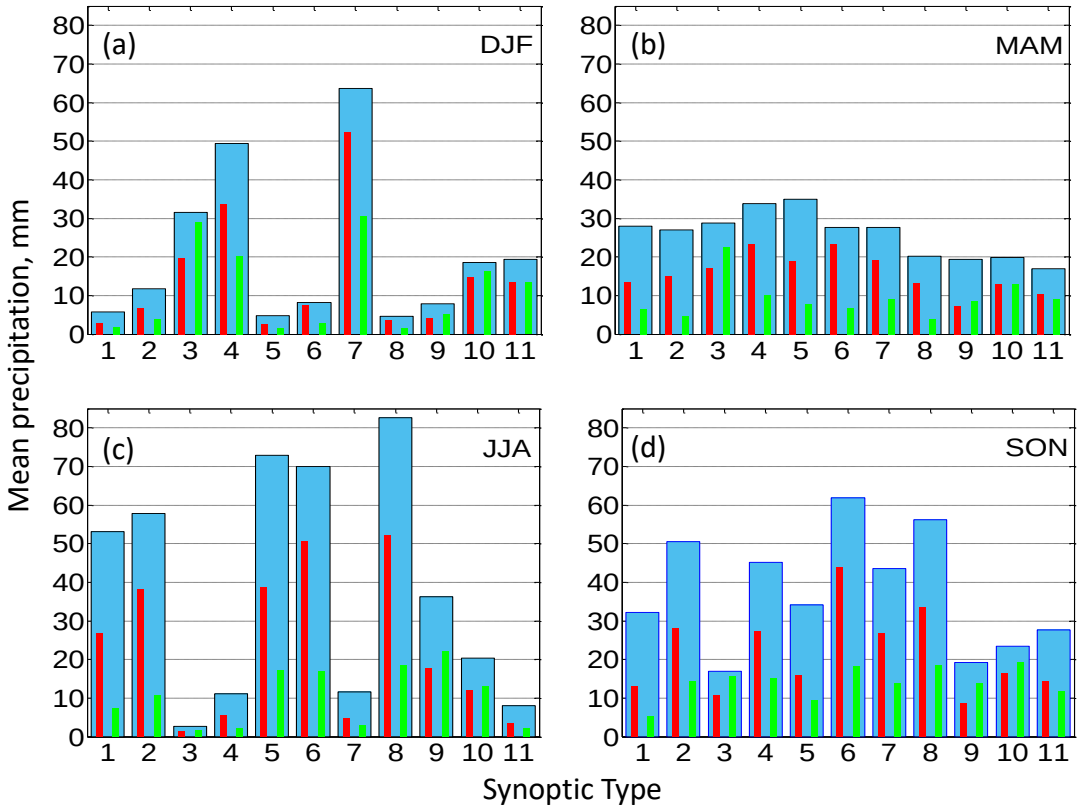

Figure 4.12 Intra-annual distribution and variability of mean precipitation (per precipitation day) associated with each synoptic type for (a) DJF, (b) MAM, (c) JJA and (d) SON. Wider, blue bars represent high elevations, narrow red bars represent western elevations, and narrow green bars the eastern elevations.

Table 4.4 summarises the mean precipitation from all days per season and reinforces previous studies that show this region is dominated by cool-season precipitation (nearly 60%), often associated with frontal and closed-low systems in the lower-to-mid troposphere (surface-500 hPa; Figures 4.11 and 4.12). However, this study highlights that a significant proportion of inflow-generating precipitation days of ≥ 10 mm (approximately 20%) are recorded during summer months, often related to the occurrence of inland heat troughs (i.e. T4 and T7), and increased convection. A further 20% of days occurred in the transitional autumn season. Mean daily precipitation from all synoptic types is similar in all seasons consistent with Simmonds and Hope (1997), but the fewer number of precipitation days occurring in summer and autumn and the higher PW, indicate a higher intensity for warm-season precipitation days (Table 4.4).

Table 4.4 Mean number of days and seasonal precipitation received from all synoptic types, across all elevations, for the period 1958–2012.

Season	Mean number of precipitation days ≥ 10 mm	Percentage of total precipitation ≥ 10 mm	Mean seasonal precipitation ≥ 10 mm	Mean daily precipitation from all types, mm
DJF	12	19.6	175	43.6
MAM	13	20.8	185	43.1
JJA	20	29.6	264	39.6
SON	18	30.0	268	44.7

In Austral summer (DJF), precipitation is dominated by warm-cored heat-trough types T3, T4 and T7. Summer types are associated with weaker mid-level troughs and weaker cyclonic vorticity, often displaced upstream of the Snowy Mountains. Instead, stronger ridges, increased moisture, enhanced WAA and low-level (upper-level) convergence (divergence) dominate and act as ascent mechanisms. Warm, moist air, with high PW is advected from tropical latitudes toward the Snowy Mountains region (Figures 4.5–4.9). High elevations still receive enhanced precipitation from these types, and days classified as T3 deliver higher amounts of precipitation across the eastern catchment (Figure 4.10c, 4.12a).

The occurrence of each synoptic type and their associated precipitation are more consistent in autumn (MAM) although T1, T3, T4 and T5 dominate slightly, representing a mix of warm- and cold-core synoptic types. This is a transition season with precipitation still generated from a moist airflow and WAA from tropical latitudes (T3 and T4). However, the northward movement of the STR and mid-latitude westerly wind belt is apparent as pre-frontal troughs and cold fronts associated with embedded lows in the Southern Ocean (T1 and T5) begin to cross the region more frequently.

Cold-cored frontal types T1, T2, T5, T6 and T8, and offshore low pressure centres (T9) dominate in winter (JJA). All demonstrate CVA with a maximum either over SEA (T1, T2 and T9) or upstream (T5, T6 and T8). Winter types generally display higher maximum cyclonic vorticity than do summer types. Only half of these types have a tropical moisture corridor at 700 hPa, and the influence of the mid-latitude westerly wind belt is clear, with a moisture source in the lower atmosphere (850 hPa) over the Southern Ocean or Tasman Sea. Low-level convergence, a northwest moisture corridor and WAA is a common feature for T6 and T8, which deliver the highest winter precipitation totals. In eastern elevations, orographic influence is apparent with much lower precipitation resulting from the predominantly westerly flow (Figure 4.10a, b). Instead, low pressure centres situated off the east coast (T9) and easterly dips (T10) are the dominant source of precipitation.

Similar to autumn, spring (SON) observes an even spread in the percentage of total seasonal precipitation days, although cold-core types T2, T6 and T8, along with T4 occur slightly more frequently. Pre-frontal and closed-low systems (T2, T6 and T8) make the highest contributions to precipitation totals, but, given that this is a transitional season, systems connected to tropical latitudes are also common (e.g. T4 and T7). Occurrence of these warm systems, on top of a late-season isothermic ('ripe') snowpack, is considered to generate the greatest snowmelt and inflow in the Snowy Mountains.

4.4 Discussion

Presented here has been a 55-year (1958–2012) synoptic climatology of daily synoptic circulation systems that deliver greater than 10 mm of precipitation to the Snowy Mountains region of south-east Australia. This is the first study to link synoptic circulation throughout the tropospheric column to precipitation either in the Snowy Mountains or elsewhere, using an objective and automated typing scheme. The use of a suite of variables throughout the depth of the troposphere, applied to a large gridded analysis area, expands on previous studies (e.g. Wilson et al 2013) and results in 11 synoptic types. The clustering method reveals subtle differences in, for example, the position and orientation of surface troughs and location of moisture corridors, which directly affect the amount of precipitation received at different sites in the Snowy Mountains region. Some types display similar attributes at certain levels, but each represents a particular synoptic atmospheric circulation for this region. The method used in this study has demonstrated that difficulties in combining variables from different atmospheric levels (Kidson 2000) can be overcome, providing a vertical profile of atmospheric conditions during specific precipitation days. It offers an automated approach to the traditional map classification (Yarnal 1993), and generates synoptic types with no *a-priori* forcing of the clustering algorithm, thereby minimising subjectivity. The importance of moisture

source regions and ascent mechanisms in delivering precipitation to the region of interest is demonstrated.

The use of a daily precipitation threshold of ≥ 10 mm differs from previous south-east Australia studies in which all precipitation days have been considered. Importantly, it allows classification of synoptic circulation associated with precipitation days that trigger a quantifiable increase in streamflow in the headwater catchments of Australia's iconic and economically important river system – the Murray Darling Basin.

Seasonal variations in the frequency of occurrence of each synoptic type highlight the variability of atmospheric circulation affecting the Snowy Mountains region. Although certain synoptic systems are predominant during the cool or warm seasons, and a clear seasonal signal in their incidence is apparent (Figure 4.11), they may occur at any time (Wright 1989).

The seasonal movement of the STR is critical to the synoptic systems experienced in SEA. In winter the STR is in its most northerly position over central Australia, allowing the passage of frontal systems associated with the mid-latitude westerly wind belt to traverse southern Australia. Accordingly, winter synoptic types frequently relate to the passage of cold fronts and closed lows and are typically associated with CVA. Areas of descent coincide with CAA, whilst CVA and ascending motion are enhanced downwind of the front or trough (Risbey et al 2009a). Jet-streaks display greater intensity in winter. Divergence in their poleward exit quadrant, along with CVA in mid-levels results in rising motion (Sturman and Tapper 2006) and is a common ascent mechanism in winter. In addition, the highest mean winter precipitation totals result from types demonstrating convergence at 850 hPa and trajectories of warm, moist air from tropical latitudes (T6 and T8).

In summer, the southwards movement of the STR sees southern Australia under the influence of a band of high pressure, associated with the descending branch of the Hadley Cell. Accordingly, frontal systems associated with the mid-latitude westerly wind belt are pushed south of Australia. Instead, downstream anticyclones and ridging enhance WAA and entrainment of tropical moisture. The warmer seasons are indicative of higher PW and weaker ascent (Milrad et al 2014). Areas of low-level convergence that are present in the dominant summer types, indicate positive vertical velocity and, in addition to strong WAA, provide an ascent mechanism, in the absence of the CVA present in winter (Risbey et al 2009a).

In all seasons, interaction between tropical and extra-tropical systems (Wright 1989), tropical moisture pathways, and vertical ascent profiles with low-level (upper-level) convergence (divergence) (Gyakum 2008) are highlighted as important factors generating precipitation ≥ 10 mm, confirming trajectory analyses conducted by McIntosh et al (2007) and Chubb et al (2011). In a

similar way, event precipitation isotope analyses conducted by Callow et al (2014) identified significant synoptic-type variability in the isotopic signature of precipitation in the Snowy Mountains. The results of this study further support the dominance of moisture-source pathways in controlling isotopic variability in this region.

It is acknowledged that using daily variables may mask some of the contributions of sub-daily systems such as pre- and post-frontal flow to precipitation over the region (Gallant et al 2012), and excludes multi-day and multi-type events. Accordingly, slow-moving synoptic systems may be over-represented. However, when considering synoptic-scale circulation, which generally operates on time-scales of a few days, the use of daily variables is considered appropriate (Pook et al 2006; Sturman & Tapper 2006; Barry & Carleton 2001). In addition, the nature of the composite plots may result in some features in the synoptic-scale circulation becoming masked (Milrad et al 2014). Highly variable precipitation, complex terrain and relatively low density gauge network in the SILO dataset, may all contribute to interpolation errors. Extensive testing and comparison of the SHL and SILO datasets have been used to quantify the uncertainty in using these interpolated precipitation data. This has permitted construction of a continuous daily precipitation record for the Snowy Mountains region; such a record is considered to be essential for compiling a long-term climatology (Chappell and Agnew 2001).

4.5 Summary

In summary, this novel application of an established synoptic clustering method has demonstrated that synoptic typing can be successfully based on atmospheric variables throughout the depth of the troposphere. The higher number of types in this study compares well with other automated typing schemes, which have generally produced more types than manual methods, with more subtle differences between types (e.g. Newton et al 2014a, b; Plavcova et al 2014; Kidson 2000). Although the k-means technique has been widely used in synoptic classifications, this is the first time that it has been applied to multi-level and multi-parameter gridded meteorological data. It has revealed the complex 3-dimensional nature of synoptic-scale circulation, including the importance of the influence of moisture pathways from tropical latitudes in the generation of high precipitation totals. Although synoptic types delivering inflow-generating precipitation have moisture sources in all oceans surrounding Australia, those with tropical connections are consistent in delivering the highest precipitation totals in all seasons. The spatial distribution of precipitation associated with synoptic types has implications for water resources management (Newton et al 2014a, b; Frei & Schär 1998) in this region.

The synoptic-typing method applied in this study allows long-term and climatologically significant periods to be examined, enabling a robust investigation of the impacts of synoptic circulation on the hydroclimate of the Snowy Mountains region. In addition, it provides a method for linking regional scale precipitation data to synoptic-scale atmospheric circulation. The following chapters in this thesis will investigate temporal variability (from intra-seasonal to inter-decadal) of the synoptic types in relation to inter-annual drivers of climate variability. Increased understanding gained from this climatology has implications for water resource availability and management in regional areas, and this method could be readily applied to other hydroclimate studies and to other regions worldwide.

Chapter 5. Trends in synoptic circulation and precipitation 1958-2012

This chapter is based on the manuscript *Theobald, A., H. McGowan, and J. Speirs, (2015): Trends in synoptic circulation and precipitation in the Snowy Mountains region, Australia, in the period 1958–2012, Atmospheric Research, 169, pp 434-448.*

This study builds on results presented in Chapter 4 by describing the temporal variability of the synoptic types over the period 1958–2012. Results from trend analyses for synoptic type precipitation, frequency and intensity are presented in this study for a range of timescales (daily, monthly, seasonal and annual). Analysis of extreme precipitation events and step changes is also presented. In addition, this study begins to assess the influence of large-scale climate drivers on synoptic types.

5.1 Introduction

The overall drying trend observed across SEA in recent decades, which culminated with the Millennium Drought, also affected the Snowy Mountains with the lowest annual inflow on record in 2006. Given the importance of inflow-generating precipitation in the Snowy Mountains discussed in Chapter 3, analysis of long-term temporal variability of precipitation-generating synoptic systems is critical to improve understanding of naturally variable precipitation patterns in the region, the causes of variability, and how these may be affected by current and future climate change.

Previous studies have investigated trends in overall cool-season (April-October) precipitation in the Snowy Mountains (Fiddes et al 2014; Chubb et al 2011). Consideration of the season as a whole however, can mask important month-to-month variations, with precipitation declines in SEA largely occurring early in the cool-season during austral autumn months (MAM; Delworth and Zeng 2014; Cai and Cowan 2013; Gallant et al 2007). Conversely, prior to the Millennium Drought, increased annual rainfall was observed between 1910 and 1990 over much of eastern Australia, linked to positive rainfall trends during summer months (November–March; Suppiah and Hennessey 1998; Nicholls and Lavery 1992). Significant increases in the proportion of precipitation from extreme events were reported during the 20th Century across eastern Australia (Alexander and Arblaster 2009; Hennessy et al 1999). For example, an increase in rainfall >95th percentile occurred in all seasons except winter when considering average rainfall across Australia. For New South Wales, a significant 31% increase in 99th percentile autumn rainfall and an increase in 90th percentile summer rain of up to 33% were reported. Whilst not statistically significant, the increase in summer rain was hydrologically important, and occurred in conjunction with a significant increase in the number of summer rain days (Hennessy et al 1999).

Trends in climate drivers known to affect precipitation across SEA are a key factor in the variability of precipitation-bearing synoptic systems. Noted features associated with the positive trend in the SAM (Murphy and Timbal 2008; Marshall 2003) include a poleward shift in the mid-latitude westerly storm tracks and strengthening of the EAC, leading to warming in the Tasman Sea. Both are proposed as mechanisms for increasing summer precipitation in SEA (Gallant et al 2012; Shi et al 2008; Cai et al 2005). Integral to SAM is the position of the STR. Delayed northward movement of the STR during the austral autumn since 1975 has impacted the passage of westerly winds over SEA, reducing precipitation at this time of year (Whan et al 2014; Cai and Cowan 2013; Murphy and Timbal 2008). Furthermore, the STR has exhibited a poleward expansion of approximately 0.5° per decade since 1979. Climate models predict continued intensification and a mean position further south for the STR, and continued positive trends in SAM, over the 21st Century, with associated decreased (increased) winter (summer) rainfall in SEA (Whan et al 2014; Timbal and Fawcett 2013; Post et al 2012).

Increased frequency and severity of El Niño events and fewer La Niña events, since the mid-1970s have been linked to decadal climate variability throughout the Pacific Ocean (Trenberth and Hoar 1996), which co-varies with, and modulates ENSO. Together, these factors may partially explain recent decreases in SEA rainfall (Gallant et al 2007). Whilst there has been no significant trend in ENSO since the 1950s (Harrison and Chiodi 2010), phase changes have occurred in the ENSO-like PDO. In the late 1970s, the PDO switched from a sustained negative to a sustained positive phase

(Garreaud and Battisti 1999). More recently, a switch back to a negative phase occurred in the late 2000s (McGowan et al 2009), with an overall negative trend from the late 2000s to 2014 when 6-year moving averages are used (Newman et al 2016). Although there has been a return to positive phase conditions since 2014 (http://research.jisao.washington.edu/pdo/PDO.latest), this is beyond the timespan of the analyses in this thesis. Model predictions show continued intensification of the ENSO cycle with longer dry spells interspersed with periods of increased precipitation (Alexander and Arblaster 2009). An upward trend towards more positive IOD values has occurred since the 1950s (Cai et al 2013), and is a likely contributor to winter and spring precipitation declines across SEA (Ummenhofer et al 2009a, b).

Rainfall projections for the Snowy Mountains catchments for 1°C of global warming (compared to the global average temperature in 1990), expected by 2030, indicate this region will experience drier dry periods (-8% or -35 mm for 10^{th} percentile rainfall), drier conditions on average (-3% or -25 mm for median rainfall), and wetter wet periods (+3% or +40 mm for 90^{th} percentile rainfall) (Post et al 2012), with regards to annual precipitation over the period 1958-2012. The magnitude of the projected changes increases for 2°C warming by 2070 (Post et al 2012). For median precipitation, this represents a decline of 6% (or -51 mm) in annual precipitation. For extreme wet (90^{th} percentile) precipitation an increase of 5% (+67 mm) is expected, whilst for the extreme dry projection, annual precipitation is expected to decline by 16% (-70 mm). Similar magnitude projections are given for SEA as a whole (Reisinger et al 2014; Sturman and Tapper 2006).

In addition to the widely studied cold front and closed-low weather systems, the synoptic typology presented in Chapter 4 found a strong emphasis on tropical moisture pathways from oceans to the north-east and north-west of Australia for delivering inflow-generating precipitation to the Snowy Mountains region. A high degree of intra-annual variability is present in the synoptic classification of weather systems. Winter and spring are typically the wettest seasons, when precipitation is heavily influenced by the interaction between the prevailing mid-latitude westerly airflow and orographic effects (Chubb et al 2011; Ummenhofer et al 2009a; Cai and Cowan 2008; Pook et al 2006), and frontal and closed-low systems dominate. However, Chapter 4 revealed the importance of warm-season precipitation for the generation of inflows, with more than 40% of precipitation days $\geq$ 10 mm occurring during the warmer months (November-March). During these months, inland heat troughs prevail and high intensity precipitation associated with trajectories of warm, moist air from tropical latitudes is common.

This study focuses on investigating temporal trends of the synoptic types described in Chapter 4, allowing recently observed precipitation declines to be placed in context of longer-term hydroclimate variability spanning the period 1958-2012. In addition, this study sheds light on the

impact of future precipitation regime changes on the hydroclimate of the Snowy Mountains due to climate change.

The chapter is structured in the following manner. Section 5.2 describes the data and methods, including descriptions of the synoptic types used throughout this study. The results of the trend analyses are presented in Section 5.3. A Discussion and Summary are presented in Sections 5.4 and 5.5 respectively.

5.2 Data and methods

Precipitation data refer to those described in Chapter 4 for days on which ≥ 10 mm was recorded. In addition, the same data sources were used to calculate all days on which ≥ 1 mm was recorded, as a reference against which to compare trends in inflow-generating precipitation. Synoptic types are those described in Chapter 4, section 4.3.1, and are typically separated by synoptic time scales (i.e. a few days). Only approximately 3% of classified days occur with the same type on consecutive days.

5.2.1 Trend Analyses

Temporal trends in synoptic type precipitation, frequency, intensity and extreme values (> 90th percentile) are obtained using least squares regression, and statistical significance assessed using the non-parametric Mann-Kendall test at the 90% or 95% level throughout (Cinco et al 2014; Risbey et al 2013; Almazroui et al 2012; Alexander et al 2010; Meneghini et al 2007). In a similar method to Chubb et al (2011) and Alexander et al (2010), precipitation intensity was calculated as the total precipitation (≥ 10 mm) from each synoptic type in a particular month, divided by the number of days on which that precipitation fell, resulting in a type-specific average intensity for each month.

Whilst linear trends can mask shorter term variability (Alexander et al 2010), they provide an overall assessment of change, and in conjunction with step change analysis can provide information on the timing of changes (Risbey et al 2013). Step changes in precipitation amount and frequency were assessed using the RHtestsV4 software package (Wang and Feng 2013; Wang 2008a, b). This is well-tested and freely available (http://etccdi.pacificclimate.org/software.shtml). The method used in this study is based on the penalised maximal *F* test (PMF) for mean shifts in a time series without a trend change, which can identify multiple heterogeneities in a time series (Wang and Feng 2013; Alexander et al 2010; Wang 2008a, b). The PMF test was used to identify 'type 1' changes, namely those that are statistically significant without supporting metadata. The software accepts data with normally-distributed Gaussian errors, and requires precipitation data to be log-transformed prior to analysis (Wang and Feng 2013). For the purposes of this study, it was not

necessary to correct the time series for any inhomogeneity, but simply identify the timing of any changes.

The physical mechanisms behind the precipitation trends were examined using the same ECMWF reanalyses data used to define the synoptic types (Chapter 4, section 4.2.1). Linear trends and their significance were calculated at each grid point within the analysis area for a number of key meteorological variables, and plotted as contour maps. Data were standardised on a monthly basis (i.e. by subtracting the monthly mean and dividing by monthly standard deviation) over the full study period using the z-score method to remove much of the seasonal cycle. A strong seasonal signal is apparent in the meteorological data for the Snowy Mountains region, and it is therefore important to remove this cycle in order that the synoptic types better reflect daily changes in the atmospheric circulation (Yarnal 1993). This process has been successfully demonstrated in previous studies (e.g. Gao et al 2014; Jiang 2011; Wilks 2006; Kidson 2000; Yarnal 1993). Accordingly, the trends presented in Section 5.3.3 and Figure 5.9 focus on the sign and significance of the changes, rather than their absolute magnitude (Meehl et al 2005). Initial analyses of these spatial trends focus on precipitation days for the entire period of study. Further spatial trends were then calculated for each synoptic type on a monthly basis (not shown).

5.2.2 Climate indices

ENSO can be represented by either its oceanic (Oceanic Niño Index, ONI) or atmospheric (Southern Oscillation Index, SOI) component. The SOI is chosen for this study because it has higher correlation with Australian precipitation (Maher and Sherwood 2014; Risbey et al 2009b). The SOI is represented by the data available from http://www.bom.gov.au/climate/current/soihtm1.shtml. Warm (El Niño) and cold (La Niña) episodes were determined based on a threshold of ± 8.0 sustained for at least three months (Murphy and Timbal 2008).

The IOD is represented by the Dipole Mode Index (DMI; Saji et al 1999), calculated as the difference in SST anomalies between the western (50 – 70°E, 10°S – 10°N) and eastern (90 – 110°E, 10°S – Equator) Indian Ocean (http://www.jamstec.go.jp/frcgc/research/d1/iod/e/iod/dipole_mode_index.html). Values are normalised by the standard deviation and phases are based on a threshold of ± 1 standard deviation or sustained anomalies ± 0.4°C for at least two months during May to November (Ummenhofer et al 2011; Meyers et al 2007).

The monthly SAM index of Marshall (2003; available at http://www.antarctica.ac.uk/met/gjma/sam.html) is used in this study. This index has been shown to

be robust prior to commencement of satellite data availability in 1979 (Ho et al 2012), and is available for the full period of this study. Positive and negative phases are based on a monthly threshold of ± 1 standard deviation (Marshall et al 2012).

Positive and negative phases of each teleconnection were determined according to the above criteria in the monthly indices described above. For each phase, mean monthly precipitation for the corresponding period and from each synoptic type was calculated.

5.3 Results

Precipitation Trends

For completeness, and as a reference against which trends in inflow-generating precipitation can be assessed, results are also included for days on which any precipitation ≥ 1 mm was observed.

5.3.1 Annual Trends

Overall, the annual number of precipitation days ≥ 1 mm and 10 mm (including contributions from all synoptic types) has decreased over the study period at a rate of -3.6 days per decade (non-significant) and -1.4 days per decade (significant only at the 80% level, p=0.13) respectively (Figure 5.1a). Considering the annual precipitation from all precipitation days ≥ 1 mm, a non-significant negative trend of -13.1 mm per decade is found, whilst the annual precipitation associated with ≥ 10 mm days demonstrates a non-significant positive trend of +5.7 mm per decade (Figure 5.1b).

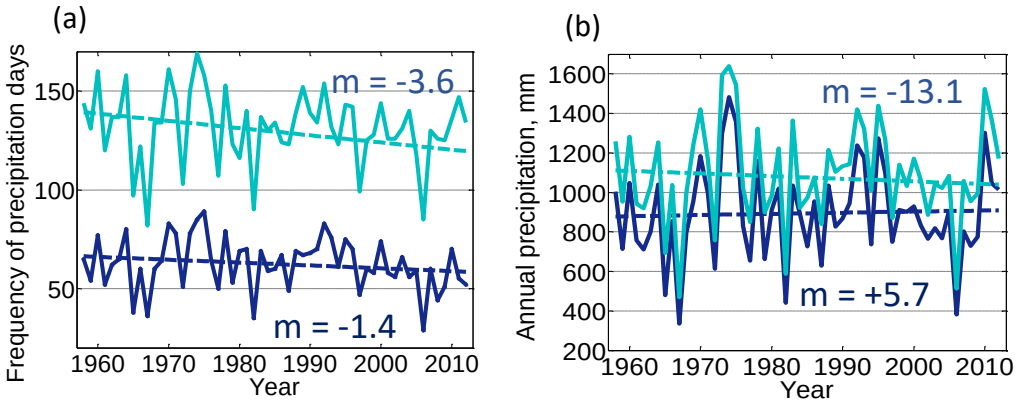

Figure 5.1 (a) Annual frequency of occurrence of all precipitation days ≥ 1 mm (cyan line) and precipitation days ≥ 10 mm (dark blue line); (b) annual precipitation of all precipitation days ≥ 1 mm (cyan line) and precipitation days ≥ 10 mm (dark blue line). Trends per decade, m, are shown.

5.3.2 Seasonal Trends

Warm season trends (calculated from November–March, with the year referring to January-March) in frequency of occurrence of +0.82 and +0.30 per decade are found for precipitation days ≥ 1 mm and ≥ 10 mm respectively (both non-significant). Negative frequency trends occur in the cool season (April–October) of -2.1 and -1.7 per decade respectively (both significant at 90%, Figure 5.2a).

Considering seasonal precipitation, positive trends of +14.3 mm and +18.2 mm per decade are found for precipitation days ≥ 1 mm and ≥ 10 mm respectively during the warm season (both non-significant, Figure 5.2b). The historically wetter months throughout the April to October cool season demonstrate a mixture of both positive and negative trends. Overall cool season trends however of -9.3 mm and -8.4 mm per decade are found for precipitation days ≥ 1 mm and ≥ 10 mm respectively (both non-significant, Figure 5.2b). Interestingly, trends in extreme days (> 90th percentile) are positive for both warm and cool seasons, however, they are more pronounced during the warm season (+3.6 mm (significant at 80%, p = 0.12)) and +0.8 mm (non-significant) per decade respectively (not shown).

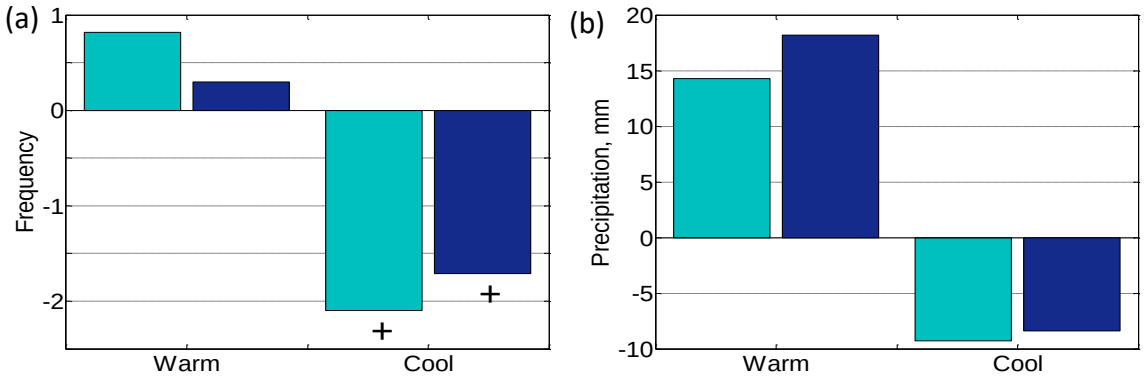

Figure 5.2 Seasonal trends (per decade) in (a) frequency of occurrence of all precipitation days ≥ 1 mm (cyan bar) and precipitation days ≥ 10 mm (dark blue bar); (b) precipitation on all days ≥ 1 mm (cyan bar) and days ≥ 10 mm (dark blue bar). Crosses indicate trends significant at 90%.

5.3.3 Monthly Trends

In order to determine the specific timings of trends outlined in the previous sub-sections, and in previous studies (e.g. Cai and Cowan, 2013), particular attention is paid to monthly trend analyses. Monthly frequency of each synoptic type is shown in Figure 5.3.

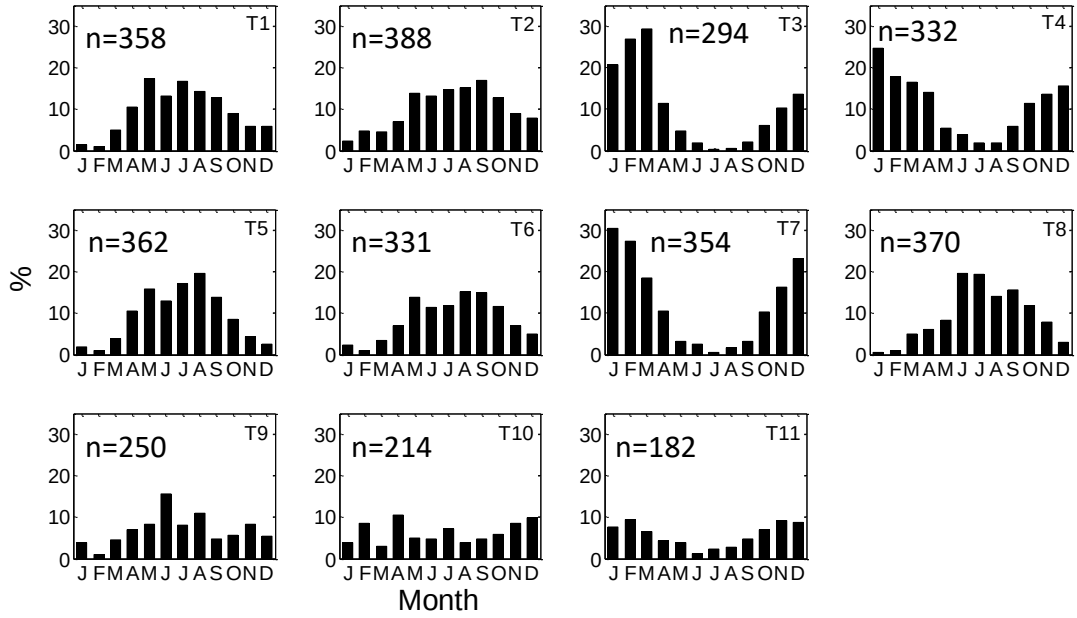

Figure 5.3 Monthly frequency of each synoptic type as a percentage of total occurrences of all synoptic types over the study period 1958-2012. The total number of occurrences, n, is also shown.

Results of the trend analysis applied to monthly precipitation accumulation, intensity (defined in Section 5.2.1), and frequency are shown in Figures 5.4, 5.5 and 5.6. Evaluation of trends for each synoptic type for the period 1958–2012 indicate five significant trends in monthly precipitation accumulation, at the 90 or 95% confidence level. These statistically significant trends in monthly precipitation accumulation are summarised below in conjunction with precipitation intensity and frequency (statistical significance shown in brackets).

- January – T3 (inland heat troughs aligned N-S) precipitation increase (95%; Figure 5.4) corresponds to significant increases in both intensity (Figure 5.5) and frequency (95%; Figure 5.6).
- May – whilst individual synoptic type precipitation trends are not significant, the cumulative precipitation total of all types display a significant decline (90%; Figure 5.4), with a corresponding significant negative trend in frequency (95%; Figure 5.6).
- June – T5 (pre-frontal troughs) precipitation increase (90%; Figure 5.4) corresponds to increases in precipitation intensity (90%; Figure 5.5).
- July – T11 (inland heat troughs aligned NW-SE) precipitation decline (90%; Figure 5.4) corresponds to decreases in intensity (Figure 5.5) and frequency (both 90%; Figure 5.6).
- October – cumulative precipitation from all synoptic types has declined (90%; Figure 5.4), caused by a decrease in cumulative frequency (90%; Figure 5.6).

With the exception of January, the warm season months of November to March (late spring to early autumn) have experienced non-significant increasing precipitation from all synoptic types combined. In all months, precipitation amount from days ≥ 1 mm demonstrate trends of the same sign as precipitation amount from days ≥ 10 mm.

Precipitation intensity across all synoptic types has increased cumulatively in nine out of twelve months, with only April, May and October experiencing declines (Figure 5.5). There is a consistent trend of more intense rainfall (as defined in section 5.2.1) during November–March. Intensity of precipitation days ≥ 1 mm has increased significantly in August (95%) and September (90%), and decreased significantly in April (90%). Frequency of precipitation days ≥ 10 mm has decreased in 7 out of 12 months, with notable decreases in autumn and spring months (Figure 5.6). Implications of decreased frequency of precipitation days and decreasing intensity are likely to exacerbate the effects of lower precipitation in these months, including reduced runoff. These trends are reflected in all precipitation days ≥ 1 mm (with the exception of January, August and December), and are consistent with the decline in annual precipitation days (Figure 5.1a).

With the exception of March, these trends remain when a shorter analysis period 1958–2009 is considered, thereby eliminating any influence of the strong 2010–2011 and 2011-2012 La Niña events.

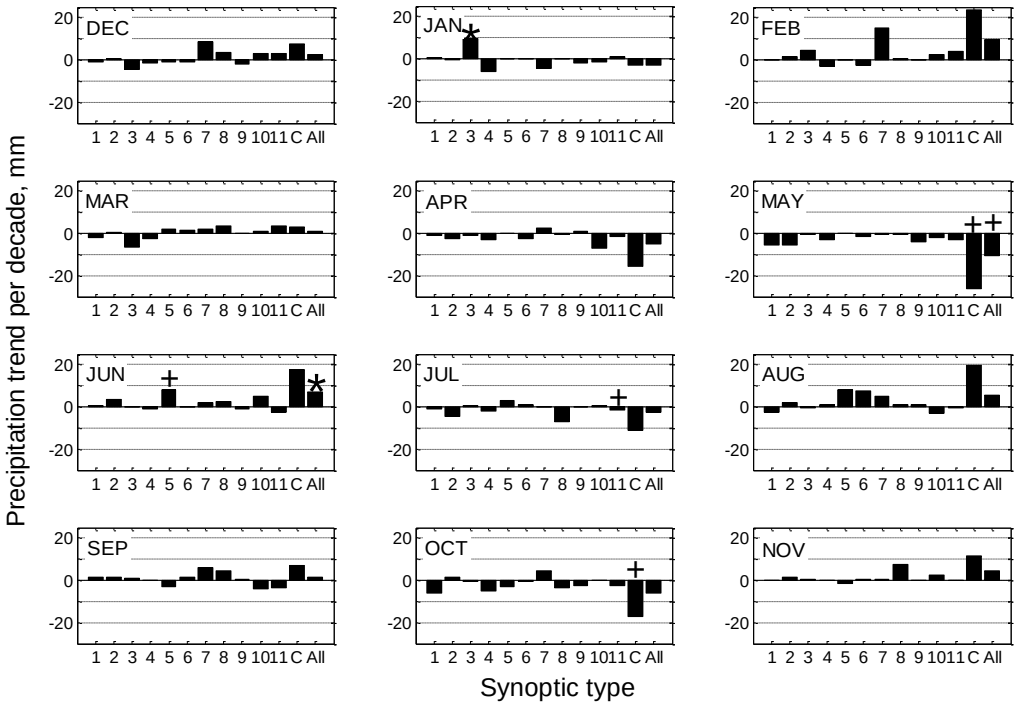

Figure 5.4 Linear trends in monthly precipitation accumulation per decade (precipitation days ≥ 10 mm) for each synoptic type (1 – 11), precipitation from all synoptic types combined, C, and precipitation from all days ≥ 1 mm, All. Asterisks (crosses) indicate significance at 95% (90%).

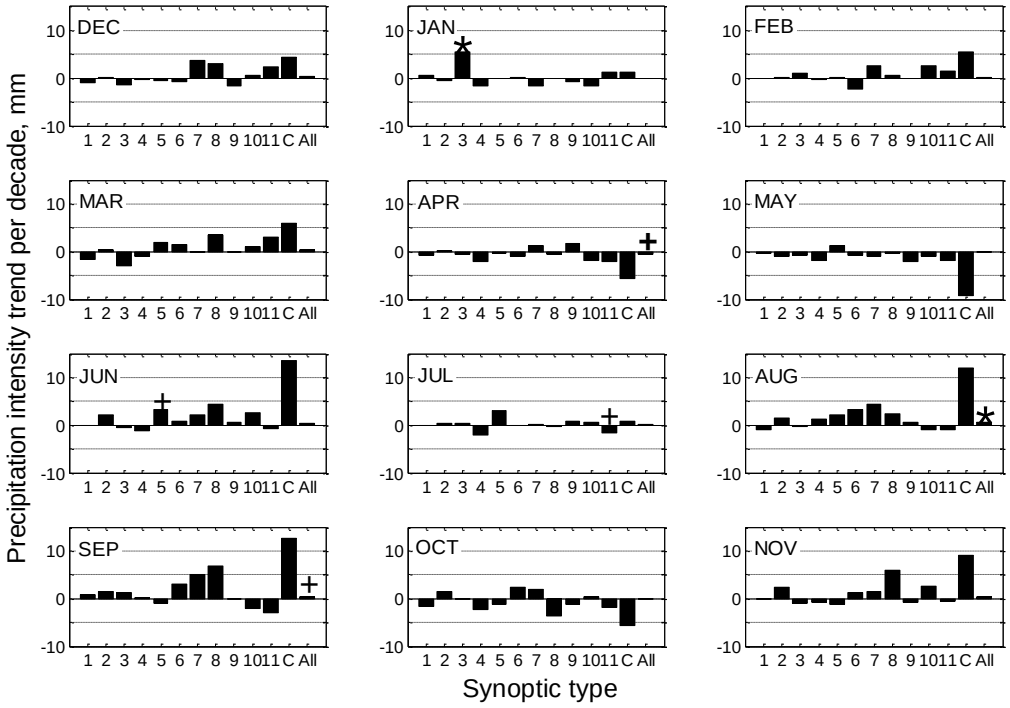

Figure 5.5 As Figure 5.4, but for precipitation intensity trends per decade.

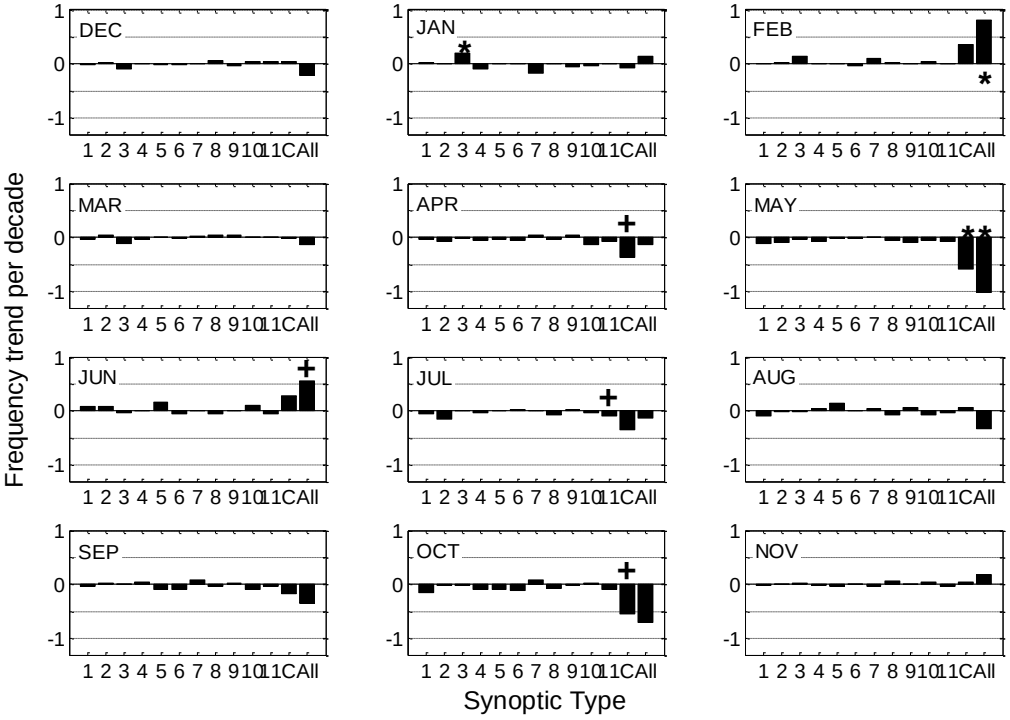

Figure 5.6 As Figure 5.4, but for frequency trend per decade.

5.3.4 Daily Trends

When considered on a daily basis, there is a highly significant increasing trend in the precipitation ≥ 10 mm from all synoptic types of +0.43 mm per day per decade (p<0.01; Figure 5.7), whereas daily precipitation ≥ 1mm displays a negligible highly non-significant trend of +0.14 mm per decade (not shown). The significant trend in daily, but not in annual, precipitation could be an effect of relative sample sizes. However both timescales show increasing trends for precipitation ≥ 10 mm per day.

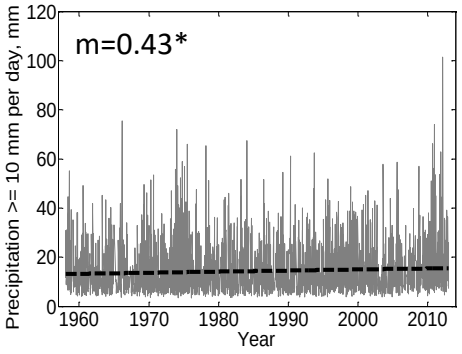

Figure 5.7 Daily precipitation associated with precipitation days ≥ 10 mm. Trend per decade, m is shown, with an asterisk denoting significance at 95% level.

5.3.5 Trends in 90th percentile precipitation

Given the increase in precipitation from days on which ≥ 10 mm is observed, trends in upper decile days are calculated (> 90th percentile, based on all data) to provide an indication of extreme precipitation events (referred to as "extreme day" hereafter). Figures 5.8(a) and (b) show that both the frequency and associated precipitation of extreme days display linear increases over the analysis period of +0.41 per decade (non-significant) and +1.8 mm (significant at 90%) per decade respectively. Figure 5.8c compares the percentage frequency of each synoptic type occurring during precipitation days ≥ 10 mm and extreme days, and indicates the main synoptic types responsible for driving these extreme days are T6, T7 and T8 (18%, 15%, 14% of extreme days respectively). These three types stand out as having strong tropical moisture pathways from warm oceans north-west of Australia to the Snowy Mountains (Figure 4.7).

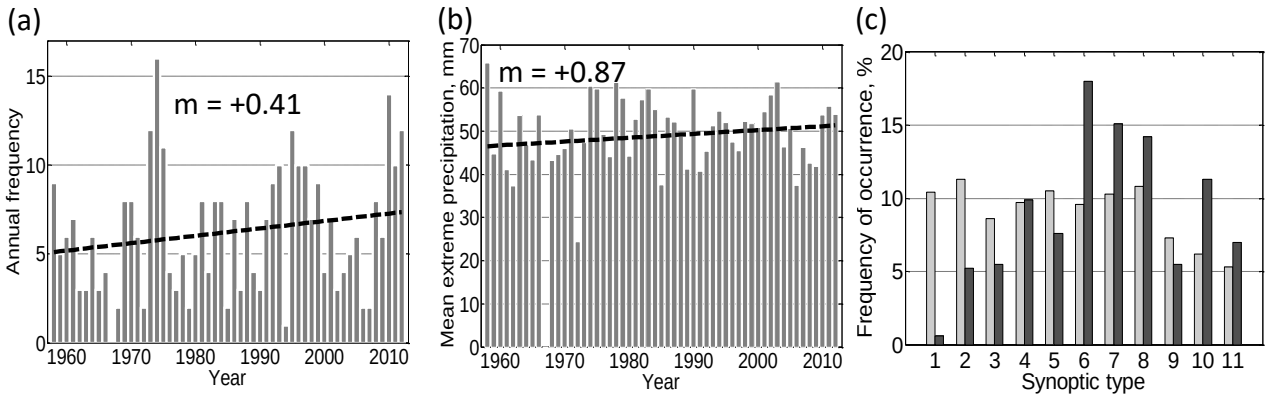

Figure 5.8 (a) annual frequency of days on which 90th percentile is exceeded; (b) mean daily precipitation in each year, mm, from days on which 90th percentile precipitation was exceeded, and (c) frequency of occurrence of each synoptic type on precipitation days ≥ 10 mm (light grey) and days on which 90th percentile precipitation was exceeded (dark grey), %. Trends per decade, m are shown.

5.3.6 Step changes

Step changes were calculated for monthly precipitation accumulations for each synoptic type using the RHtestsV4 software (Wang and Feng 2013; Wang 2008a, b), and are shown in Table 5.1. In this study, the precipitation record is based on the mean of several stations which diminishes any potential effects of changes in instrumentation in identifying step changes. Inspection of gauge records reveals that a number of high resolution, heated precipitation gauges were added to the network from 2004 onwards. Four gauges were decommissioned between 2010 and 2011 and replaced with new gauges at the same sites. Prior to 1975, an increased amount of interpolated Patched Point Data (PPD; Jeffrey et al 2001) data is included in the daily precipitation record. None of these periods are apparent in the step changes listed in Table 5.1, and it is therefore considered unlikely that the steps identified are non-climatic.

Where significant trends in monthly precipitation exist and no step changes are identified, the trend can be inferred to have occurred continually over the period of the analysis. Analysis of the step changes show that the majority occurred in the years prior to and during the Millennium Drought, consistent with Risbey et al (2013) who found that most step changes in SEA occurred in the early 1990s and around 2000. The remainder occur in the late 1960s and early 1970s, consistent with shifts in the STR, SAM and an increased rate of global warming at that time (Murphy and Timbal 2008). A possible relationship between downward trends in embedded cold fronts (T1) and increasing positive trends in SAM and STR is explored further in Chapters 6 and 7. In particular, the September and October downward step changes in T1, and downward steps in T7 and T11 are

likely to have contributed to the overall decline in cool-season precipitation reported in previous studies.

There is an approximately equal number of decreasing and increasing steps. With the exception of T5, all synoptic types exhibiting upward step changes have strong tropical connectivity and reflect positive trends in humidity along tropical moisture pathways.

Table 5.1 Timing of change-points identified in the monthly precipitation time series. Italicised entries denote change-points corresponding to a linear trend of the same sign. Entries in bold denote a corresponding significant trend of the same sign. Letters in brackets denote corresponding step-changes in frequency (F) and intensity (I).

Synoptic Type	Change-points (upwards)	Change-points (downwards)
T1		Jan 1992 (I), Sep 2002, *Oct 2002 (I)*
T2	*Jun 1969*	
T3	***Jan 1991***	
T4		*Jan 1997 (F)*
T5	***Jun 1989*** *(F)*	
T7	*Mar 1997 (F, I)*	Jun 2002 (I)
T8	*Sep 1997*	
T11		*Oct 1973 (I)*

5.3.7 Trends in meteorological variables

Spatial trends in the standardised meteorological variables for all precipitation days are shown in Figure 5.9. Considering all months simultaneously, statistically significant increases in MSLP are found over northern and Western Australia, extending south into the Southern Ocean. Significant declines in MSLP in the region of the Great Australian Bight and to the south of Australia are evident, and suggest a deepening trough to the south of the continent.

A statistically significant negative trend in atmospheric thickness is found along important moisture pathways for the Snowy Mountains, in line with decreasing temperatures in the mid-levels of the troposphere. Positive trends in thickness are found over the Tasman and Coral Seas, and over the Southern Ocean to the south-west of the analysis area, coinciding with a warmer atmosphere in these areas.

Significant positive trends in relative humidity are found over much of the Australian continent between 850–500 hPa, with the increase extending from tropical latitudes. Significant negative trends in relative humidity are located over much of the Southern Ocean and Tasman Sea between

850 and 500 hPa levels. With the exception of small regions in the far north-west and south-west of the analysis region, these trends are largely reflected by trends of the same sign and similar extent in absolute (specific) humidity (not shown), indicating that the relative humidity trends are not necessarily driven by temperature effects.

Significant negative (cooling) temperature trends are found over much of the continent throughout the 850–500 hPa layer, and are especially evident at 850 and 700 hPa. Areas of significant warming are located in the SW of the analysis area, over the Southern Ocean at all levels; and over the Tasman (850–500 hPa) and Coral Seas (850 hPa).

To further investigate possible reasons for the precipitation trends, spatial trends for the same variables shown in Figure 5.9 were calculated for each month (not shown). During May and October, warming trends between 850 and 500 hPa and an increase in atmospheric thickness (1000-500 hPa) over the Snowy Mountains region suggest a more stable atmosphere with limited opportunity for convection. Also in May, an increasing (though not significant) trend in MSLP over eastern Australia extends from northern Australia. This pattern, along with a decrease in subtropical moisture transport, and associated WAA, is conducive to less precipitation and supports findings of Cai and Cowan (2013) of a poleward expansion of the subtropical dry zone.

The cumulative precipitation decreases in January, April and July have in common a positive trend in atmospheric thickness and a decline in humidity along moisture pathways. Those months with increasing precipitation (Figure 5.4) consistently demonstrate lower MSLP, lower temperatures between 850-500 hPa, and increasing humidity in the Snowy Mountains region, indicative of increased cloud cover. Positive trends in relative humidity are not confined to one particular season. Although most warm season months (except January) display this trend, it is also apparent in June, August and September.

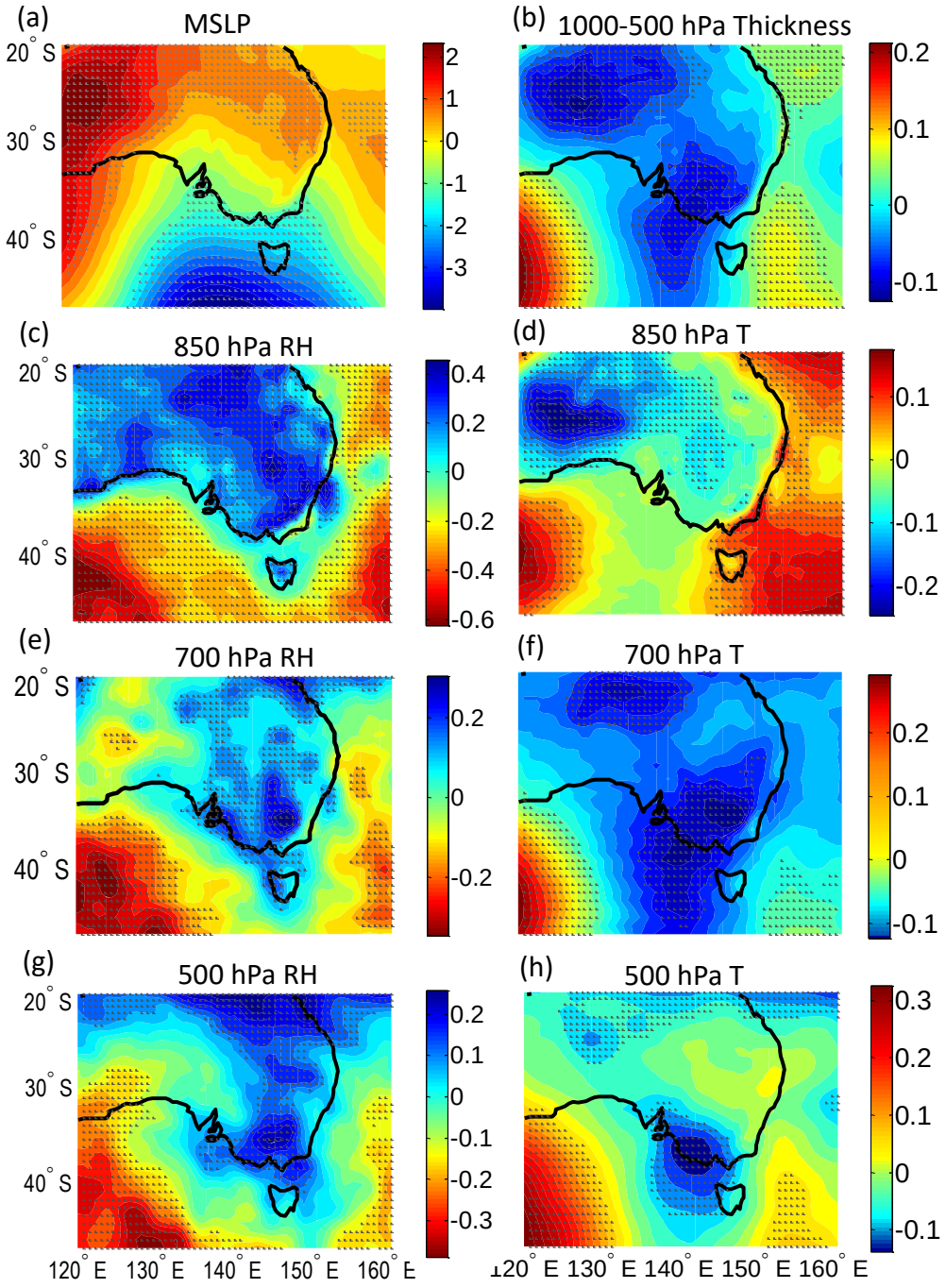

Figure 5.9 Spatial trends in (a) MSLP; (b) 1000 – 500 hPa thickness; (c, e, g) humidity, RH; and (d, f, h) temperature, T (coloured contours) over the analysis area shown in Figure 3.1(a), for all precipitation days ≥ 10 mm. Significance at 95% level is shown as stippled areas. Note that for humidity, positive (negative) trends are depicted by blue (red) colours.

5.3.8 Relationship with large-scale teleconnections

Table 5.2 shows the average value of each teleconnection for each synoptic type for precipitation days ≥ 10 mm, and for extreme high precipitation days (> 90th percentile). The analysis demonstrates that the La Niña-like state of ENSO (positive SOI), with warm SSTs in the western tropical Pacific Ocean plays a key role in driving synoptic types that generate precipitation totals ≥ 10 mm, and extreme events. Mean positive SOI values are found during extreme precipitation days for all types except T5. In particular, high SOI values are found for T3, 4, 7, 8 and 9, where low-level north or north-easterly winds entrain moisture from the Coral or Tasman Seas (Figure 4.6). Mean values for T1 should be interpreted with caution given just two occurrences of this synoptic type during extreme high days. The two synoptic types (T1, T5) with negative average SOI values (indicative of El Niño conditions) are embedded cold front and pre-frontal types which have a moisture source in the Southern Ocean with no direct tropical connection.

Table 5.2 Mean teleconnection value (ENSO (SOI), IOD (DMI) and SAM) associated with each synoptic type, and number of occurrences, n, for precipitation days ≥ 10 mm and days exceeding 90th percentile (in brackets). DMI values were calculated for May–November only. Asterisks indicate values that are significantly different from each other and random clusters.

Synoptic Type	SOI	DMI	SAM	Absolute frequency, n
1	-0.25 (5.65)*	0.08 (0.09)	-0.69 (-1.50)*	358 (2)
2	0.90 (0.81)	0.07 (-0.06)	-0.01 (-0.33)	388 (18)
3	1.85 (4.64)	0.10 (0.05)	0.30 (0.40)*	294 (19)
4	0.73 (5.01)	0.09 (0.02)	0.08 (0.65)*	332 (34)
5	-0.30 (-0.98)*	0.11 (0.16)	-0.37 (-0.25)*	362 (26)
6	1.19 (0.29)	0.06 (0.12)	-0.11 (0.07)	331 (62)
7	0.75 (4.28)	0.15 (0.19)*	0.20 (0.28)*	354 (52)
8	1.61 (3.42)*	0.04 (-0.01)*	-0.19 (0.14)	370 (49)
9	1.00 (3.27)	0.08 (0.14)*	0.14 (0.17)	250 (19)
10	1.27 (1.27)	0.10 (0.04)	0.25 (-0.08)*	214 (39)
11	0.62 (2.31)*	0.09 (0.15)	0.04 (-0.28)*	182 (24)
			Total days:	3435

A clear relationship exists between SAM and synoptic types representing cold frontal systems, with types T1, T2, T5, T6, and T8 associated with a negative mean SAM value (Table 5.2). A similar pattern is found for extreme days (T1, T2 and T5). In addition, extreme days associated with T10 and T11, where low level moisture is entrained along tropical and Southern Ocean pathways, display mean negative SAM values. Dominant summer types (T3, T4 and T7) are associated with positive mean SAM values (Table 5.2), consistent with the enhancement of moist easterly onshore

flow (Murphy and Timbal 2008; Shi et al 2008; Meneghini et al 2007) and greater influx of moisture from NWWA (O'Donnell et al 2015) during the warm-season.

While most synoptic types are related to a mean "wet" (La Niña) phase of ENSO, the mean DMI value is positive, indicative of the "dry" phase of the IOD (Table 5.2). A similar relationship between precipitation days and positive mean values of the DMI was found by Verdon-Kidd & Kiem (2009a). The influence of negative IOD phases becomes apparent for precipitation > 90th percentile associated with T2 and T8, both of which have a strong northwest tropical moisture pathway at 700 hPa. The strongest relationships between the known "wet" phases of the drivers occur with the SOI and SAM.

Mean monthly precipitation during positive and negative phases of ENSO, IOD and SAM is shown in Table 5.3. These data indicate on a broad scale how precipitation varies in accordance with different teleconnection phases and combinations. Whilst mean precipitation is not calculated here on a seasonal basis, the IOD is only considered for the May–November period and as such demonstrates a seasonal dependency of precipitation on IOD. Analysis reveals that similar patterns exist between precipitation days ≥ 1 mm and ≥ 10 mm. Individually, the highest monthly totals occur during negative IOD events, followed by La Niña phases. The lowest average monthly totals are received during El Niño events, followed by positive phases of IOD and SAM. The combination of negative IOD phase and La Niña observes three times as much precipitation (on average) than positive IOD phases and El Niño. Overall the highest (lowest) mean monthly precipitation is a result of the combined effects of La Niña (El Niño) and negative (positive) IOD, consistent with Meyers et al (2007). Relatively high monthly mean precipitation is also experienced when La Niña occurs in combination with negative SAM phase, and for combinations of SAM with negative IOD phase.

These analyses shed light on the complex inter-relationships between teleconnections and precipitation in the Snowy Mountains region of SEA, and the need for combined analyses of all teleconnections. The trend towards positive IOD events since the 1950s (Cai et al 2013) and longer, more frequent El Niño events (Gallant et al 2007) may in part be related to the decline in the annual number of precipitation days (Figure 5.1a). A number of years (1965, 1967, 1982 and 2006) stand out as having fewer precipitation days ≥ 10 mm (Figure 5.1a) and coincide with periods of below average rainfall related to El Niño events (Gallant et al 2012) in addition to a positive IOD event in 1967. Similarly, 1974, 1975 and 1992 experienced high numbers of precipitation days coinciding with La Niña events, and the two La Niña events of 2010–2012 are reflected in an increase in annual precipitation days after a period of sustained lower frequency since the early 2000s. The

increase (decrease) in precipitation during most warm (cool) months is likely related to the continued positive trend in SAM.

Table 5.3 Mean monthly precipitation across all elevations combined (for precipitation days ≥ 1 mm and ≥ 10mm), for positive and negative phases (± 1 σ) of ENSO, IOD and SAM. In addition, mean monthly precipitation for combinations of ENSO, IOD and SAM are also included.

Phase	Mean monthly precipitation, mm days ≥ 1mm	Mean monthly precipitation, mm days ≥ 10 mm	Number of months
El Niño	74.3*	57.9*	87
La Niña	111.4*	94.3*	86
IOD +	82.3*	64.1*	81
IOD -	140.4*	119.4*	21
El Niño & IOD +	67.0*	51.3*	31
La Niña & IOD -	176.4*	155.5*	4
SAM +	81.4	66.2	83
SAM -	94.4	75.1	92
SAM + & La Niña	85.5	74.3	26
SAM - & La Niña	106.5	86.8	18
SAM - & El Niño	89.3	64.9	22
SAM + & El Niño	82.5*	59.7*	13
SAM + & IOD -	104.4	83.2	3
SAM + & IOD +	78.9	58.6	12
SAM - & IOD –	125.8	102.3	4
SAM - & IOD +	81.4*	66.3*	10
		Total months considered = 455	

5.4 Discussion

The synoptic climatology on which this study is based (Chapter 4) revealed the complex three-dimensional nature of atmospheric circulation responsible for inflow-generating precipitation, and the importance of considering multiple levels through the troposphere. The identification of critical moisture pathways originating in the tropical oceans to the north-east and north-west of Australia, and over the Southern Ocean supports previous trajectory and isotope studies in SEA (Callow et al 2014; Chubb et al 2011; McIntosh et al 2007), and confirms the importance of tropical moisture influx for the generation of precipitation totals ≥ 10 mm.

This study has examined synoptic and precipitation trends relating to precipitation days ≥ 10 mm, however extreme precipitation days (> 90th percentile) and all precipitation days ≥ 1mm are also presented for context. The multi-decade trend analyses offer detailed insight into the precipitation regime of the Snowy Mountains.

Overall, this study finds a decline (1958–2012) in the total number of precipitation days ≥ 10mm and an increase in precipitation on these days, suggesting that precipitation in this region is becoming more intense. Precipitation intensity increases in both cool and warm seasons. This is in accordance with widely reported climate change projections of fewer, yet more intense precipitation events in a warming climate (Fischer et al 2014; Stocker et al 2013 2013; Zappa et al 2013; Landvogt et al 2008; Ghassemi and White 2007; Meehl et al 2005; Alpert et al 2002). Similar trends have been detected in studies from the USA, in association with increasing temperature and humidity since the 1950s (Gillies et al 2012; Rasmussen et al 2011).

Precipitation trends in the Snowy Mountains since 1958 show significant reductions during the autumn and spring transition months, with an overall decline in cool-season precipitation amount and frequency of precipitation days ≥ 1 mm and ≥ 10 mm. This study sheds light on synoptic processes leading to the reduction in cool-season precipitation during the Millennium Drought. In particular, significant declines in monthly precipitation and frequency of all synoptic types combined are observed in May and October, with a step change (decrease) in the dominant cold front synoptic type T1, in September and October 2002. The cold fronts associated with T1 are typically embedded in the mid-latitude westerly storm-track, and in addition to other synoptic types with a low-level moisture source over the Southern Ocean are more typically linked to negative phases of SAM. Given projected continued positive trends in SAM in winter, it is expected that precipitation from embedded cold frontal systems will continue to decline, with their frequency maxima further south (Catto et al 2014; Grieger et al 2014; Whan et al 2014). Meanwhile, the SAM trend is likely to contribute to continued increases in summer precipitation of tropical origin.

The October precipitation decline is also likely to have a marked effect on inflow generated from snow-melt. During spring months as much as 50% of annual inflows to rivers in the Snowy Mountains are generated, when rain on snow events flush snowmelt into streams and rivers (McGowan et al 2009). Wise et al (2015) describe the importance of precipitation during cool season transition months for areas of the western USA, where a similar reliance exists on snowmelt for annual water supply. A statistically significant decline in May precipitation for all synoptic types combined and an increasing trend in MSLP over much of the synoptic analysis area, demonstrate a trend in precipitation patterns towards drier conditions at this time of year. This supports a poleward shift of the subtropical dry-zone and dry-season precipitation regimes from northern Australia (Delworth and Zeng 2014; Cai and Cowan 2013) as a proposed mechanism for lower autumn precipitation. The lack of step-changes in May suggests that the changes have occurred more gradually over the analysis period.

Positive trends in overall precipitation frequency, amount and intensity are found for the warm season as a whole and most warm season months, for precipitation days ≥ 10 mm and all days ≥ 1 mm. These trends are largely influenced by dominant warm-season inland heat troughs associated with synoptic types T3 and T7. Step changes (increases) in warm season precipitation from summer-dominant inland heat trough types T3 and T7 are evident from 1991 and 1997 respectively. These synoptic types display strong tropical connectivity and align well with positive humidity trends along their moisture pathways. These results provide further evidence that the historic pattern of precipitation in SEA may be shifting towards a regime with increasing warm-season precipitation, with associated consequences for water storage replenishment (Verdon-Kidd et al 2013). Similar observations of increasing rainfall during spring and summer in south-west Western Australia by Bates et al (2008) indicate larger-scale precipitation regime changes. Cooling temperature trends at the 500 hPa level, and increasing humidity between 850 and 500 hPa, during most warm months (November–February) coincide with increasing trends in precipitation amount, and indicate that this warm season precipitation will increasingly be convective, in a cooler, more unstable mid-level atmosphere. In turn, convective precipitation is largely associated with high intensity precipitation which has been shown to have adverse effects including flash flooding and soil erosion in Mediterranean catchments (Vallebona et al 2014).

The timing of most downward change-points prior to and during the Millennium Drought, is consistent with Risbey et al (2013), who found step reductions in SEA rainfall in the early 1990s and around 2000. In their study the reduction was closely associated with cutoff circulation and cold fronts on the western slopes of the Snowy Mountains region. This suggests that fundamental changes in atmospheric circulation occurred at this time.

The high inter-decadal variability of precipitation in this region means that any trend analysis reflects the period chosen (Risbey et al 2013). However, by considering a multi-decade period, this study allows for example, short-term, drought-related trends to be placed in the context of longer-term climate variability. The period chosen for this study encompasses anthropogenic climate forcing (Reisinger et al 2014; Gallant et al 2012). It also includes the multi-year Millennium Drought, several shorter, though equally intense droughts and one of the strongest La Niña events on record that broke the Millennium Drought in the summer of 2010–2011 (Verdon-Kidd et al 2013; Gallant et al 2012). The results presented in this study of increasing warm season precipitation are consistent with studies conducted prior to the Millennium Drought, which found similar trends over much of eastern Australia during summer months (Suppiah and Hennessey 1998; Nicholls and Lavery 1992). The inclusion of the recent drought period however, may offer insight into likely future precipitation trends, consistent with expansion of the subtropical dry zone,

and intensification of precipitation in a warmer atmosphere (Cai and Cowan 2013; Chiew et al 2011). Monthly trends in precipitation from all synoptic types remain robust when the analysis period is ended prior to the 2010–2012 consecutive La Niña events (thereby eliminating these events as possible causes of the trends), with the exception of March, when record 7-day precipitation totals were recorded in the Snowy Mountains (Bureau of Meteorology 2012). Accordingly, this study identifies potentially important precipitation regime changes such as the 2010–2012 La Niña events.

Noticeably fewer precipitation days (≥ 10 mm) occur in drought years such as 1967, 1982/83 and 2006 (associated with strong El Niño events) when record low rainfall was recorded in SEA (Verdon-Kidd et al 2013; Gallant et al 2012). This suggests that variability in synoptic circulation reflects patterns in large-scale teleconnections, in particular ENSO, with all types that display tropical moisture pathways having a positive mean SOI value.

Mean teleconnection values for each synoptic type provide insight into the complexity of determining the contribution of each teleconnection to precipitation in the Snowy Mountains region. For instance the average value of the IOD for each synoptic type is positive, whereas more precipitation days would be expected to be associated with a negative IOD. This may, in part, result from positive IOD events having greater amplitude and frequency than negative events throughout the IOD time series, and the observed positive trend in the IOD (Cai et al 2013). In addition, because precipitation anomalies usually begin to manifest prior to the May onset of IOD events, they cannot be said to be caused solely by the IOD, and may be more likely due to the forcing of other teleconnections (Murphy and Timbal 2008), offering further possible explanation for the positive DMI values shown in Table 5.2. The importance of the NW tropical moisture pathway in generating precipitation, however, is apparent in the mean monthly precipitation associated with negative IOD phases and combinations of a negative IOD with both La Niña and SAM shown in Table 5.3. An increase in the precipitation and frequency of extreme days has been associated with synoptic types T6, T7 and T8. These three synoptic types are concurrent with mean positive SOI values, with particularly strong mean positive values during T7 and T8 extreme days, indicative of a dominance of La Niña conditions. Similarly, extreme days classified as T8, often associated with north-west cloud bands, occur in conjunction with a negative DMI. Furthermore, areas of positive trends in humidity are aligned with critical moisture pathways from tropical latitudes.

It is acknowledged that more influences on SEA precipitation exist than have been examined in this study. For example the Pacific Decadal Oscillation and Madden-Julian Oscillation are also known to influence the frequency of precipitation-bearing synoptic patterns on long and short timescales respectively (Gallant et al 2012; McGowan et al 2009; Pezza et al 2007; Mantua and Hare 2002). In

addition, localised phenomena such as the annual cycle of the subtropical ridge (Murphy and Timbal 2008), strength and position of the subtropical jet-stream and SST anomalies in the Tasman Sea (Risbey et al 2009a, b) are purported to affect the seasonality of precipitation in SEA. Furthermore, the influence of each teleconnection on precipitation and synoptic circulation varies on a seasonal basis (e.g. Ding et al 2012), which is not examined in this study. The combined effect and relative influence of multiple drivers on precipitation variability in the Snowy Mountains region is the focus of Chapter 7.

Results presented here are consistent with previous regional (e.g. Chiew et al 2011; Alexander et al 2010, Alexander and Arblaster 2009) and global studies of fewer, more intense precipitation days. Similar responses have already been detected in the Mediterranean (Alpert et al 2002) and are predicted for the European Alps (Fischer et al 2014), North Atlantic and European regions (Zappa et al 2013) and South Pacific region (Caloiero et al 2015), due to changes in the hydrological cycle in a warmer climate.

5.5 Summary

Although not all trends in this study are statistically significant, it is likely that a precipitation response to climate change may already be occurring, even if not yet detectable statistically (Timbal and Fawcett 2013). Changes in synoptic circulation associated with precipitation days in the headwater catchments of the Snowy Mountains are likely to have had, and will continue to have significant impacts on inflow volumes. Implications for agriculture, environmental flows and water resource management stem from declines in shoulder season precipitation and subsequent compression of the cool season, as well as increasing extreme precipitation events. Minor changes to air temperature and precipitation have had substantial impacts on distribution of water resources in western Canada (Newton et al 2014a, b), and changes in both mean precipitation and extreme precipitation events have adversely affected global crop productivity in many countries (Lobell et al 2011; Gornall et al 2010). Declines have already been detected in wheat yields since 1990 in countries such as France (Lobell et al 2011) as well as Australia, where the onset of autumn rains necessary for crop sowing has been occurring later (Pook et al 2009). Hydrological effects of precipitation trends may also be experienced in the Snowy Mountains, where the timing of precipitation changes may increase the need for altered water management strategies. Furthermore, changes to any synoptic systems that generate snowfall have the potential to alter the snow season, adversely affecting alpine tourism and reservoir replenishment of the Snowy Mountains hydroelectric scheme. A study outlining the proportion of rain versus snow for each synoptic type is the subject of the following chapter.

This study represents the first long-term study of precipitation influences and trends in the Snowy Mountains region of Australia. The monthly analyses shed light on overall declines (increases) in cool (warm) season precipitation. Given the importance of precipitation in this region to agriculture, environment and industry, and the susceptibility of marginal alpine areas to climate change (Demiroglu et al 2016; Beniston 2003; Martin and Durand 1998), a comprehensive understanding of precipitation influences is critical for efficient water use and management, and is the subject of Chapter 7. Accordingly, this study may have relevance for regional water management and availability, as well as climate change impact and adaptation studies in similar areas worldwide.

Chapter 6. Determination of the proportion of rain versus snow for synoptic types

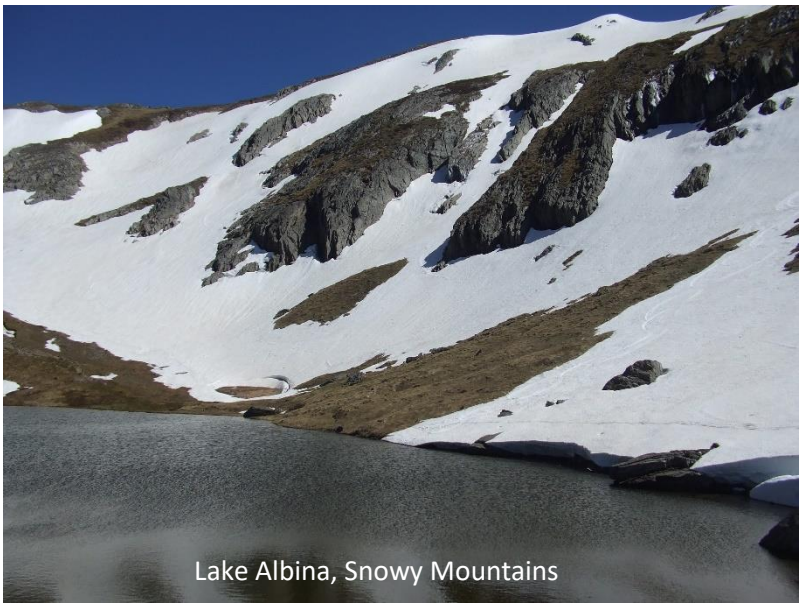

Following the description of the precipitation-bearing synoptic types and the total amount of precipitation they deliver (discussed in Chapters 4), this study seeks to determine the proportion of rain versus snow for each synoptic type. In conjunction with the synoptic type trends described in Chapter 5, implications for the snow season and water storage replenishment are discussed.

6.1 Introduction

The retention and release of water from snowpack is a key factor in maintaining the hydrological cycle in regions affected by seasonal snow cover. For example, widespread warming that has occurred across the western United States in recent decades has resulted in a greater fraction of precipitation falling as rain rather than snow, subsequently reducing the snowpack (Gillies et al 2012). The marginal nature of Australia's alpine regions makes the Snowy Mountains especially sensitive to climate change, particularly increasing temperatures. The snowpack is an important source of inflows to reservoirs in the Snowy Mountains with heavy, warm spring rains falling on top of the snowpack generating approximately 50% of total annual inflows to the hydroelectric catchments (Snowy Hydro Ltd 2003). Maximum snow depth, however, has declined by up to 15% since the 1960s, particularly in spring (Davis 2013; Nicholls 2005), and model predictions suggest that this trend will continue along with a reduction in the length of the snow season (Hennessy et al 2003, 2008). Declines in shoulder-season precipitation, identified in Chapter 5, suggest that this

trend may already be apparent, and are consistent with thaw dates believed to be occurring on average two days earlier per decade since 1954 (Green and Pickering 2009).

Measurement of solid precipitation is notoriously difficult (as discussed in Chapter 2, section 2.7), and the ratio of snow to liquid water is an important issue. Snowfall can be recorded in several ways: total solid precipitation, snow water equivalent, and snow depth. Snow depth however, is considered a better indicator of availability for inflow, and avoids some of the challenges related to precipitation gauge measurements.

Snowfall in the Snowy Mountains is synoptic in origin (Green and Pickering 2009). Winter orographic lifting in combination with westerly or north-westerly winds associated with the passage of cold fronts has been demonstrated as the major snow producing mechanism (Green and Pickering 2009; Budin 1985; Colquhoun 1978). Case studies from Colquhoun (1978) demonstrated that a cold NW-WNW airstream ahead of a cold front and westerly airstreams associated with the passage of a cold front are key synoptic patterns for generating snowfall. Any variations in the synoptic systems producing snowfall are therefore likely to affect both the amount and distribution of snowfall in the Snowy Mountains region (Green and Pickering 2009).

Occurrence of snow is strongly related to ambient air temperature (Pepler et al 2015; Feiccabrino et al 2013; Yuter et al 2006). Yuter et al (2006) showed that a daily maximum temperature threshold of 0.5°C produced a dramatic shift between rain and snow in the western United States, whilst a more recent study by Feiccabrino et al (2013) found that misclassified precipitation at sites across Sweden reduced by half when an air temperature threshold of 1.0°C was used instead of 0.5°C.

Snow depths in the Australian alpine regions have been shown to strongly decline during El Niño and/or positive Southern Annular Mode (SAM) events. In particular, significant correlations exist between SAM and maximum snow depth and length of the snow season. Furthermore, late winter and spring snow depth is influenced by the phase of the IOD (Pepler et al 2015). Spencers Creek snow depth in the Perisher Valley near the Australia alpine divide (Figure 6.1 and 3.1b) was found to have a strong relationship with the mean position of the subtropical ridge (Budin 1985). The combination of positive trends in SAM and the IOD (Cai et al 2009; Marshall 2003) and a poleward expansion of the sub-tropical dry zone (Whan et al 2014) over recent decades is likely to further exacerbate the snow depth decline.

This study built on this previous body of work by demonstrating that snowfall can be allocated to a distinct set of synoptic types, and suggests mechanisms by which the snowpack may alter due to the key changes in synoptic circulation discussed in Chapter 5.

6.2 Data

Daily maximum surface air temperatures were calculated using the temperature records from SHL gauges within the high elevation group (Figure 3.1b) where available, infilled with SILO data (Jeffrey et al 2001) to give a continuous daily record for the period 1958-2012 (thereby matching the synoptic classification in Chapter 4 and encompassing the length of the snow course records). Snowy Hydro Ltd operates three snow course sites (Figure 6.1, Table 6.1) where snow depth is measured at weekly intervals during the cooler months (April-November).

Table 6.1 Location and elevation of snow course sites operated by Snowy Hydro Ltd.

Snow course site	Latitude	Longitude	Elevation, m	Start date
Spencers Creek	36.43°S	148.35°E	1805	10/06/1954
Deep Creek	36.03°S	148.38°E	1609	03/07/1957
Three Mile Dam	35.88°S	148.45°E	1463	25/06/1955

Weekly snow depth measurements from Spencers Creek snow course from the start of 1958 to 2012 have been used in this analysis. This is the highest elevation of the three snow course sites thereby giving maximum possible recorded snow. Precipitation days and synoptic type classifications are those described in Chapter 4.

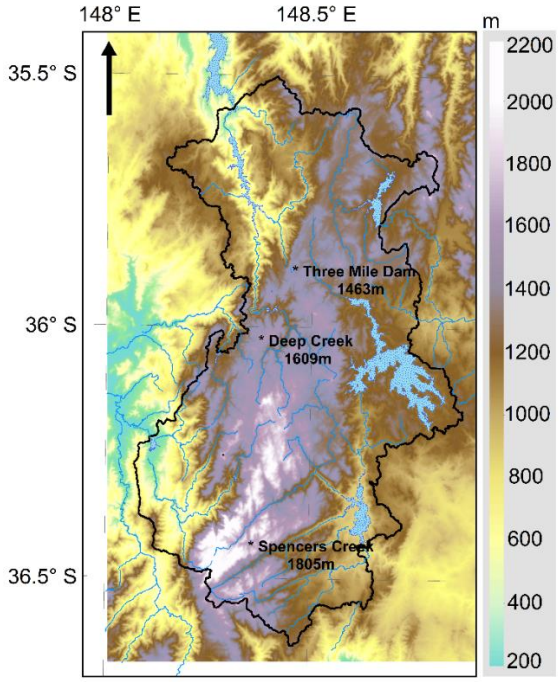

Figure 6.1 Location of the three snow course measurement sites operated by Snowy Hydro Limited.

6.3 Methods

Daily maximum temperature was extracted for each precipitation day (≥ 10mm) for the period 1958-2012, identified in Chapter 4. Following previous studies from the USA (Yuter et al 2006) and Sweden (Feiccabrino et al 2013), maximum daily temperature thresholds of 0.5°C and 1.0°C were tested. Since snow depth is recorded weekly (rather than daily), if the snow depth increased during the week that a precipitation day was observed it was inferred that this precipitation contributed to the snow accumulation. A comparison was made for precipitation days under each temperature threshold.

All precipitation days with daily maximum temperature < 0.5°C coincided with weekly accumulation in snow depth in the Spencers Creek snow record, however there were many other instances (28%) of increasing snow depth, i.e. the temperature must have been > 0.5°C, but snow fell. Conversely, for a daily maximum temperature of < 1.0°C, all precipitation days (except 6 out of a total of 315) coincided with increasing snow depth. It is noted also that the definition of a precipitation day (≥10mm) excludes the contribution of low precipitation events to snow depth and may account for some days of increasing snow depth. Local drifting of snow may have also contributed to increases in snow depth at Spencers Creek that were not associated with precipitation. In conjunction with local knowledge, a maximum daily temperature threshold of 1.0°C was therefore decided upon to differentiate between rain and snow.

6.4 Results

Over the period 1958-2012, approximately 10% of 3435 days delivering inflow-generating precipitation (≥ 10 mm) resulted in snowfall based on a maximum daily temperature threshold of 1.0°C, giving a total of 315 precipitation days that generated snowfall according to this criterion. The proportion of snow days allocated to each synoptic type is shown in Table 6.2, which also shows that the snow season extends between April and November. Figure 6.2 demonstrates the high inter-annual variability of annual maximum snow depth at Spencers Creek, and illustrates a noticeable decline in annual maximum snow depth since the early 1990s, consistent with previous studies, and the significant decline in cool season precipitation since that time. Fewer above average snow depth years, and none that exceeded +1 σ, are also apparent since the early 1990s.

Table 6.2 Proportion of inflow-generating precipitation days resulting in snow for each synoptic type between 1958 and 2012.

Synoptic Type	Precipitation days	Snow days	% Snow	Timing
T1	358	114	31.8	Apr-Nov
T2	388	96	24.7	Apr-Nov
T3	294	2	0.7	Jun, Oct
T4	332	2	0.6	Jul-Aug
T5	362	49	13.5	May-Sep
T6	331	8	2.4	Jul-Aug
T7	354	0	0	
T8	370	21	5.7	May-Aug
T9	250	18	7.2	May-Aug
T10	214	5	2.3	Jul-Aug
T11	182	0	0	
Total	3435	315		

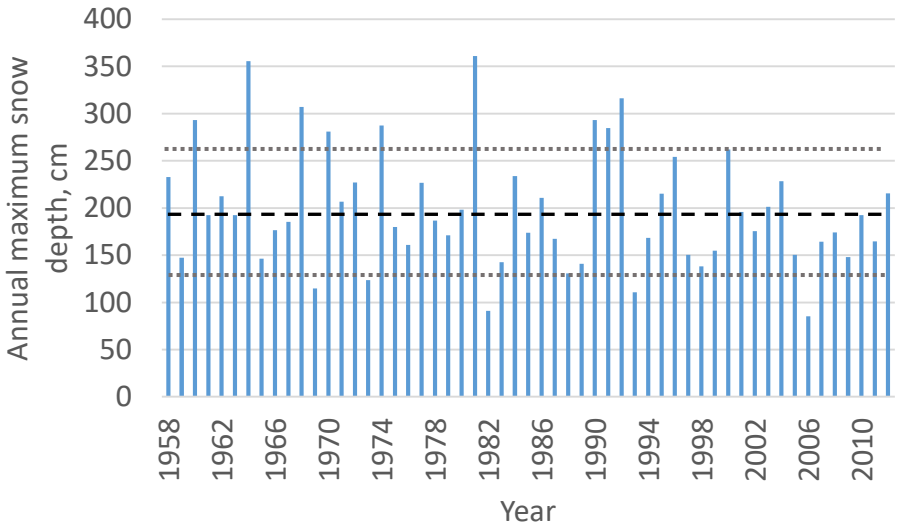

Figure 6.2. Annual maximum snow depth from 1958-2012 based on weekly snow depth observations from Spencers Creek snow course. Black dashed line indicates mean snow depth, and grey dotted lines indicate ± 1σ.

This study reveals that relatively few synoptic types result in the majority of snowfall. Synoptic types T1 (embedded cold fronts), T2 (closed lows) and T5 (prefrontal troughs) account for 82.3% of all snow days (when ≥10 mm precipitation was observed) for the period 1958-2012. Consistent with expectations, these synoptic weather systems are dominant cool season types which originate in the mid-latitude westerly wind belt. These systems have in common a low-level (850 hPa) moisture

source from the Southern Ocean and westerly-north westerly winds. A small percentage of snowfall results from north-west cloud bands (T8) with north-westerly winds, and offshore lows (T9) with prevailing south-south easterly winds. Overwhelmingly, the vast amount of snowfall is delivered by embedded cold fronts and closed lows between April and November. A trend analysis reveals that the annual frequency of T1 snow days has declined significantly (-3 days over the period 1958-2012), and faster than total T1 precipitation days (-2 days). Similarly, the annual amount of snow that embedded cold fronts deliver has significantly declined by -59.53 mm over 1958-2012 (> 99% significance), comprising much of the decline in total precipitation from cold fronts. Other synoptic systems result in snow only during more limited periods (T5 May–September; T8 and T9 May–August). No snow resulted from synoptic types T7 and T11, both of which are associated with strong warm air advection from tropical north-west Australia, with negligible amounts from those types dominant during warmer months (T3, T4 and T7).

6.5 Discussion

For precipitation days ≥ 10 mm, the snow season is shown to occur between April and November. The two main synoptic types responsible for delivering snowfall – embedded cold fronts (T1) and cutoff lows (T2), occur throughout this entire period. Consistent with expectations and previous studies (Chubb et al 2011; Colquhoun 1978), the majority of snow fall derives from synoptic types with a low-mid level westerly airflow, often with a west-northwest or northwest component (Figures 4.6-4.8). Whilst these synoptic types are not typically associated with the highest precipitation totals or greatest atmospheric moisture content (especially embedded cold fronts), low to mid-level airflow is perpendicular to the Snowy Mountains, forcing ascent and producing large vertical ascent of water vapour (Colquhoun 1978). Dominance of the mid-latitude westerly belt during winter months can ensure a persistent airflow from this direction, bringing extensive snowfall to western and higher elevations (Colquhoun 1978). The spatial distributions of precipitation across the Snowy Mountains catchments for types T1 and T2 (Figure 4.10) are consistent with this understanding.

Offshore lows (T9) deliver a small percentage of snowfall events per year. These systems are associated with cold southerly to south-easterly airstreams over the Snowy Mountains, which can produce snowfall to low altitudes in southern and central areas of New South Wales, with only lighter falls on the higher parts of the ranges (Colquhoun 1978). Again, this pattern is consistent with the spatial distribution of precipitation shown for synoptic type T9 in Figure 4.10. The attribution of snow to pre-frontal troughs, NWCBs and offshore lows during a shorter period covering May to September is largely consistent with their peak periods of occurrence shown in Figure 5.3, and with their dependence on the wintertime position of the westerly wind belt and STR.

Similar to the results of Gillies et al (2012), there is no overall decline in the total amount of inflow-generating precipitation over the period 1958-2012 (Chapter 5, Figure 5.1). However, declines in the frequency, as well as precipitation and intensity of the main synoptic types associated with snowfall (T1 embedded lows and T2 cutoff lows) are apparent during several months of the cooler months (Figure 5.4-5.6), notably in the shoulder seasons. Compared to overall precipitation from T1, a significant decline in the annual number of snow days associated with embedded cold fronts, and the amount of snow they deliver, has occurred over the period 1958-2012. This suggests that temperature effects described by Pepler et al (2015), and a faster decline in snow-bearing synoptic systems in a warming climate (Gillies et al 2012) are apparent in the Snowy Mountains. The declines in annual maximum snow depth in the Australian Alps identified by Nicholls (2005) between 1962 and 2001, and Davies (2013) during 2001-2010, particularly in spring are consistent with annual maximum snow depth data for Spencers Creek (Figure 6.2) and a decline in the spring frequency of embedded cold fronts (T1) identified in this study (Chapter 5, Figure 5.6). Positive values of SAM were associated with a strong decrease in Australian snow cover by Pepler et al (2015), and Budin (1985) found a very strong association between Spencers Creek snow depths and the mean position of the subtropical ridge. Whilst snowfall in this region displays high inter-annual variability (Figure 6.2), the dependence of the main snow-producing synoptic types on the mid-latitude westerly wind belt, and the trend towards increasingly positive values of SAM, along with the associated poleward migration of the STR suggests that the decline in occurrence of snow-producing synoptic types and snow depth will likely continue. Consequences for annual inflows to the headwater catchments of the Snowy Mountains are apparent, given that up to half of annual inflows have historically been generated from snowmelt (McGowan et al 2009).

This study, in combination with the trends discussed in Chapter 5, demonstrates that a decline in the frequency, precipitation and intensity of snow-producing synoptic types particularly during autumn and spring (Figures 5.4-5.6) combine to shorten the snow season, with potential adverse effects for the alpine ski industry. These results are consistent with predictions of continued snow depth declines in future (Hennessy et al 2003, 2008) and warming trends in alpine areas as a result of climate change (Demiroglu et al 2015; Pepler et al 2015). Earlier and faster snowmelt may eventuate from an increase in frequency and precipitation of synoptic types resulting in warm air advection from NWWA during spring months. In addition to increased precipitation during warmer months, subsequent effects exist for the temporal distribution of inflows throughout the year and associated water management.

The maximum daily temperature threshold method of delineating the occurrence of rain or snow does not take into account a cross-over range where both precipitation types may have fallen

simultaneously. However, this method and the threshold were chosen following a study that investigated the percentage of misclassified precipitation events based on different temperature thresholds (Feiccabrino et al 2013). As this thesis is not focussed solely on the rain versus snow debate, this method was considered satisfactory for the purposes of assigning snowfall to synoptic types. It is acknowledged that measurement of solid precipitation is notoriously difficult and may be affected by wind-blown snow at the snow course sites. In addition, the weekly resolution of snow depth measurements may mask some variability in the accumulation and ablation of the seasonal snow pack. Furthermore, small differences in surface wind direction may affect orographic enhancement, with subsequent impacts for snowfall and snow depth.

6.6 Summary

A distinct set of synoptic types deliver the majority of snowfall to the Snowy Mountains, all of which are associated with the mid-latitude westerly wind belt. Whilst previous studies have demonstrated that warming temperatures over the alpine area are an important driver of decreasing snow depth (Demiroglu et al 2016; Pepler et al 2015), this study has shown that in addition to any temperature effects, a decline in the frequency of the main snow producing synoptic types, and the precipitation they deliver, during autumn and spring is also a key driver of snow depth decline over recent decades. The trend towards more positive values of SAM, which forces the westerly wind belt polewards is likely to result in continued changes to snow-producing synoptic circulation (specifically a continued decline in embedded cold fronts) and further declines in snow depth over the Snowy Mountains. This will affect the timing of inflows to headwater catchments of the region and regional water availability, particularly during spring months - a critical time for water storage replenishment.

Chapter 7. Teleconnection forcing of precipitation-bearing synoptic types

This study builds on the results presented in chapters 4, 5 and 6 by shedding light on the causes of synoptic type variability in the historic record, and underlying physical mechanisms for synoptic circulation variability related to large-scale climate drivers. A novel application of a statistical technique is presented to quantify the relative influence of all climate drivers on synoptic type frequency. This study has recently been re-submitted as a manuscript to the Journal of Climate following peer review.

7.1 Introduction

Severe droughts, interspersed with flooding rains, are a natural feature of the Australian hydroclimate presenting significant challenges for water resource management and supply security. Understanding the drivers of such variability is therefore crucial. Developing understanding of the mechanisms that force precipitation variability in the Snowy Mountains region has gained attention over the past decade following an uninterrupted series of years with below median precipitation across SEA that comprised the Millennium Drought (1997-2009; Timbal and Fawcett 2013).

As discussed in Chapter 4, the Snowy Mountains climate is dominated by the hemispheric scale mid-latitude westerly wind belt during winter and by tropical moisture sources during warmer months. Specific synoptic patterns are therefore responsible for delivering precipitation at different times of year. Accordingly, synoptic type frequency is influenced by tropical and extra-tropical

modes of atmospheric variability including ENSO, PDO, IOD, SAM, as well as SSTs in the Tasman Sea (Gallant et al 2012; Schepen et al 2012; Kirono et al 2010; Risbey et al 2009b).

Effects of individual teleconnections on Australian rainfall are well documented. Positive phases of the SOI and negative phases of the IOD contribute to above average precipitation in SEA as a result of warmer SSTs and enhanced convection in the western tropical Pacific, and eastern tropical Indian Ocean respectively (Verdon-Kidd et al 2013; Gallant et al 2012; Timbal and Hendon 2011; Ummenhofer et al 2009a; Cai and Cowan 2008; Murphy and Timbal 2008). The impact of SAM is highly seasonal, with below (above) average winter (summer) precipitation for SEA during positive phases. Conversely, negative SAM phases in winter enhance the mid-latitude storm track, resulting in more frequent cold fronts crossing southern Australia (Whan et al 2014). In addition, anomalous SSTs in the Tasman Sea are reported to affect onshore moisture transport, and therefore precipitation, particularly in summer when precipitation can be enhanced by positive anomalies (Risbey et al 2009b; Shi et al 2008). Furthermore, lower frequency variability associated with the PDO, whilst not directly affecting the synoptic-scale circulation (Kiem et al 2003), influences precipitation variability via modulation of the ENSO cycle (McGowan et al 2009; Gallant et al 2007; Garreaud and Battisti 1999; Trenberth and Hoar 1996).

Importantly, the teleconnections do not act in isolation (Gallant et al 2012; Kiem and Verdon-Kidd 2011; Timbal and Hendon 2011), making knowledge of their combined influence critical to improving understanding of variability of precipitation-bearing synoptic types.

In the Australian region, particular combinations of teleconnection states are more likely to occur whilst others are infrequent. For example, La Niña events tend to co-occur with cool phases of the PDO and negative IOD (Meyers et al 2007) and vice versa – interactions which can reinforce wet or dry conditions over SEA. Conversely, out of phase SOI/PDO phases i.e. warm and cool phase, act to moderate effects on precipitation (Praskievicz and Chang 2009). On a seasonal basis, an El Niño and positive SAM in autumn indicate dry conditions over SEA, whilst a La Niña event (usually considered ‘wet’) in autumn can result in rainfall anomalies comparable to El Niño unless it occurs in conjunction with negative SAM (Chiew et al 2011; Kiem and Verdon-Kidd 2009a, 2011). The mechanism behind this relationship is not yet fully understood (Kiem and Verdon-Kidd 2011), however it may have similar origins to the negative correlation between La Niña SST patterns in the tropical western Pacific and SAM during JJA described by Ding et al (2012), which implies higher rainfall during negative SAM phases and La Niña. Furthermore, a positive SAM is found to co-occur with above average SSTs off the West Australian coast in summer and, in conjunction with poleward expansion of the subtropical ridge (Whan et al 2014), has been linked to increased

summer rainfall in northwest Western Australia (NWWA) over the last two decades (O'Donnell et al 2015).

Climate model projections show continued intensification of ENSO events with prolonged dry spells interspersed with periods of increasingly extreme precipitation (Cai et al 2014a; Alexander and Arblaster 2009). Moreover, upward trends towards more positive IOD and SAM values have occurred since the 1950s and 1970s respectively (Cai et al 2013; Murphy and Timbal 2008; Marshall 2003). The positive trend in SAM and strengthening of the EAC are proposed as mechanisms for the observed Tasman Sea warming in recent decades (Oliver et al 2014; Gallant et al 2012; Shi et al 2008; Cai et al 2005), and have likely contributed to increased summer precipitation in NWWA (O'Donnell et al 2015) and SEA respectively (Chapter 5). Similarly, background SST warming has occurred across the tropical western Pacific (Wang et al 2016) and tropical Indian Ocean (Alory et al 2007) since the 1950s and 1960s respectively.

Many studies have focussed on direct relationships between teleconnections and surface variables such as temperature, precipitation and streamflows (e.g. Kingston et al 2015; Bonsal & Shabbar 2013; Whitfield et al 2010), and several have investigated the extent to which teleconnections modify synoptic type frequency (e.g. Newton et al 2014a, b; Brigode et al 2013; Lorenzo et al 2007; Stahl et al 2006). Fewer have sought to identify the combined effects of teleconnections. For example, using ENSO, IPO, SAM and IOD as predictors, Kiem and Verdon-Kidd (2009a, 2011) demonstrated that single indices were rarely best at predicting seasonal rainfall, and that the combined state of the three oceans surrounding Australia is a key driver of rainfall variability in the southern Murray-Darling Basin. Similarly, stream flows across Victoria were shown to respond to the intensity of the STR and a tripole of tropical SSTs extending from the tropical Indian Ocean, to the central equatorial Pacific Ocean (Fiddes and Timbal 2016). Further studies have sought to attribute rain day occurrence or synoptic type frequency to a particular teleconnection phase (Gallant et al 2012; Verdon-Kidd and Kiem 2009a). These studies have developed a broad knowledge of dominant influences on SEA precipitation. However, a knowledge gap remains regarding quantifying the combined influence and relative contribution that each teleconnection makes to synoptic type frequency variability.

To address this knowledge gap, this study focuses on methods that reveal covariance of synoptic type-teleconnection relationships and assess relative influence of teleconnections. Results demonstrate that, depending on the moisture source region for the synoptic type, frequency appears to be modulated by the underlying phase of the PDO, and by the interaction between the tropical Pacific and Indian Oceans.

The chapter is outlined as follows. Sections 7.2 and 7.3 describe the data and methods respectively; Section 7.4 outlines the results and discussion. These are separated into tropical and extra-tropical sources of variability, and suggest possible physical mechanisms for the patterns found; a summary is given in section 7.6.

7.2 Data

7.2.1 Synoptic types

The synoptic classification of inflow-enhancing synoptic precipitation systems (determined as ≥ 10 mm) described in Chapter 4 is used here (1958-2012), and extended back to 1900 using the recently released ECMWF ERA-20C reanalysis dataset (http://apps.ecmwf.int/datasets/data/era20c-daily). ERA-20C spans 1900-2010 and uses the same analysis method as ERA-Interim. It assimilates surface observations only and uses new data assimilation methods to tackle the problem of observing system changes (Poli et al 2013). Although not as accurate as the established ERA-40 and Interim reanalyses, comparison of an overlapping period (1979-2010) between ERA-Interim and ERA-20C showed ERA-20C to be approximately 70% as accurate in classifying precipitation days. Whilst the limitations of using this dataset are acknowledged, importantly its availability at the same finer resolution as ERA-Interim and ERA-40 resolves surface features that coarser-scale reanalyses cannot. The synoptic type time series therefore spans 113 years, capturing multi-decadal variability. Each synoptic type (described in Table 4.2) was allocated subjectively to a group based on its dominant moisture pathway at 700 hPa, as shown by relative humidity in Figure 7.1. Types within the northeast (NE) group represent north-east inland troughs (T3) and easterly dips (T10), which transport moisture from the tropical ocean north-east of Australia. The northwest (NW) group contains closed lows (T2 and T6), inland heat troughs [those that interact with cold fronts (T4 and T7), and one that does not (T11)], as well as atmospheric circulation conducive to north-west cloud bands (T8). Embedded cold fronts (T1) and pre-frontal troughs (T5) are represented by the Southern Ocean (SO) group. Offshore lows (T9) form the Tasman group, and include lows that form directly offshore, as well as those with tropical (e.g. inland trough lows and ex-tropical cyclones) and extra-tropical (e.g. southern secondary lows) origins. Daily frequency of each of the four synoptic type groups identified was aggregated to standard climatological seasonal totals (summer (DJF), autumn (MAM), winter (JJA) and spring (SON)).

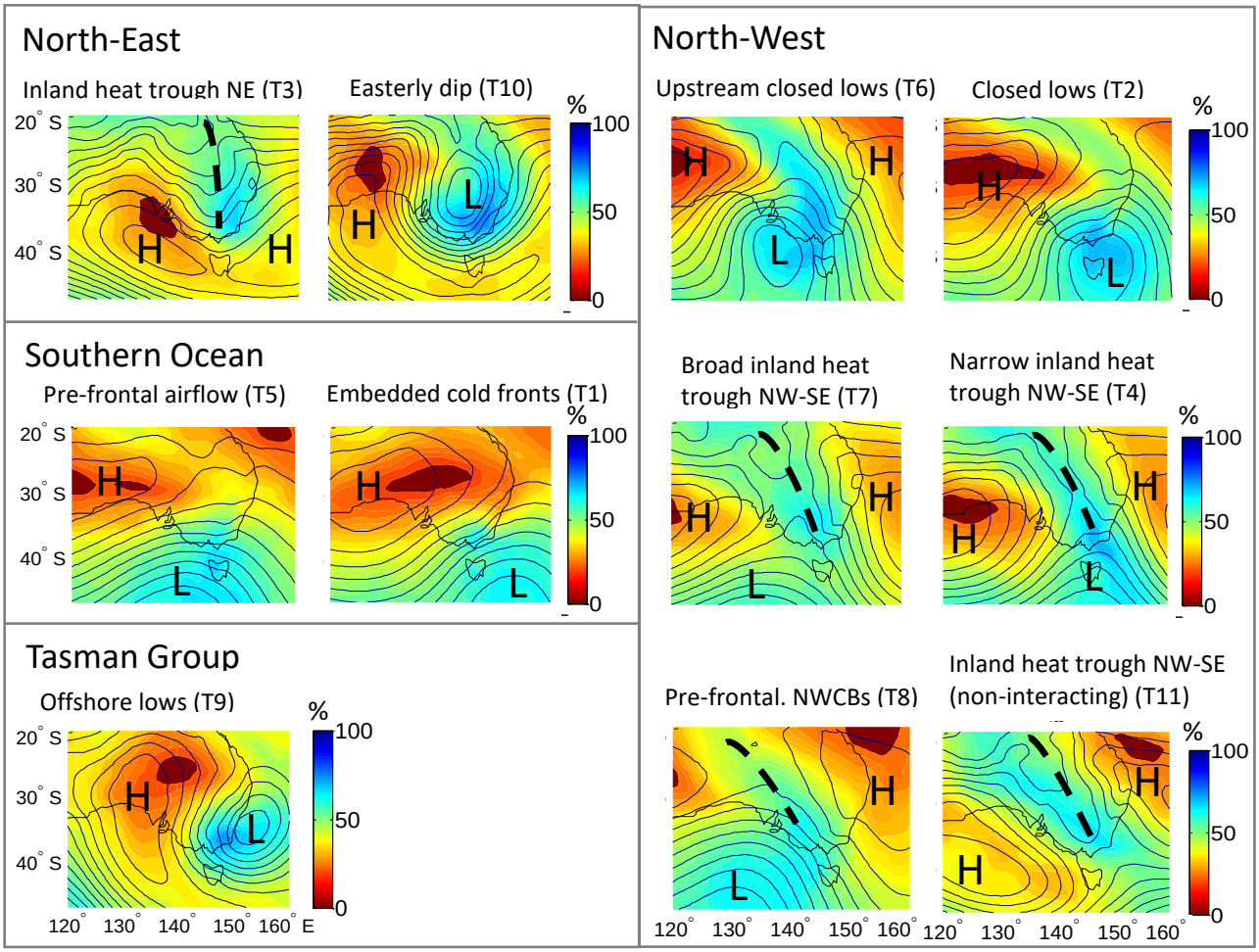

Figure 7.1 Grouping of 11 synoptic types based on relative humidity at 700 hPa (coloured contours, %). Mean sea level pressure pattern (line contours), surface high (H) and low (L) pressure regions, and trough lines (thick dashed lines) are also shown. This figure is a combination of ERA20, ERA40 and ERA Interim datasets.

7.2.2 Teleconnections

For the SOI and IOD, the indices used in this study are the same as those described in Chapter 5, section 5.2.2, but for the extended period 1900-2012. SAM is represented by the index of Marshall et al (2003) (www. antarctica.ac.uk/met/gjma/sam.html) for the period 1957-2012, and by the index of Visbeck for the earlier period 1900-1956 (Visbeck 2009; M. Visbeck, personal communication). Both of these indices are calculated using station-based observations. The two versions of SAM were compared for the period 1957-2005 and the correlation found to be excellent (R^2=0.86). In addition, the following indices are used to represent additional teleconnections known to influence precipitation variability in SEA.

A PDO index was obtained from the Joint Institute for the Study of the Atmosphere and Ocean (JISAO) (www.research.jisao.washington.edu/pdo). This index is defined as the leading principal

component of North Pacific monthly SST variability (poleward of 20°N). This index identifies the major phases of the PDO: 1923-1942 (warm; positive values), 1946-1976 (cool; negative values), 1979-1996 (warm) and a return to a cool phase after 2009.

SST anomalies (SSTA) in the Tasman Sea are represented by the Tasman Sea Index (TSI), calculated as the average SSTA for the Tasman Sea (30°S-40°S, 150°E-160°E; Schepen et al 2012; Murphy and Timbal 2008). Long-term monthly mean SSTs (for the whole analysis period) were subtracted from the monthly SST data to calculate the anomaly over the area described above, using data from ECMWF Interim, ERA-40 and ERA-20C datasets.

For all teleconnections, monthly index values were obtained for the period 1900-2012, and seasonal means calculated for DJF, MAM, JJA and SON. Although the IOD is not usually considered active in warmer months (November-April), Kiem and Verdon-Kidd (2009a) showed that several significant results exist in January between Victorian rainfall and IOD phase, and it is included in these analyses for completeness.

7.3 Methods

7.3.1 Synoptic types

Consistent with Schepen et al (2012), Kirono et al (2010), Risbey et al (2009b) and Verdon-Kidd and Kiem (2009a) for rainfall in regions of SEA, initial correlation analyses showed significant linear correlations between synoptic types and SOI (up to 31% variance), PDO (up to 25% variance), DMI (up to 34% variance), SAM (up to 38% variance) and TSI (up to 51% variance). These correlations remained when autocorrelation in the teleconnection time series was considered and thus only these teleconnection indices are considered further.

7.3.2 Boosted regression tree analysis

To assess the relative influence of each teleconnection on synoptic type frequency, a boosted regression tree (BRT) analysis was performed in R using the gbm library with the additional brt.functions package developed by Elith et al (2008). The BRT works in the same way as a conventional classification and regression tree (CART) analysis i.e. data are recursively partitioned based on a binary split of a predictor variable. Each split maximises the homogeneity of the resulting groups with respect to the response variable. Boosted regression trees are an extension of CART and were chosen in this study as a novel application of an established technique to assess the relative influence of each predictor variable (teleconnection indices) on the response variable (synoptic type frequency) for several reasons: their non-linearity assumption; ability to account for complex interactions between predictors; ability to fit the model with relevant predictor variables;

returning a percentage influence for each predictor (Elith et al 2008). For each synoptic group frequency, 452 consecutive seasons were modelled against the five teleconnection predictor variables described in Section 7.2.2, using a Poisson distribution suitable for frequency data. Three key parameters control the optimal model fit: 1) learning rate (*lr*) determines the contribution of each tree to the model. A slower *lr* is preferable as the contribution of each tree is shrunk, allowing the model to more reliably predict the response; 2) tree complexity (*tc*) controls the fitting of interactions, e.g. a *tc* of five fits a model with up to five-way interactions; 3) bag fraction specifies the proportion of data to be selected at each step, i.e. bag fraction=0.7 means that 70% of the data are randomly used for each iteration.

Learning rate and tree complexity determine the number of trees. Relatively small sample sizes, such as that used in this study (n=452) generally require a slower learning rate in order to reach the recommended minimum of 1000 trees. In accordance with Elith et al (2008) and others (e.g. Jouffray et al 2015), these parameters were sequentially altered to achieve the optimal model fit. Cross validation deviance (cv) and standard error (se) were used as an estimation of best fit, with the lowest values indicating the best model fit. The combination with the lowest values that produced the recommended minimum 1000 trees was then used to fit the final BRTs (Elith et al 2008; Jouffray et al 2015) for concurrent synoptic variability with lags up to 2 years in the predictor variables, in seasonal increments. These sub-annual timescales are investigated using BRTs as they can be unclear in wavelet analyses, which are better at revealing longer period variability. Learning rates of 0.01, 0.001, 0.0001 and 0.0005; *tc* from 2 to 5 (to allow for interactions between all predictors); and bag fractions from 0.5 to 0.9 were tested. Results are summarised in Table 7.1.

Regression trees find the predictor which best splits the data into two groups. The data is separated then this process is applied separately to each sub-group (Therneau et al 2013), and continues for all trees. The contribution, or relative influence, of each predictor to the response is determined by averaging the number of times each predictor determines the split, across all trees, and scaled so the sum adds to 100. Higher numbers indicate a stronger influence on the response variable (Elith et al 2008; De'Ath 2007). The BRT does not produce significance values, however the relative influence can be considered similar to a correlation coefficient (Elith et al 2008). Partial dependency plots show the effect of each predictor on the response variable after taking into account the average effect of other predictors.

Table 7.1 Optimal parameters and performance of the final boosted regression tree for each grouping of synoptic types. The lowest values of cross validation deviance (cv) and standard error (se) were used as an indicator of model performance with the lowest values indicating the best model shown here.

Synoptic group	Learning rate	Tree complexity	Bag fraction	Number of trees	cv	se
NE	0.0001	4	0.6	3200	2.000	0.062
NW	0.001	5	0.7	1300	1.981	0.079
SO	0.001	4	0.75	1100	2.681	0.098
Tasman	0.0005	5	0.7	1000	1.866	0.06

7.3.3 Wavelet analysis

Cross-wavelet analysis was used to characterise the relationship between seasonal synoptic type frequency and seasonal teleconnection indices over the period 1900-2012. Wavelet analyses examine relationships in time-frequency space. They determine periodicity in relationships through time, show concurrent and lagged relationships, and identify regions where two time series demonstrate high common power (Kingston et al 2015; Keener et al 2010; Grinsted et al 2004; Torrence and Compo 1998). Accordingly, they can be considered a correlation coefficient in time-frequency-space (Grinsted et al 2004). Importantly, wavelet analysis reveals the non-stationarity of relationships through time. All analyses were performed in Matlab using software available at http://noc.ac.uk/using-science/crosswavelet-wavelet-coherence. The software is based on an auto-regressive (AR)1 model, and was considered appropriate for the data in this study following autocorrelation analyses. Wavelet analyses have been demonstrated as appropriate for climate data in several studies (e.g. Kingston et al 2015; Grinsted et al 2004). All time series were first de-trended to ensure that results are based on actual relationships rather than artefacts of trends or the strong seasonal cycle. Each SAM index was detrended separately. For there to be a cause and effect relationship between two time series the oscillations should be phase-locked or slowly varying, e.g. the two time series are in anti-phase in all regions with significant common power across a particular periodicity (Grinsted et al 2004).

7.4 Results and Discussion

Composite maps of MSLP anomalies for positive and negative phases of each teleconnection were constructed using the ERA-20C and Interim datasets for the whole analysis period, and are shown in Figure 7.2. These represent the average MSLP conditions that can be expected during each phase.

For the purposes of this study, sub-annual timescales are periods less than one year, and describe BRT results; inter-annual and inter-decadal timescales span 1-9 years, and greater than 10 years respectively, and discuss wavelet results.

For wavelet plots, in-phase (anti-phase) coherence between a teleconnection and synoptic type frequency is indicated by arrows pointing right (left). Arrows pointing right also indicate zero phase lag, whereas arrows pointing up or down indicate ¼ phase lag and those pointing left a ½ phase lag. Lag time is a function of the period of the significant coherence: e.g. for coherence at two year periodicity, arrows angled down (up) represent a ¼ phase lag (i.e. ¼ of two years=six months) with series one (two) leading series two (one); horizontal arrows pointing right represent zero lag, and those pointing left represents a ½ phase lag (i.e. ½ of two years=one year) (Grinsted et al 2004). These properties are illustrated in Figures 7.3-7.6h.

Regions where the two time series share significant common power, and therefore co-vary significantly at the 95% level are indicated by the thick black lines in Figures 7.3-7.6c-g. Significance is determined using 1000 Monte Carlo simulations (Grinsted et al 2004). The thin curved line indicates the cone of influence (COI) outside of which relationships should be interpreted with caution. Only those significant regions exhibiting phase-locked or slowly-varying oscillations at a particular periodicity are discussed in the text and are highlighted by a white box in the corresponding figures. Regions shown as significant but where arrows change direction across the period, are not discussed, as these are not considered to have a cause and effect relationship (Grinsted et al 2004).

Whereas wavelet analyses can reveal relationships up to multi-decadal timescales, BRT offers the opportunity to explore relationships at shorter terms (sub-annual to annual; which can be difficult to discern in wavelet analyses), including the effect of the previous season's indices on concurrent synoptic type frequency.

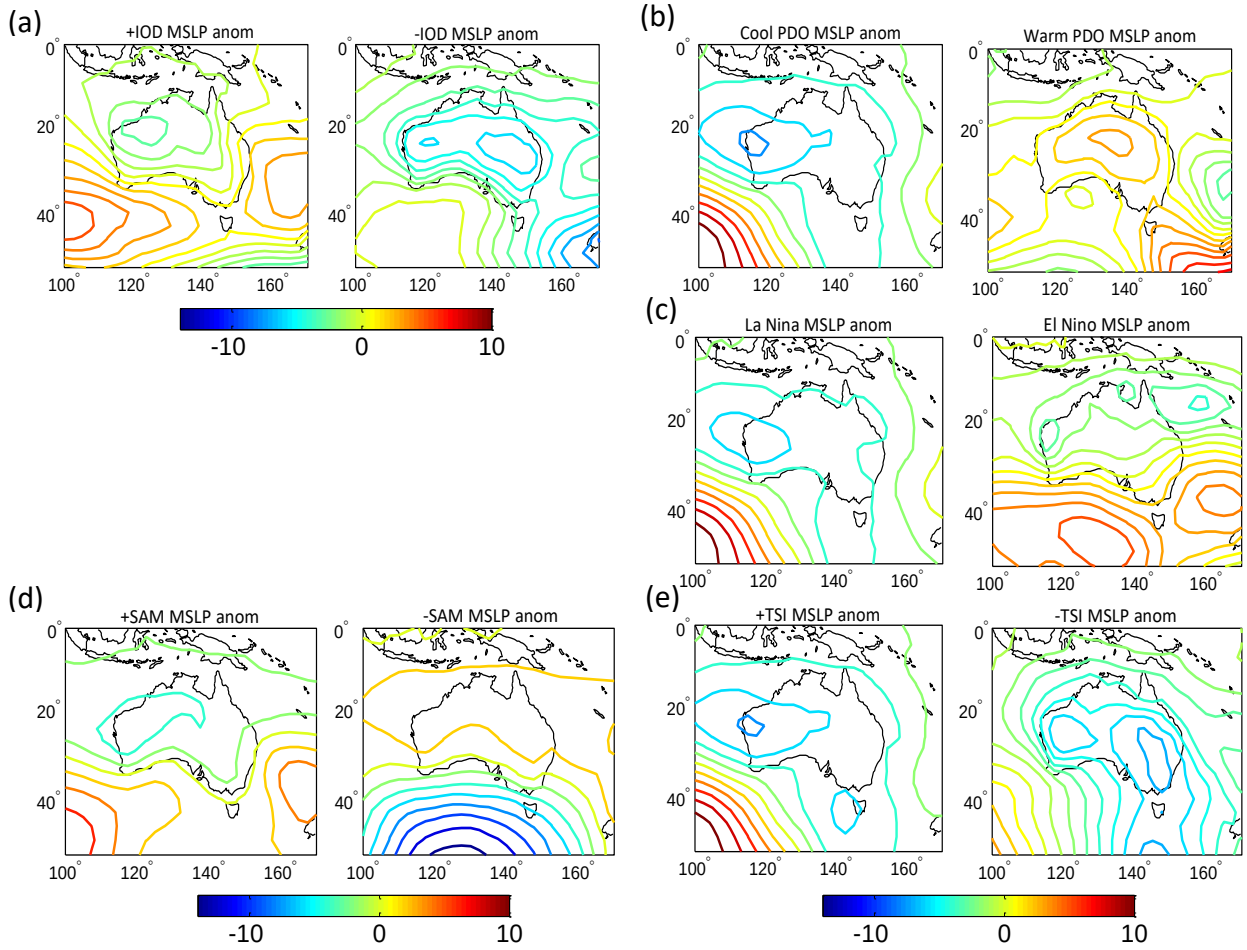

Figure 7.2 Mean sea level pressure anomalies (with respect to the mean) during positive and negative phases of (a) IOD, (b) PDO, (c) ENSO, (d) SAM) and (e) TSI for all occurrences of each phase over the period 1900-2012. Measurement is in hPa.

Tropical influences on synoptic type frequency

7.4.1 Results

North-East Group (NE)

Sub-annual to annual

Seasonal frequency of synoptic types within the NE group is enhanced by concurrent positive phases of SAM, SOI and TSI (25.9%, 25.8% and 24.5% relative influence respectively, Figure 7.3a). Cool PDO phases contribute 15.1% relative influence, with synoptic type frequency increasing once the value of the PDO falls below -1.5. The influence of positive SOI and SAM values persists at lags up to and including 2 and 7 seasons respectively. The influence of cool PDO phases remains at all lags up to 2 years (Figure 7.3b). Furthermore, synoptic frequency is enhanced by positive DMI values 4-8 seasons previously.

Inter-annual and *inter-decadal* results from the wavelet are shown in Figure 7.3c-g, and summarised in Table 7.2.

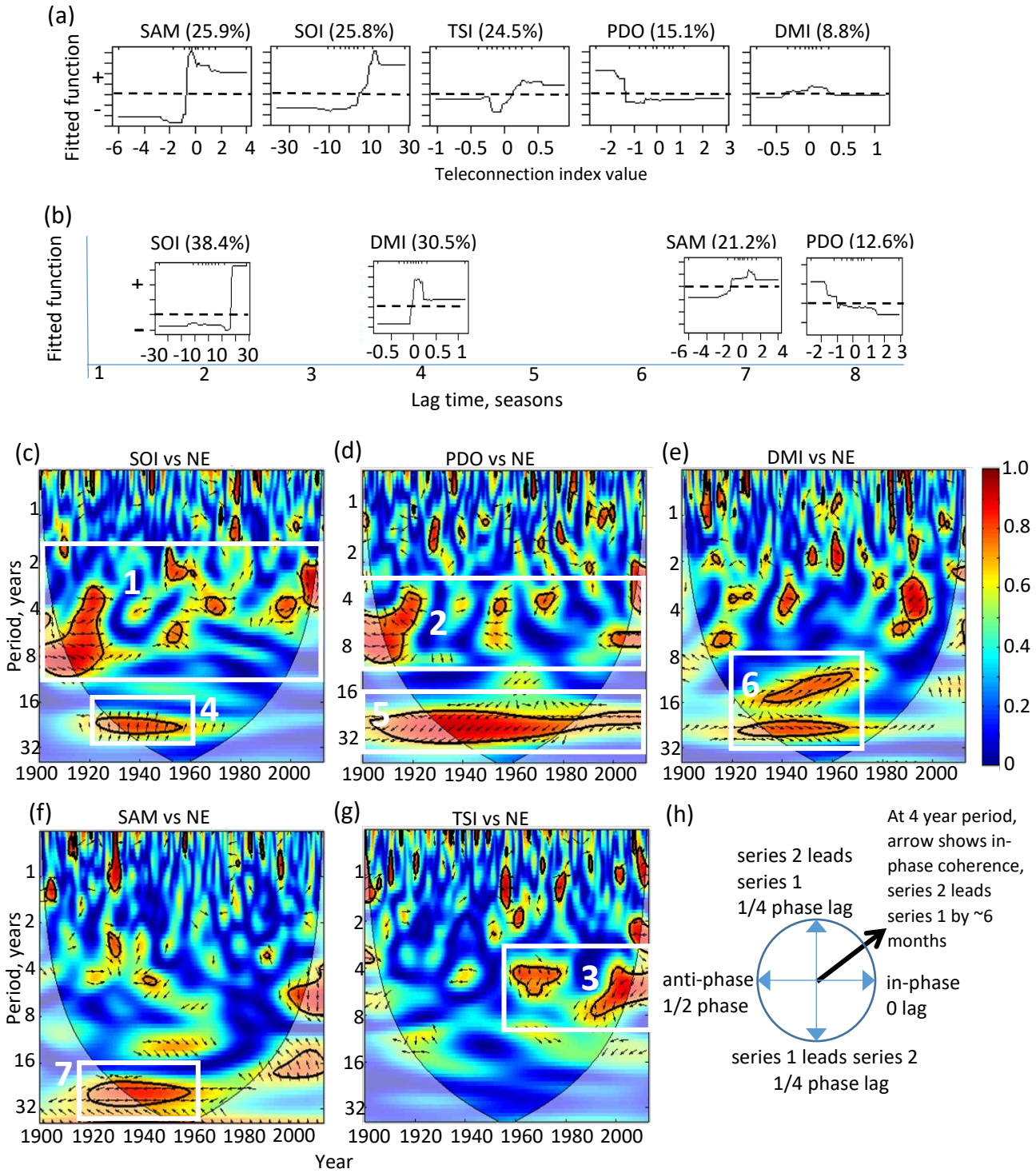

Figure 7.3 (a) Partial dependency plots showing relative influence of each teleconnection on concurrent NE synoptic type frequency from the boosted regression tree analysis. Relative influence of each predictor is shown in parentheses. Dashed line shows zero influence, above (+) and below (-) the dashed line represents increased and decreased frequency accordingly. (b) Partial dependency plots for selected lagged relationships discussed in the text. Dashed lines indicate zero influence on synoptic type frequency. A 4 season lag corresponds to 1 year, and an 8 season lag to

2 years. In (a) and (b) x-axis shows the teleconnection index value, and y-axis the fitted function i.e. when the plot is one increment above the horizontal dashed line, synoptic type frequency is interpreted to be twice as frequent as when the plot is one increment below the horizontal dashed line. (c)-(g) Coherence and phase of the cross-wavelet analysis between frequency of synoptic types in the northeast group and (c) SOI, (d) PDO, (e) DMI, (f) SAM and (g) TSI. Relationships described in Tables 7.2-7.5 are highlighted by the white boxes and numbers. Higher magnitude coherence is shown by red colours with significance at 95% indicated by the thick black lines. Period is expressed in years. Phase relationships are indicated by (h) and are described in the text. In each case, series 1 is the teleconnection and series 2 the synoptic type frequency. The thin curved lines indicates the cone of influence, outside of which the analysis should be interpreted with caution.

Table 7.2 Summary of wavelet results for NE group.

Timescale of influence	Teleconnection	Period (yrs)	Phase	Years of influence	Teleconnection lead/lag	Figure
Interannual	SOI	2-8yrs	In	1900-1920; 1950-1970; late 1990s	0	3c, box 1
	PDO	4-8yrs	Anti	1900-1920; 1950; 1970 >1990s	1.5-2.5yr lead	3d, box 2
	TSI	4-8yrs	Anti	1960s-late 1970s; >1990	1-2yr lead	3g, box 3
Interdecadal	SOI	16-32yrs	In	1920s-late 1950s	4-7yr lag	3c, box 4
	PDO	16-32yrs	Anti	1900-2012	6-12yr lead	3d, box 5
	DMI	10-32yrs	In	1920-1960s	1yr lead	3e, box 6
	SAM	16-32yrs	Anti	1920-1960	10-15yr lead	3f, box 7

North-West Group (NW)

Sub-annual to annual

Negative DMI values are the optimal predictor of concurrent synoptic type frequency (42.9% relative influence; Figure 7.4a) in the NW group, which increases once DMI values fall below -0.4. Positive SAM and SOI phases contribute 21.8% and 19.8% relative influence respectively (Figure 7.4a). Synoptic type frequency increases once TSI values increase above -0.5, and positive TSI values remain an influence at all lags to 3 seasons. At lags of 7 (Figure 7.4b) and 8 seasons, positive values of the DMI area strong influence. Positive SAM values continue to influence higher synoptic type frequency at all lags up to 4 seasons. The influence of cool PDO phases persists at all lags between 3 and 8 seasons (Figure 7.4b), which along with positive DMI and SAM are often amongst the most influential predictors at these shorter timescales.

Inter-annual and *inter-decadal* results from the wavelet analyses are shown in Figure 7.4c-g, and summarised in Table 7.3.

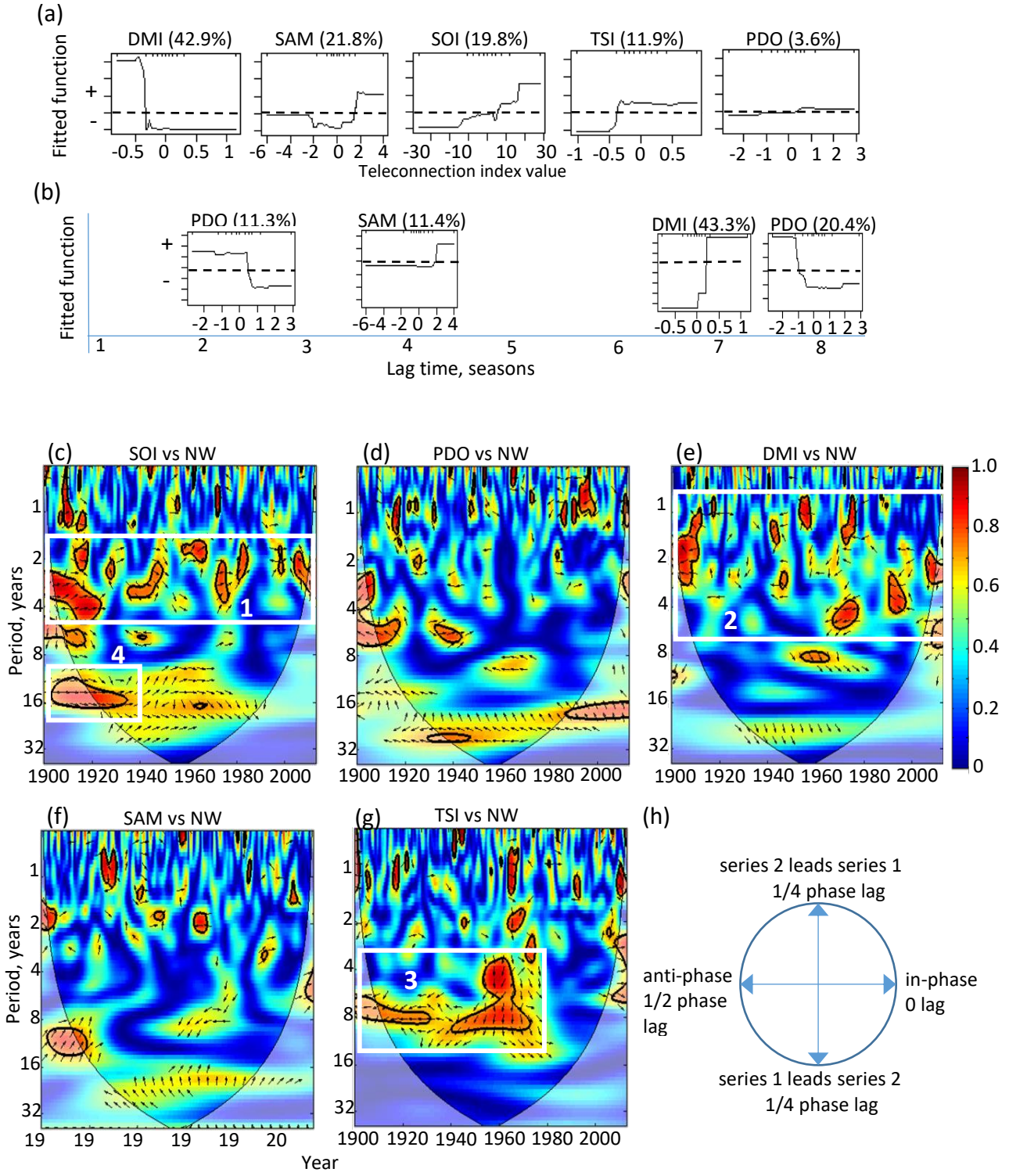

Figure 7.4 As Figure 7.3 but for synoptic types in the northwest group.

Table 7.3 Summary of wavelet results for the NW group.

Timescale of influence	Teleconnection	Period, (yr)	Phase	Years of influence	Teleconnection lead/lag	Figure
Interannual	SOI	1.5-5yrs	In	Occasions throughout 1900-2012	0-2 months lead (1940s)	4c, box 1
	DMI	1-6yrs	Anti	Occasions throughout 1900-2012	1-2yr lead	4e, box 2
	TSI	6-8yrs 3-10yrs	Anti	1900-1930 1940-1970	3-4yr lead 0.75-2.5yr lead	4g, box 3
Interdecadal	SOI	16yrs	In	1900-1930s	0	4c, box 4

7.4.2 Discussion

NE Group

The optimal predictors of concurrent synoptic circulation patterns that transport moisture from the tropical Pacific Ocean northeast of Australia to the Snowy Mountains region (classified in Chapter 4) are positive phases of SOI, SAM and TSI. Synoptic frequency is also enhanced by cool phases of the PDO. For both the SOI and PDO, this enhancement occurs during cool phases of the PDO that prevailed from 1890-1924, 1947-1976 and in the late 1990s (http://research.jisao.washington.edu/pdo/). The lag time of the PDO (1.5-2.5 years, Table 7.2) is consistent with cross-wavelet analysis lag times between the PDO and SOI of approximately 2 years (not shown). Given the different source regions for these two teleconnections, it is plausible that there would be a delay between the north Pacific and tropical Pacific Oceans. Consistent with the moisture source for this group, enhanced evaporation to the overlying atmosphere from above average SSTs in the Coral Sea subsequently feeds humid, tropical air into and along inland meridional troughs towards the Snowy Mountains. Previous studies have demonstrated similar effects of the PDO on eastern Australian rainfall (Gallant et al 2012 and references therein) and streamflow variability in the Murray River, SEA (McGowan et al 2009). Furthermore, regions of inter-annual coherence with the SOI appear to coincide with specific La Niña events (http://www.bom.gov.au/climate/enso/lnlist/). Conversely, lack of inter-annual coherence with either the SOI or PDO during warm PDO phases (mid-1920s-mid-1940s and late 1970s-late 1990s) suggests that warm PDO phases suppress inter-annual synoptic type frequency, by impeding southwards transport of tropical moisture (Figure 7.2b). The importance of warmer SSTs in the western tropical Pacific Ocean for enhanced synoptic frequency extends to inter-decadal timescales for the PDO.

The inter-decadal lead of the DMI indicates more frequent NE synoptic types approximately 1 year after a positive DMI event, when eastern tropical Indian Ocean SSTs are below average. This relationship and lag time is consistent with the effect described in Izumo et al (2013, 2010), whereby positive DMI events induce La Niña conditions in the Pacific ~18 months later.

The anomalous southerly position of the STR during positive SAM phases (Figure 7.2d) is conducive to advection of tropical moisture (Speer et al 2011), including that from the western Pacific (Figure 7.2d). The relationship at sub-annual timescales between synoptic type frequency and positive SAM phases is not found at longer timescales, suggesting that this is a short-term seasonal effect, related to the southerly position of the STR during summer. The inter-decadal coherence with SAM implies increased synoptic frequency during negative SAM phases. The regions of interdecadal coherence that co-occur between 1920-1950 in the DMI, SAM and SOI results requires further research to fully understand the lead/lag mechanisms. Although this coherence appears in the results of 3 teleconnections, it is acknowledged that without a clear physical mechanism, this must be interpreted with caution. It is proposed that at inter-decadal timescales the influence of cool PDO on synoptic type frequency, which extends across the entire analysis period, is greater.

The concurrent (sub-annual) influence of above average Tasman SSTs on higher synoptic type frequency is likely related to enhanced evaporation from underlying warmer SSTs in summer and warm air advection of that moisture via onshore easterlies (Risbey et al 2009b) towards the Snowy Mountains. The lagged interannual relationship with the TSI occurs at 'ENSO timescales' (~4-8 years). Whilst this relationship requires further elucidation, it may be linked to ocean circulation changes during the ENSO cycle and the transfer of warm surface waters from the tropical western Pacific along the east coast of Australia via the EAC. The positive trend in SAM, in all seasons since the 1970s (Whan et al 2014; Marshall 2003), suggests that offshore moisture is entrained from over a warmer Tasman Sea.

NW group

The frequency of synoptic types that transport moisture from the tropical Indian Ocean, northwest of Australia is enhanced during cool phases of ENSO (i.e. La Niña) at sub- to inter-annual periods. A similar relationship exists at inter-decadal periods with the SOI. The influence of cool phases (above average tropical western Pacific and Coral Sea SSTs) of ENSO may, in part, be related to a low-level (850 hPa) moisture source from the northeast for several synoptic types in this group (T4, T6, T7, T8 and T11; Chapter 4, Figure 4.6). Circulation anomalies for cool ENSO phases (Figure 7.2c) suggest transport of tropical air from both the northeast and northwest of Australia, likely

leading to more frequent NW types. The low-level influence of above average Coral Sea SSTs may in part explain why these synoptic types have remained prevalent (Chapter 5) despite a sustained positive trend in the IOD.

Consistent with expectations, negative DMI phases and especially negative events that exceed the threshold of -0.4 are the dominant driver of concurrent synoptic type frequency within the NW group at sub- to inter-annual timescales. The enhancement (diminishment) of synoptic frequency during negative (positive) phases of the DMI is consistent with the mechanism of the IOD, where higher SSTs in the tropical eastern Indian Ocean drive greater evaporation and moisture advection from the northwest of the continent towards the south-east (Ummenhofer et al 2009a). The occurrence of this relationship during cool PDO phases at inter-annual periods, and the lag time of approximately 9 months to 2 years is consistent with the transport time of warm water from the western Pacific warm pool via the Indonesian Throughflow (ITF) to the eastern tropical Indian Ocean, and oceans surrounding northern and north-west Australia (Sprintall and Révélard 2014; van Sebille et al 2014; England and Huang 2005). Subsequently, higher rates of evaporation from warm SSTs off NWWA enhance the tropical hydrological cycle there (Godfrey 1996; Graham 1995), allowing advection of warm humid air via inland troughs aligned NW-SE towards the Snowy Mountains. In addition, the Western Pacific warm pool has warmed significantly since 1955, implying transport of increasingly warmer waters through the ITF (Wang et al 2016; Cravatte et al 2009).

Despite the increasingly positive trend in DMI, background warming of SSTs in the tropical Pacific and Indian Oceans (Alory et al 2007) propose a mechanism for the lagged inter-annual DMI relationship found in this study. Furthermore, anomalous easterly winds across the equatorial western Pacific over a region of above average SSTs during cool PDO states also help to increase warm water transport through the ITF (van Sebille et al 2014).

BRT results show an increase in synoptic type frequency with positive SAM values. A positive SAM in summer and autumn has been linked to higher subtropical precipitation in NWWA, as the southerly position of the subtropical ridge is conducive to tropical moisture advection (O'Donnell et al 2015; Figure 7.2d). This is consistent with moisture advection along the NW-SE trough lines in this study and prior correlation analyses with synoptic type T7 (broad inland heat troughs aligned NW-SE) - one of the dominant summer types in this group. At all lags up to 2 years, positive SAM values continue to aid the advection of northwest tropical moisture. Continuing positive trends in SAM (Whan et al 2014; Marshall 2003), suggest a transition to increased warm season precipitation in SEA and dominance of the northwest moisture pathway (Chapter 5).

Before the onset of rapid warming in the Tasman Sea, it appears that higher Tasman SSTs coincided with lower frequency of NW types, and vice versa. This occurrence largely during cool PDO phases indicates perhaps a greater frequency of synoptic types from the NE or Tasman during these periods. The physical mechanism for this multi-year lagged relationship may be related to Pacific Ocean circulation changes (possibly related to ENSO), but without further research of ocean processes the causal nature of this relationship must be considered with caution. It is also possible that this result may be an artefact of the data and statistics used.

Extra-tropical influences on synoptic type frequency

7.4.3 Results

Southern Ocean (SO) Group

Sub-annual to annual

The dominant concurrent influence on SO types is SAM, with negative values contributing 46.2% of relative influence. A peak in synoptic type frequency occurs for SAM values between -1 and -3 (Figure 7.5a). This relationship with negative SAM values does not persist past two seasons lag (Figure 7.5b). Synoptic type frequency increases when TSI values are between -0.2 and +0.5 (18% relative influence). At lagged timescales however, TSI influence is generally positive (not shown). Negative DMI events coincide with increased synoptic frequency (Figure 7.5a). Concurrent cool PDO phases have only a weak influence, however this increases in strength at all lags greater than two seasons. SOI values either remain neutral or are negative at all lagged timescales up to 2 years. This is consistent with higher frequency of SO types during El Niño periods, and reveals a potential relationship at annual periodicities that is not apparent in the wavelet results.

Inter-annual and *inter-decadal* results from the wavelet analyses are shown in Fig. 5c-g, and summarised in Table 7.4.

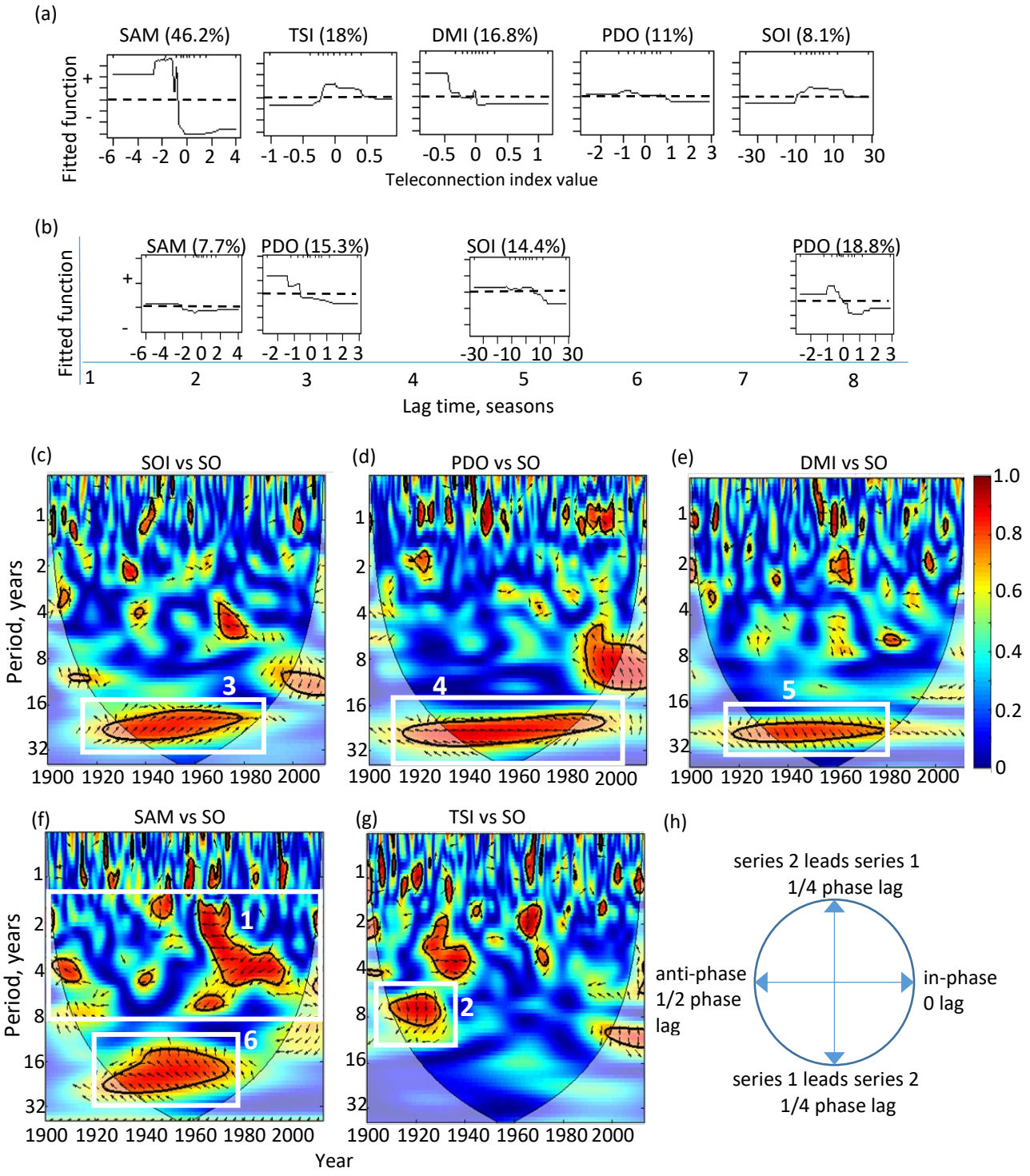

Figure 7.5 As Figure 7.3 but for synoptic types in the Southern Ocean group.

Table 7.4 Summary of wavelet results for SO group.

Timescale of influence	Teleconnection	Period, (yr)	Phase	Years of influence	Teleconnection lead/lag	Figure
Interannual	SAM	1.5-8yrs	Anti	Occasions throughout 1900-2012	0.75-4yr lead	5f, box 1
	TSI	6-10yrs	In	1910-1930	1.5-3yr lead	5g, box 2
Interdecadal	SOI	16-32yrs	In	1920-1980	0	5c, box 3
	PDO	16-32yrs	Anti	1910-2000	12yr lead	5d, box 4
	DMI	16-32yrs	In	1920-1980	4yr lead	5e, box 5
	SAM	16-32yrs	Anti	1920-1970s	6-10yr lead	5f, box 6

Tasman Group

Sub-annual to annual

Three teleconnections contribute nearly 95% influence to concurrent synoptic type frequency in this group: negative DMI, and positive SAM values contribute 34.6% and 30.9% relative influence respectively to higher synoptic type frequency; the TSI contributes 29.2% relative influence, and synoptic frequency increases once values increase above -0.2 (Figure 7.6a). Positive TSI values continue to influence higher synoptic frequency at 1 and 2 years lag (Figure 7.6b). The influence of positive SOI and SAM values does not extend past two seasons lag (Figure 7.6b for SAM). Negative DMI values remain a dominant influence at all lags up to four seasons (not shown).

Inter-annual and *inter-decadal* results from the wavelet analyses are shown in Figure 7.6c-g, and summarised in Table 7.5.

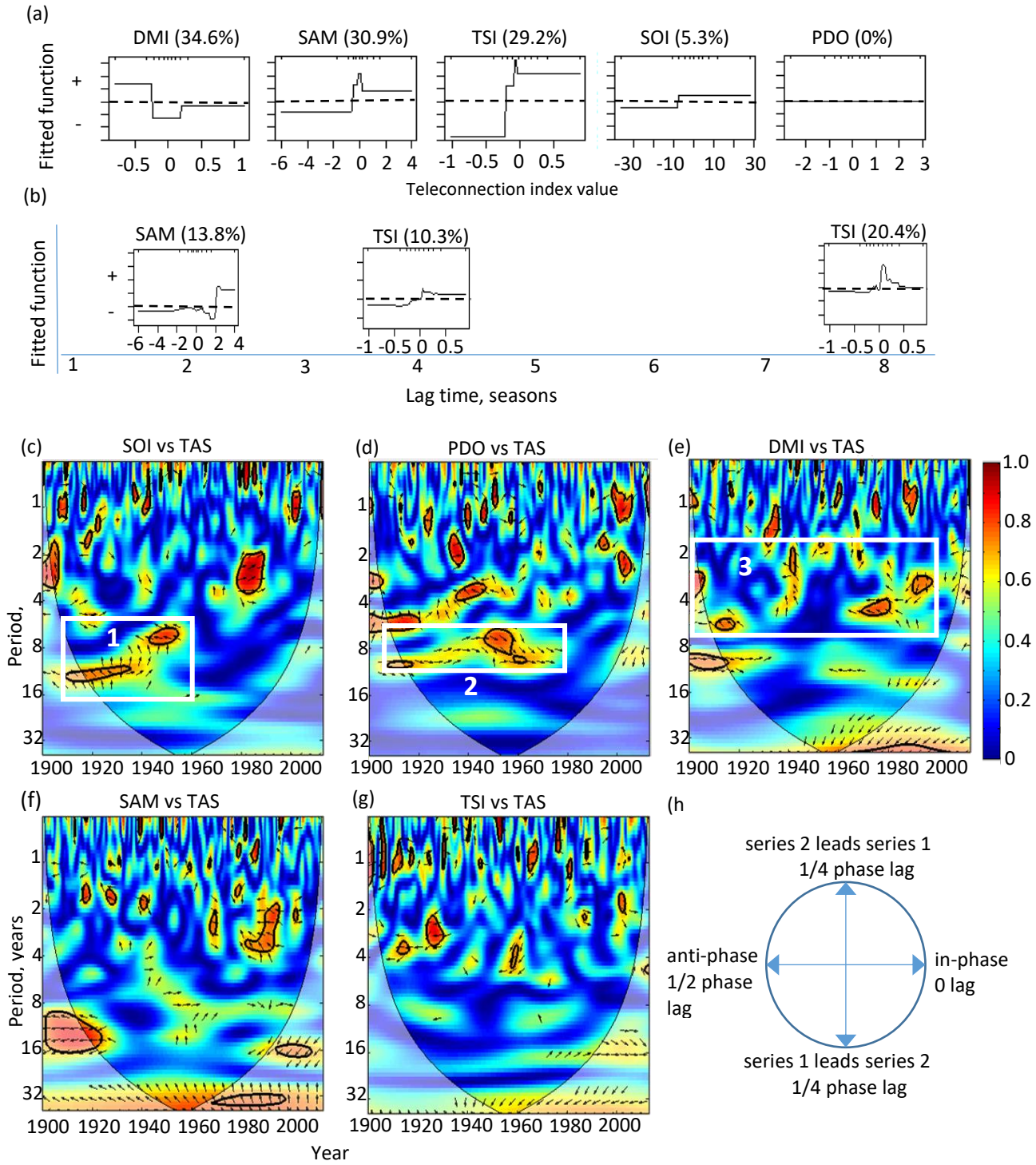

Figure 7.6 As Figure 7.3 but for the synoptic type in the Tasman group.

Table 7.5 Summary of wavelet results for Tasman group.

Timescale of influence	Teleconnection	Period, (yrs)	Phase	Years of influence	Teleconnection lead/lag	Figure
Interannual	SOI	6-12yrs	Anti	1910-1930s; 1940-1950	3-4.5yr lag	6c, box 1
	PDO	6-12yrs	In	1910; 1940s-1960s	0	6d, box 2
	DMI	2-7yrs	Anti	Occurrences throughout 1900-2012	1.5-3yr lead	6e, box 3

7.4.4 Discussion

SO Group

Synoptic types in this group occur predominantly in winter. Consistent with the well-described relationship between SAM and embedded cold fronts, it is therefore not surprising that negative values of SAM contribute almost half of concurrent variability of synoptic type frequency in this group. These results are consistent with circulation anomalies in Figure 7.2d and with Verdon-Kidd and Kiem (2009a) who associate winter synoptic types, including cold fronts, with negative SAM values. Similarly, Fiddes et al (2014) demonstrated correlation coefficients of -0.22 and -0.29 between the frequency of extreme (>95th percentile) precipitation events and SAM in JJAS and autumn respectively. This consistency with previous studies increases confidence in the use of BRTs for their ability to describe relative influence of predictors. Interestingly, the apparent threshold of -1 in the SAM index, above which synoptic type frequency decreases markedly, suggests that the frequency of cold fronts reduces before the threshold of a positive SAM event (+1 standard deviation; Marshall et al 2012) is reached.

The SAM exhibits little persistence (no autocorrelation) and the effects of a negative phase on synoptic frequency do not persist at timescales beyond two seasons lag in the BRT analysis. This is in accordance with the limit of predictability for SAM of intra-seasonal to seasonal timescales (Hendon et al 2014). However, when considering longer periodicities, anti-phase coherence suggests that SAM has been a useful indicator of synoptic type frequency at lag times up to a decade. Whilst SAM is usually considered a high-frequency mode, the lag time observed here is consistent with the low-frequency variability of SAM as reported by Kidson (1999) and Lim et al (2016). The inter-decadal coherence with SAM is phase-locked and extends over a large area, and is therefore unlikely to be a random artefact (although this does remain a remote possibility). Whilst forcing of SAM on inter-decadal timescales is thought to be related to ENSO, observed SSTs, sea-

ice distribution and increased greenhouse gases (Karoly 1989; Kidson 1999; Mo 2000), there remains an aspect of this lead relationship that is yet to be fully understood, in terms of the effect on mid-latitude weather. Any underlying physical mechanism responsible for this lead relationship could be investigated by the application of the statistical techniques in this chapter to climate model output. The cessation of the inter-annual (inter-decadal) anti-phase relationship with SAM since the late 1990s (1970s) is consistent with a decline in the passage of embedded cold fronts across southern Australia during positive SAM phases, likely associated with the positive trend in SAM in recent decades (Whan et al 2014). This is also consistent with a decline in cool season precipitation associated with frontal systems during the Millennium Drought (Risbey et al 2013; Verdon-Kidd and Kiem 2009b).

Although cold fronts, in general, have declined in frequency in conjunction with the positive trend in SAM over recent decades (Catto et al 2014), those bringing precipitation in excess of 10 mm per day also appear to be driven, in part at least, by cool Pacific indices. Cool PDO phases towards longer lag times in the BRT analysis are consistent with wavelet results, and both analyses indicate that the background state for higher frequency of synoptic types within this group includes a cool phase of the PDO. Accordingly, the influence of the PDO spreads far beyond its source region in the North Pacific. The influence of cool Pacific indices extends to inter-decadal timescales for both the PDO and SOI. The mechanism of this relationship initially seems counter-intuitive given the Southern Ocean source of these synoptic types. It is proposed however that the significant negative correlation between tropical western Pacific SSTs and SAM during JJA described by Ding et al (2012) is consistent with La Niña SST patterns, and implies higher frequency of SO synoptic types during negative SAM phases and La Niña in austral winter. In addition, the frequency of synoptic types, including cold fronts, bringing wet conditions to SEA in winter was shown to increase during cool PDO phases (Verdon-Kidd and Kiem 2009a) and La Niña events (Pezza et al 2008). Conversely, the inter-decadal influence of positive DMI phases is consistent with more frequent SO types when SSTs in tropical latitudes north-west of Australia are below average.

The association of synoptic type frequency and TSI early in the 20th century and re-emergence after the late 1990s is consistent with low-level airflow drawn in ahead of fronts. The latter period may be linked to the warming trend in the Tasman Sea in recent decades (Oliver et al 2015). This more energetic Tasman Sea environment (a result of greater heat transport by the EAC) may also, in part, be responsible for the increased intensity of cold frontal precipitation described in Chapter 5.

Tasman Group

The variability of offshore lows is influenced at sub-annual timescales by above average SSTs in the eastern tropical Indian Ocean and Tasman Sea. The concurrent influence of TSI and SAM is consistent with warmer surface waters over the Tasman Sea inducing greater evaporation, onshore easterly flow and enhanced precipitation respectively (Fiddes and Pezza 2015; Risbey et al 2009b), and may be related to increasing summer precipitation in the Snowy Mountains, especially across eastern elevations (Chapter 4, section 4.3.1; Fiddes et al 2014). The increasing trend in Tasman SSTs, which has occurred since the 1950s (Oliver et al 2015) is likely to be an influencing factor in the BRT results, leading to a more energetic environment, and a projected increase in offshore low during warmer months (November-April; Pepler et al 2016). Similarly, during positive SAM phases the subtropical ridge is situated over southern Australia, including over the Tasman Sea, which in turn modulates underlying Tasman SSTs. Increased SSTs in this region and associated higher rates of evaporation may aid offshore low formation or persistence. These results are consistent with patterns found in previous studies, where southern secondary lows (i.e. those that form outside the tropics) occur more frequently during high latitude blocking in the Tasman Sea (ESCCI 2015), consistent with positive SAM (Figure 7.2d) in summer. The influence of positive TSI and SAM values however does not persist past sub-annual timescales, and may in part be due to seasonal effects and the Southern Ocean origin of many of these synoptic systems.

Negative DMI values are a consistent feature at all periodicities considered. The large concurrent influence of negative DMI values may indicate that the offshore lows in this group are mostly southern secondary lows, whose occurrence has also been shown to be positively influenced by above average eastern Indian Ocean SSTs (ESCCI 2015; Browning and Goodwin 2013) via interaction with warm, moist air from northwest cloud bands. This is consistent with the eastwards migration of closed lows (synoptic types T2 and 6) and their associated northwest moisture pathway, to become offshore lows. Furthermore, interaction can also take place with warm, humid air from the Tasman Sea (Browning and Goodwin 2013). The circulation anomalies for negative DMI phases support both of these interactions (Figure 7.2a).

At all periodicities, the SOI and PDO do not appear to be a major influence on synoptic type frequency, consistent with the extra-tropical moisture source of this group.

7.5 Synthesis of results and discussion

Figure 7.7 provides a summary diagram of discussions relating to sub-annual influences. In brief, NE synoptic type frequency increases when concurrent above average tropical western Pacific and Coral Sea SSTs feed moisture along inland meridional troughs, and during positive phases of SAM

which increase onshore moisture advection. Frequency of synoptic types with NW origin increases in response to above average SSTs in the tropical eastern Indian and western Pacific Oceans, and the Tasman Sea. Positive SAM phases aid tropical moisture advection towards the Snowy Mountains. SAM is the dominant influence on SO synoptic type frequency, and above average Tasman SSTs feed warm, moist air in ahead of the front. Key drivers of Tasman synoptic type frequency are above average SSTs in the eastern tropical Indian Ocean and Tasman Sea, and subsequent advection of warm humid air towards the Snowy Mountains in conjunction with positive phases of SAM (Figure 7.7).

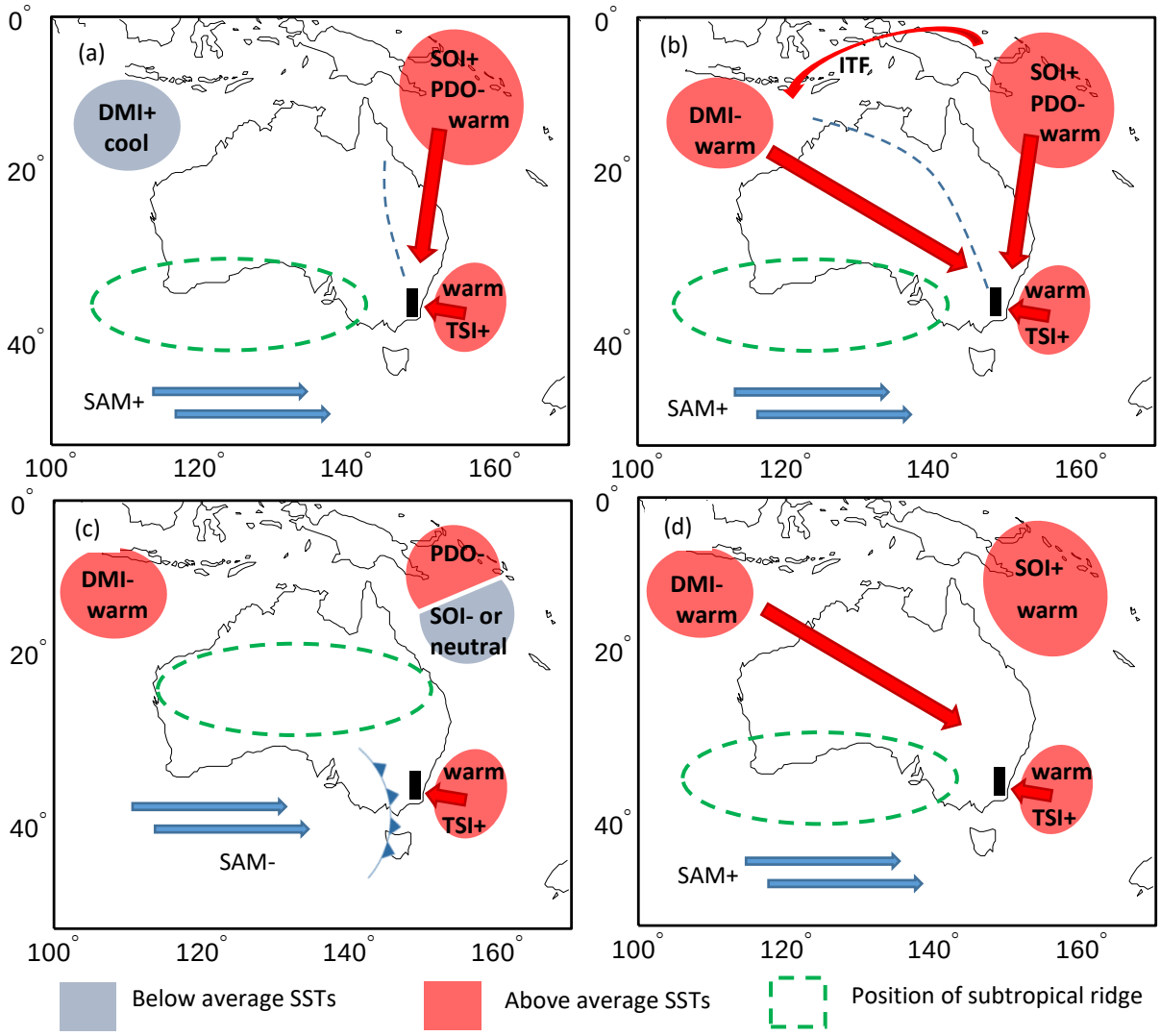

Figure 7.7 Schematic representation of the key factors influencing concurrent synoptic type frequency variability for (a) NE group, (b) NW group, (c) SO group, (d) Tasman group. Blue dashed lines represent inland troughs. Blue and red arrows indicate cool (mid-latitude westerly storm track) and warm air advection respectively, and moisture pathways towards the Snowy Mountains region (black rectangle); curved arrow represents transfer of warm ocean waters via Indonesian Through-Flow (ITF).

7.6 Summary

This study represents a further step in the continual process of establishing causes of precipitation variability. The analyses presented demonstrate the complex interactions between teleconnections and their effect on frequency of synoptic weather systems delivering precipitation to the headwater catchments of the Snowy Mountains. In particular the tropical Pacific and Indian Ocean indices are shown to be important for driving not only the influx of tropical moisture towards the Snowy Mountains, but also in driving low-frequency variability of some extra-tropical synoptic systems.

A climatic shift during the mid-20th Century (Baines and Folland 2007; Meyers et al 2007) that saw the beginning of rapid atmospheric temperature increases, and increasing tropical SSTs, including the tropical Indian Ocean (Cai et al 2014b) and western Pacific warm pool (Wang et al 2016; Cravatte et al 2009), also resulted in increasing SST trends in the Tasman Sea (Oliver et al 2015). Given the tropical nature of the moisture pathways associated with many of the synoptic types in this study, it is likely that these trends, consistent with global warming, have influenced changes in the synoptic circulation and associated moisture advection to SEA.

Cross-wavelet analyses describe non-stationarity of relationships between synoptic type frequency and teleconnections, offering insight into drivers of precipitation variability at both inter-annual and low frequency inter-decadal periodicities. Multi-year lead times of teleconnections are likely linked to ocean circulation patterns and subsequent forcing of atmospheric circulation, which could be further explored through modelling experiments. No one teleconnection acts in isolation, and the application of boosted regression trees demonstrates that the relative influence of all potential predictors can be quantified. This offers a new dimension to existing understanding of the effect of large-scale atmospheric circulation drivers on precipitation in this hydrologically, and economically, important region of SEA. Results presented here largely complement earlier studies of (e.g. Schepen et al 2012; Verdon-Kidd and Kiem 2009b; Risbey et al 2009), and broadly agree with initial correlation analyses. The overall consistency of BRT results with the cross-wavelet analyses and known teleconnection relationships indicates promise in their application to climate data. Together, these two techniques provide insight into the drivers, and underlying mechanisms, of precipitation variability. This has particular importance for regional water management, seasonal forecasting, as well as potential for early warning of wet and dry periods in the study area.

Chapter 8. Conclusions and future research

This thesis has addressed the primary research aims to develop a synoptic-scale precipitation climatology for the Snowy Mountains region of southeast Australia, assess the variability of synoptic types over a multi-decadal period, and to understand how large-scale climate drivers influence that variability. It has addressed major knowledge gaps introduced in chapter 1 by using three-dimensional data to describe synoptic types, assessing precipitation trends over multiple decades and investigating the relative influence of teleconnections on synoptic type frequency. Key findings are presented in the results chapters of this thesis (sections 4.3, 5.3, 6.4 and 7.4). This chapter summarises those key findings with respect to the research aims and objectives stated in Chapter 1, and describes the contribution of the thesis to the field of synoptic climatology. Limitations of the study are discussed, along with directions for future research.

8.1 Research findings

8.1.1. Objective 1: Develop a synoptic classification of inflow-generating precipitation events for the Snowy Mountains 1900-2012.

The primary objective of this research was achieved by the application of an automated clustering method to multi-level and multi-parameter gridded ECMWF reanalysis data. The range of data used included MSLP, wind vectors, temperature and humidity at several tropospheric levels, to describe the synoptic characteristics in terms of atmospheric stability and available moisture. Precipitation-bearing synoptic types were classified in all seasons, thereby capturing year-round variability in both tropical and extra-tropical synoptic systems. Chapter 4 detailed the eleven synoptic types responsible for inflow-generating precipitation that were described initially for the period 1958-2012, and later extended to cover the period 1900-2012. Analysis of the resultant synoptic types demonstrated the existence of key atmospheric moisture pathways that originate over the oceans surrounding Australia. These were further highlighted by the results of the WRF modelling.

Winter precipitation was dominated by synoptic types associated with the mid-latitude westerly wind belt, in particular by embedded cold fronts and closed lows. During the warmer months of summer, precipitation was dominated by inland heat troughs, and warm air advection from tropical latitudes. The importance of warm air advection in driving tropical moisture advection towards the Snowy Mountains for the generation of high precipitation totals was, however, apparent in all seasons. Validation of the automated typing showed good agreement with manual surface and 500 hPa height synoptic analysis charts, and satellite imagery for the period 2008-2012, demonstrating that the automated method was able to capture expected synoptic types. Results presented in Appendix 1show that WRF can be successfully used to produce high resolution regional modelling.

8.1.2. Objective 2: To understand the synoptic influences on inflow-generating precipitation in the Snowy Mountains.

Chapter 4 included an analysis of the spatial distribution of precipitation associated with each synoptic type. The spatial distribution was assessed using a 5km resolution gridded precipitation data product. A clear distinction was apparent between synoptic types with a northwest and northeast pathway in delivering greater precipitation amounts across the western and eastern elevations of the Snowy Mountains respectively. Higher precipitation totals across western and high elevations of the Snowy Mountains Hydro-electric Scheme's catchments were evident for synoptic types associated with the mid-latitude westerly wind belt. This was also apparent for types with a dominant moisture pathway from northwest Western Australia, some of which also bring increased precipitation to northern catchments of the Snowy Mountains. Higher precipitation across eastern elevations was apparent for those synoptic types originating over the Coral and Tasman Seas. These results are important for understanding water availability within the catchments.

Chapter 6 determined the proportions of rain versus snow for each synoptic type, using a daily maximum temperature threshold to assess whether rain or snow fell on each classified precipitation day. The study identified that a distinct set of types generated the majority of snowfall (≥ 10 mm water equivalent) in the Snowy Mountains. Importantly, and consistent with previous Australian snow studies, these were all associated with the mid-latitude westerly wind belt. Accordingly, atmospheric circulation trends that force the westerly wind belt poleward are therefore highly likely to affect the amount of snow received across the Snowy Mountains. Noticeable declines in annual maximum snowdepths, as well as fewer above average snow depth years were evident since the early 1990s. This study demonstrated that, in addition to increasing temperature trends (Pepler et al 2015), snow depths in the Snowy Mountains are also sensitive to declines in the main snow-producing synoptic type.

8.1.3. Objective 3: Investigate the variability and trends in synoptic types that influence the Snowy Mountains.

The considerable inter-annual precipitation variability that exists in the Snowy Mountains region was the motivation for this objective. Chapter 5 addressed the first two sub-objectives: to describe and quantify the temporal variability of, and identify long-term trends in, synoptic types. Analysis of synoptic type precipitation, frequency and intensity over a 55 year period (1958-2012) demonstrated trends towards fewer, more intense precipitation events, with an increase in the proportion of extreme precipitation (> 90th percentile). In addition, the study showed that important changes in the seasonality of precipitation were apparent, with precipitation totals increasing during

warmer months, and declining in the shoulder seasons of autumn and spring. Although not always statistically significant, the trends showed that a precipitation response to climate change is likely to already be occurring.

The remaining sub-objectives sought to develop understanding of this variability. This was achieved by applying wavelet and boosted regression tree methods to characterise the relationships between synoptic type frequency and teleconnection indices. The synoptic classification presented in Chapter 4 was extended to 1900 using the same methods and newly available ERA-20C reanalysis data from ECMWF, in order to include a greater number of teleconnection cycles. The results of this study were presented in Chapter 7, and highlighted the complex interactions that take place between teleconnections, and their lead and lagged effect on synoptic type frequency and variability. In particular, tropical western Pacific and eastern Indian Ocean SSTs were shown to be important for driving the advection of tropical moisture towards the Snowy Mountains.

The study showed that relationships between teleconnections and synoptic type frequency are not stationary through time, with particular combinations of indices modulating higher or lower frequency of types. For example, the frequency of synoptic types with a moisture source to the northeast of Australia was shown to be enhanced during cool phases of both ENSO and the PDO, and suppressed during warm phases of the PDO. This result is consistent with previous findings of how Pacific indices modulate eastern Australian rainfall (Power et al 1999), and indicates robustness of the results in this study. The combined effects of multiple teleconnections on synoptic type frequency were quantified using boosted regression tree methods. This technique revealed the dominant influences on synoptic type frequency at concurrent and lagged timescales.

8.2 Contribution of the research to knowledge gaps

This study has been the first to demonstrate that multi-level gridded meteorological data can be successfully combined by an automated, objective technique to define synoptic types based on atmospheric circulation throughout the depth of the troposphere (Chapter 4). In doing so, it has expanded the current understanding by revealing the complex three-dimensional nature of synoptic-scale circulation, which plays a key role in system development, steering and ultimately the weather experienced at the surface. The synoptic typing method applied in this study has aided in the identification of atmospheric moisture source regions and pathways associated with synoptic types. This includes those in the mid-levels which would otherwise have been missed if only surface circulation had been considered.

The agreement of the cool season synoptic types in this study with those of previous manual synoptic classifications for SEA, demonstrates that the novel application of k-means clustering to fine-scale reanalysis data is robust and able to identify key synoptic features without the need for additional satellite imagery. It is anticipated that the clustering method could be applied to research in other regions, and to parameters other than precipitation, to elucidate relationships between regional surface climate and the overlying synoptic-scale atmospheric circulation.

The use of gridded precipitation data may provide greater insight for water managers into the expected spatial distribution of precipitation associated with particular synoptic types moving across the region.

The results in Chapter 5 represented the first study to consider precipitation trends in all seasons over a multi-decadal period for the Snowy Mountains, thereby expanding the recent focus on cool season precipitation during and since the Millennium Drought. The results demonstrated that the seasonality of precipitation is changing in the temperate alpine region of SEA. Precipitation during the historically wetter cool season appears to be in decline, consistent with previous studies of other SEA regions. Conversely, warm season precipitation appears to have increased over the period 1958-2012. Increases in precipitation intensity in all seasons indicate that precipitation may be becoming more convective. Importantly, this study has found evidence in the observational record of changes previously predicted by climate change models. The declining cool season rainfall, and particularly the significant drying in autumn, is consistent with the poleward expansion of the subtropical arid region, and delayed northward movement of the subtropical ridge. A decline in the number of embedded cold fronts crossing the study region, particularly since the Millennium Drought, is consistent with consequences of positive trends in SAM. Hence, this study has confirmed that important changes are occurring in atmospheric circulation, with consequences for regional precipitation and runoff.

The analysis presented in Chapter 7 increases understanding of how synoptic type frequency varies in response to multiple teleconnections. The benefits of applying established statistical techniques to multi-decadal climate data include elucidation of non-stationarity in relationships, and quantification of the relative influence of several teleconnections on synoptic type frequency, thereby revealing how key teleconnections interact to influence regional precipitation. The use of boosted regression trees has demonstrated a novel and useful approach that describes how synoptic type frequency varies in response to the continuous range of teleconnection index values. This adds value to the current understanding of the response of synoptic type frequency to either positive, negative or neutral phases of a teleconnection.

In practical terms, the results of this study suggest that effects on precipitation may be felt before a particular teleconnection reaches its threshold value for an event to be declared. Importantly, this study develops new understanding of regional precipitation variability, by demonstrating that the relative influence of all teleconnections can be quantified, thereby offering an exciting new approach to seasonal precipitation forecasting. The methods applied in Chapter 7 will help inform regional water availability, management and policy development.

The wavelet and regression tree analyses presented in Chapter 7 provided insight into how trends in teleconnections may impact the frequency of particular synoptic types in the future. For example, increasingly positive trends in SAM (Marshall 2003; Whan et al 2014) will have a detrimental effect on the passage of embedded cold fronts across southern Australia. Given that these systems deliver much of the cool season precipitation and are responsible for the majority of snowfall in the Snowy Mountains, a continued decline in cool season precipitation and maximum snow depth is therefore likely. The increasingly positive trend in IOD (Cai et al 2014b, 2009) is likely to exacerbate the decline in cool season precipitation, particularly in spring. However, increasing background SSTs in the eastern tropical Indian Ocean (O'Donnell et al 2015; Alory et al 2007), will likely result in continued moisture transport from NWWA, particularly in warmer months when the IOD is not considered to operate, with consequences including increased summer rainfall.

Understanding of precipitation variability over the instrumental record provides essential data against which to assess current and future changes to precipitation regimes. The analyses in Chapters 5 and 7 demonstrate that synoptic type frequency is highly dependent on teleconnection phase and interactions. The significance of the results in this thesis for inflows in the Snowy Mountains region may include: changes to the timing of reservoir replenishment; increased summer precipitation with the potential to observe greater inflows during this season; compression of cool season precipitation (due in part to significant declines in austral autumn); and decline in inflows associated with snowmelt as maximum snow depths decrease. However the outcomes of this thesis have much broader implications. The decreases in shoulder season precipitation will have subsequent effects for the wider catchment hydrology, and the agricultural industry which relies on the 'autumn-break' to begin crop sowing (Pook et al 2006). Overall, the trends also have consequences for downstream agricultural irrigation and environmental flows along some of Australia's iconic river systems. The decline in maximum snow depths is likely to have marked effects on alpine tourism, particularly in a region which is already subject to highly variable snowfalls. The impact of increasing precipitation intensity on regional natural resource management, for example soil erosion and flooding warrants further investigation. In all cases, adaptive management practices are necessary.

8.3 Research limitations and future research directions

This thesis has presented the first comprehensive study of synoptic systems responsible for inflow-generating precipitation in the Snowy Mountains. It is acknowledged that incorporation of precipitation into the snowpack, or enhanced inflows during spring snowmelt means that any precipitation-runoff threshold is not static, and depends on many catchment conditions. As the focus of this thesis was inflow-generating precipitation, these factors were minimised by considering only precipitation during December-April for the threshold calculation. The incorporation of evaporation, snowmelt and soil moisture data into the development of a dynamic seasonal threshold for inflow generation could be the focus of future studies.

The synoptic classification presented in this study does not track synoptic systems from their formation as they migrate eastwards. Rather, following Pook et al (2006) and others since, it provides a snapshot of the atmospheric circulation on the day that precipitation was observed. Similarly, slow-moving synoptic systems may be over-represented. Calculations show however, that the majority (79%) of precipitation days ≥ 10 mm do not occur consecutively. Of those that do, only approximately 3% consist of the same synoptic type. Over-representation is therefore minimal in this study, and the daily classification is considered appropriate given typical synoptic speeds (Sturman & Tapper 2006; Pook et al 2006; Barry & Carleton 2001). These types of slow-moving systems may feature more frequently however if all precipitation days were considered (i.e. all days on which > 1 mm was observed), and may therefore benefit from a classification system that takes into account multi-day events. Synoptic typing of all precipitation days, or those with a different threshold, may shed light on precipitation patterns critical to other industries.

In addition to moisture availability in source regions of synoptic types, it is possible that surface moisture conditions in the regions over which the systems migrate may modulate the overlying airmass. It has been suggested that it may be possible to incorporate surface water conditions for the Australian landmass as an input to the clustering algorithm, using GRACE satellite groundwater storage data (G. McGrath – personal communication). In doing so, further insight into the modulation of synoptic systems and the precipitation they ultimately produce may be gained. The association of synoptic types with moisture source regions and pathways in this study allow future studies to attribute for example, palaeoclimate isotope data, collected for the Snowy Mountains, to synoptic types, offering insight of precipitation variability on much longer timescales than presented here.

The trend analyses presented in Chapter 5 span the shorter analysis period 1958-2012. Linear trend calculations are dependent on the time period considered (Risbey et al 2013), and not necessarily

suitable for longer periods that display high degrees of non-linearity. Whilst they have been useful for describing the trends in precipitation since the onset of increased rates of global warming in the 1950s, precipitation data in the Snowy Mountains exhibit strong non-linearity over the time period 1900-2012. When considering relationships between synoptic types and teleconnections over the extended period it is therefore important to use non-linear methods. Both the wavelet and boosted regression tree methods presented in Chapter 7 are non-linear. These analyses reiterated that significant changes in the precipitation regime of the Snowy Mountains occurred during the mid-20th century.

This is the first known study to apply boosted regression trees to climate data. However BRTs have been applied to many other types of environmental data. The length of the observational climate record is relatively short in comparison to datasets used in other BRT applications. However, this study assesses the influence of teleconnections over a period greater than 100 years, thereby spanning much of the observational record in Australia. Moreover, expected relationships between synoptic types and teleconnections are revealed. Furthermore, the flexibility of the BRT software to decrease the learning rate allows a more reliable prediction of the response variable in the case of small sample sizes. The overall agreement between BRT and wavelet results suggests that these methods are robust in explaining relationships between synoptic type frequency and teleconnections. Future research should focus on applying the relationships gleaned from the BRT analysis to operational data, to test their accuracy in predicting precipitation totals, particularly with regards to improving seasonal precipitation forecasts.

This study endeavoured to describe the influence of large-scale drivers on synoptic type variability. There may however, be other, more localised factors that influence synoptic precipitation in the region. For example, Kingston et al (2015) found locally derived indices to exhibit better relationships with lake inflows in New Zealand, than the SOI or SAM. This study identified a dominant moisture pathway from NWWA that is associated with many of the synoptic types. These results are consistent with increasing SSTs off the coasts of north and northwestern Australia, the transfer of heat through the ITF, and increased evaporation of moisture to the overlying atmosphere. Although the more remote IOD provides a degree of explanation of precipitation variability over SEA, a more localised index may provide greater explanation of synoptic type variability, especially in seasons when the IOD is not considered active. Similar to the Ningaloo Niña index, a key area for further research is the development of a climate index that incorporates SST and atmospheric anomalies off northwest and northern Australia. Such an index may also capture the effects of the long-term Indian Ocean warming trend (Alory et al 2007), which may make increased moisture available for advection towards the Snowy Mountains.

8.4 Summary

Despite the uncertainty surrounding long term changes in rainfall patterns in a warming climate (Whetton et al 2012), this thesis has provided evidence that the character of precipitation affecting the economically important Snowy Mountains region has changed over the last century. A more energetic atmosphere and hydrological cycle, expected as a result of anthropogenic warming is seemingly eventuating, with associated increases in precipitation intensity of inflow generating precipitation in the Snowy Mountains. With this knowledge comes the need to develop adaptive regional water management strategies with regards to changing precipitation regimes. It is envisaged that the increased understanding of precipitation variability developed in this thesis may inform water resource issues, informing adaptation and mitigation measures in agriculture, water management, energy, as well as socio-economic factors.

Appendix 1

This appendix firstly presents the results of determining the threshold for inflow-generating precipitation. This is followed by presentation of the WRF modelling of atmospheric humidity and MSLP are presented.

1. Determination of precipitation threshold

Following the application of the Lyne and Hollick filter to inflow gauge data as described in Chapter 4, quickflow was plotted against precipitation from the most relevant precipitation gauge. Fig. A1 shows the relationship between precipitation on day 0 and inflow on day +1, for the two inflow gauges at Yarrangobilly and Snowy River. In each case, inflow begins to rise (consistently) once the precipitation reaches ~10 mm (green arrow). Following advice from water managers in the region.

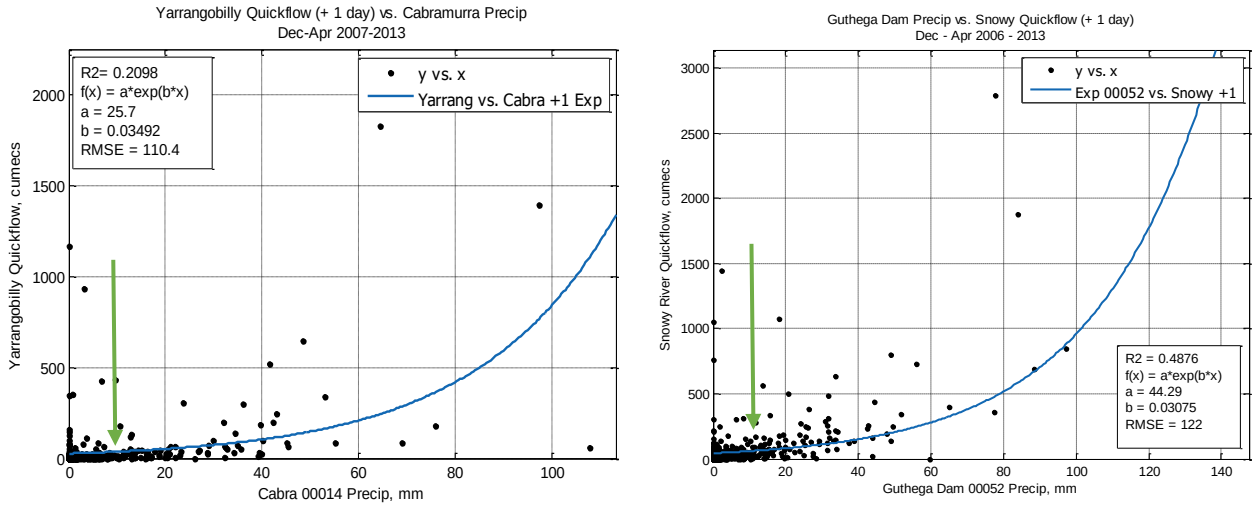

Fig. A1 Inflow (y-axis; cumecs) vs precipitation (x-axis, mm) for inflow gauges at (a) Yarrangobilly, and (b) Snowy River, fitted with exponential regression lines. In each case, the green arrow indicates the 10 mm threshold, above which inflow begins to rise consistently above zero.

2. Results of WRF modelling for MSLP and specific humidity over SEA

This section presents the results of WRF modelling for MSLP and specific humidity (water vapour mixing ratio) over SEA. Comparison against BoM analysis charts for MSLP, is also presented (no analysis chart archive is available from BoM for atmospheric moisture content). As discussed in Chapter 4, there is good overall agreement for MSLP between BoM analyses and the WRF modelling. The delineation between humid and dry airmasses in the WRF output is also particularly apparent. Animated movies of atmospheric moisture transport for each synoptic type are presented in the supplementary material.

Table A1. Comparison of MSLP between WRF modelling results for SEA domain (column 2) and BoM surface analysis charts (column 1; SEA domain highlighted by blue box) for one example of each synoptic type. MSLP (hPa; line contours) are shown for BoM charts (black contours) and WRF charts (white contours). Water vapour mixing ration at 30m above ground level (kg/kg; coloured contours) as a measure of atmospheric moisture content is shown for WRF output only.

BoM Surface Analysis Chart	**WRF Modelling, SEA 6km domain**
T1 Embedded cold fronts 1st July 2008 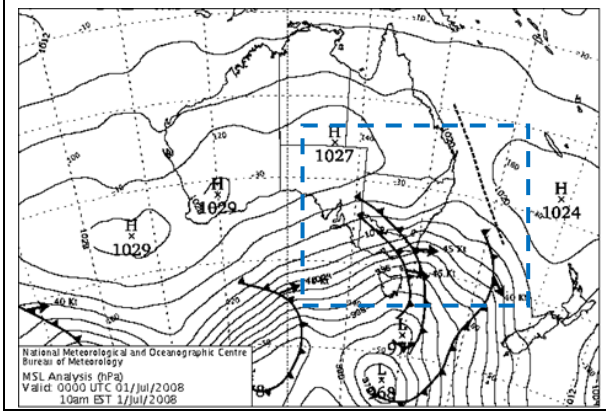	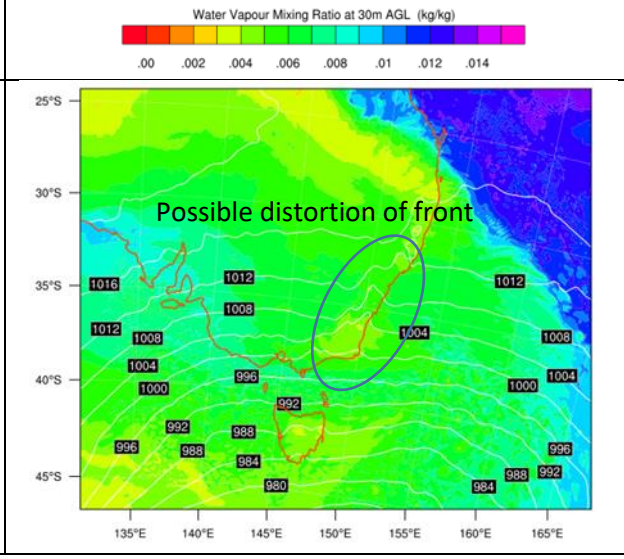

T2 Closed lows

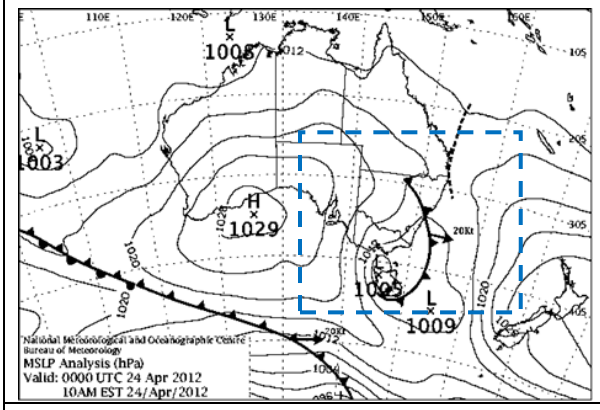

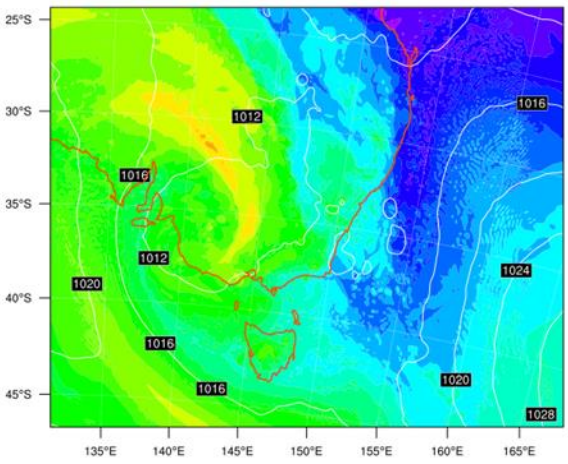

T3 Inland heat troughs

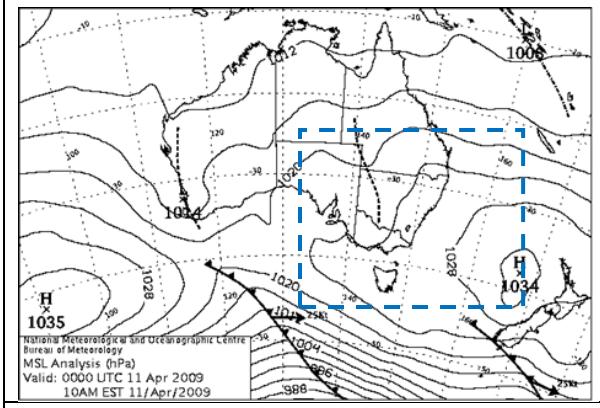

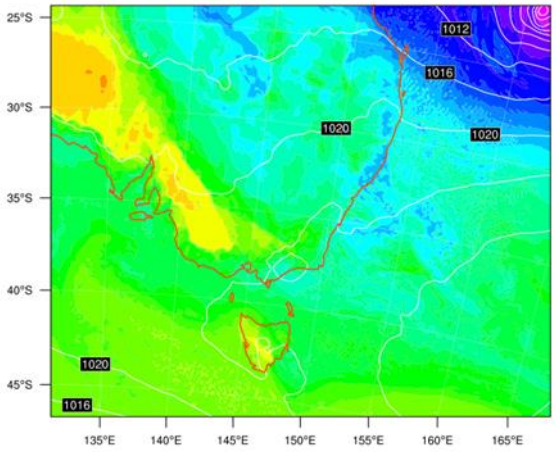

T4 narrow, interacting, inland heat troughs

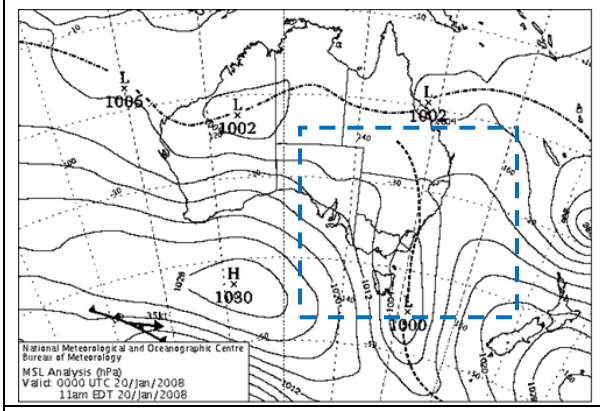

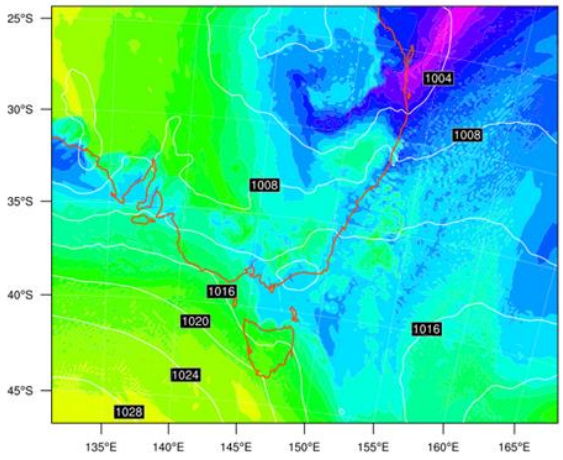

T5 Pre-frontal troughs

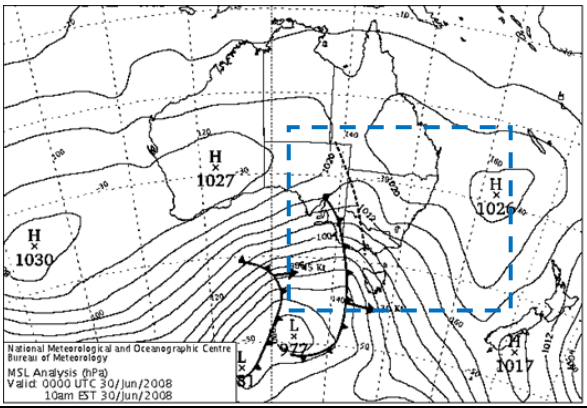

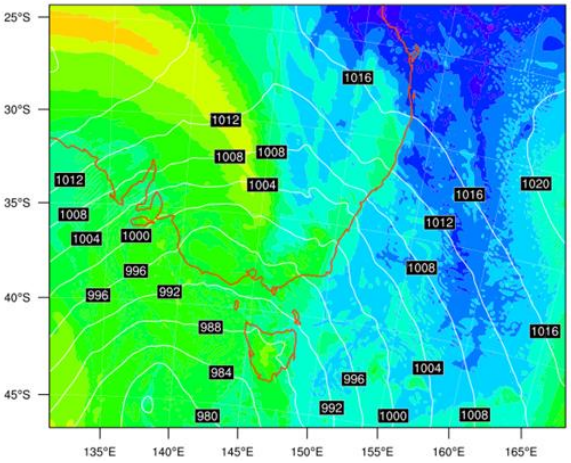

T6 Upstream closed lows

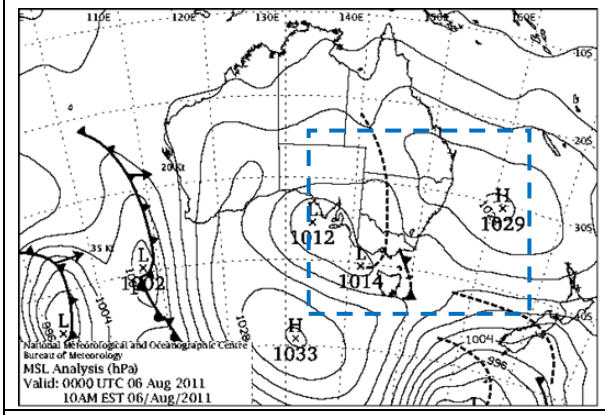

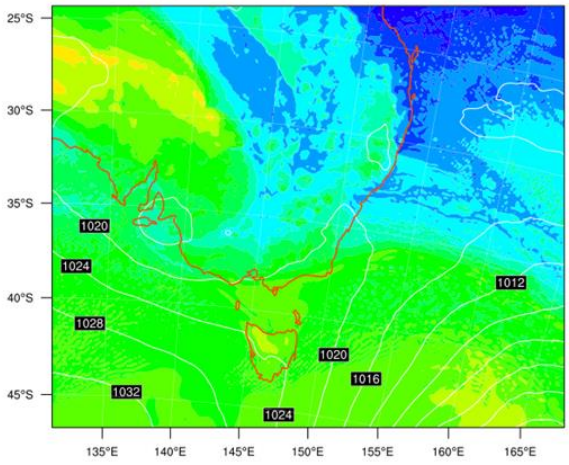

T7 Broad, interacting inland heat troughs

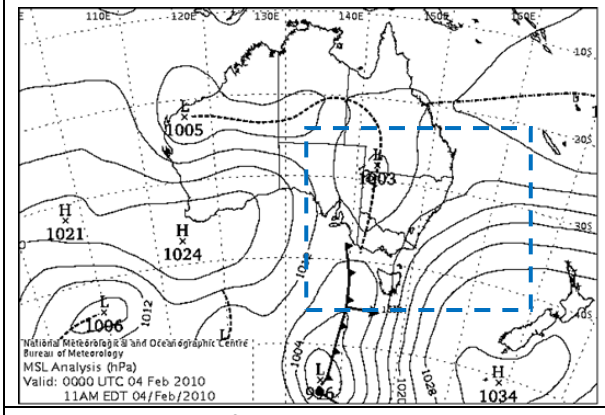

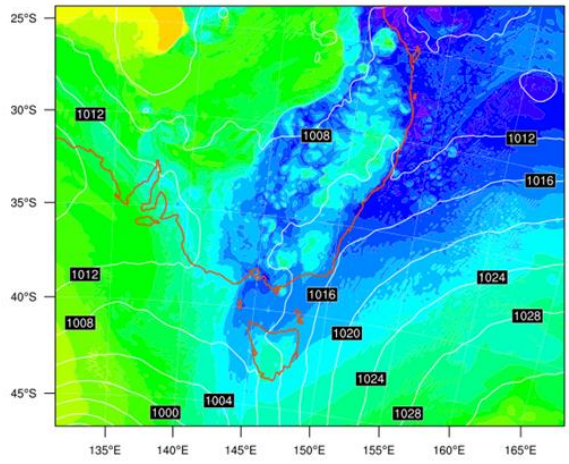

T8 Upstream pre-frontal troughs; NWCBs

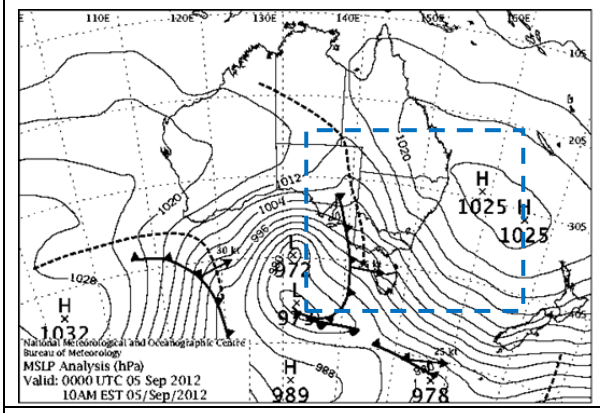

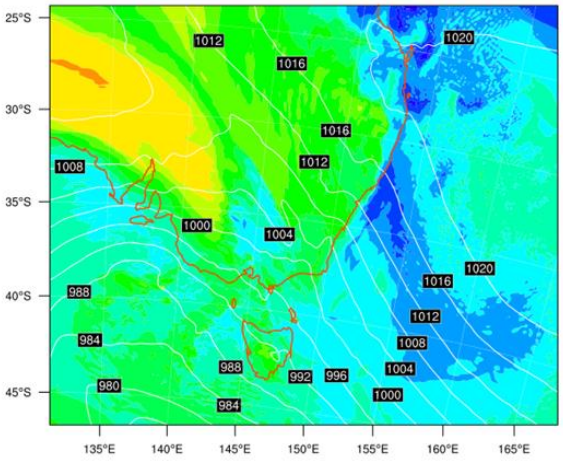

T9 Offshore lows

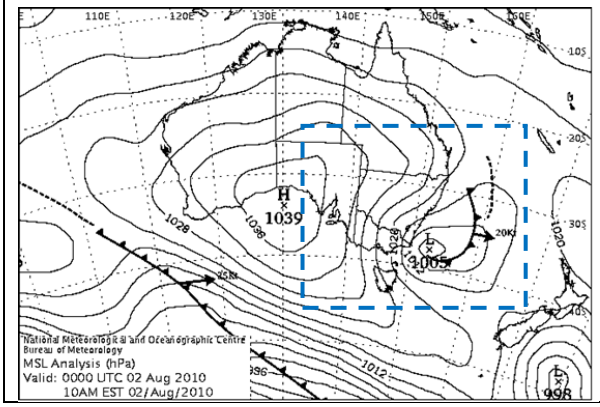

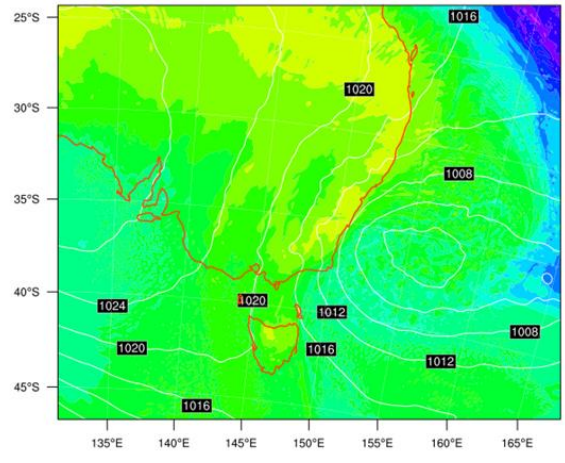

T10 Easterly dips

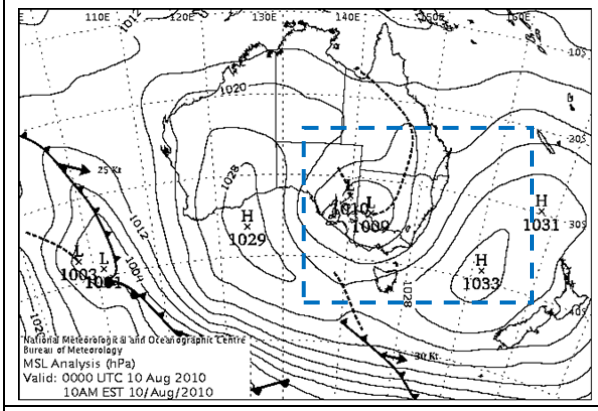

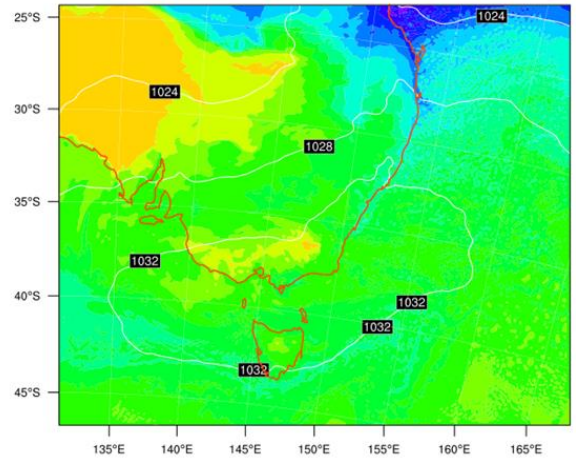

T11 Non-interacting inland heat troughs

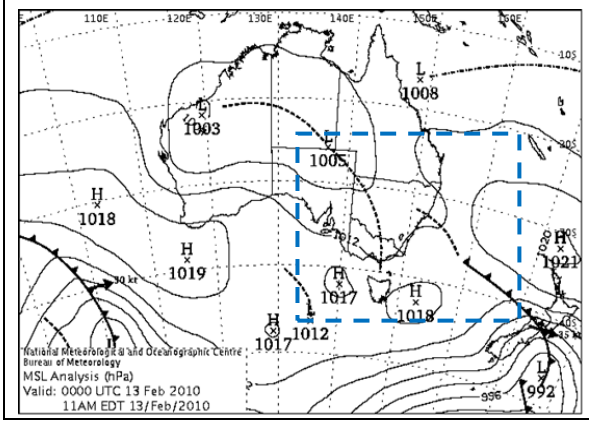

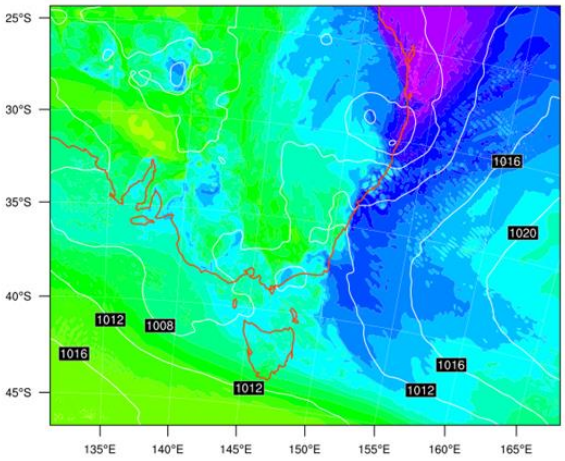

References

Alexander, L. V., and J. M. Arblaster, 2009: Assessing trends in observed and modelled climate extremes over Australia in relation to future projections. *International Journal of Climatology*, **29 (3)**, 417-435.

Alexander, L. V., P. Uotila, N. Nicholls, and A. Lynch, 2010: A New Daily Pressure Dataset for Australia and Its Application to the Assessment of Changes in Synoptic Patterns during the Last Century. *Journal of Climate,* **23**, 1111-1126.

Almazroui, M., M. Nazrul Islam, P. D. Jones, H. Athar, and M. Ashfaqur Rahman, 2012: Recent climate change in the Arabian Peninsula: Seasonal rainfall and temperature climatology of Saudi Arabia for 1979-2009. *Atmospheric Research,* **111**, 29-45.

Alory, G., S. Wijffels, and G. Meyers, 2007: Observed temperature trends in the Indain Ocean over 1960-1999 and associated mechanisms. *Geophysical Research Letters*, **34**.

Alpert, P. and Coauthors, 2002: The paradoxical increase of Mediterranean extreme daily rainfall in spite of decrease in total values. *Geophysical Research Letters,* **29 (10)**, 1536-1539.

Ashcroft, L., J. Gergis, and D. J. Karoly, 2016: long-term stationarity of El Nino-Southern Oscillation teleconnections in southeastern Australia. *Climate Dynamics*, **46**, 2991-3006.

Baines, P. G., and C. K. Folland, 2007: Evidence for a Rapid Global Climate Shift across the Late 1960s. *Journal of Climate,* **20**, 2721-2744.

Barry, R. G., 1992: *Mountain Weather and Climate.* Second ed. Routledge.

Barry, R. G., and A. M. Carleton, 2001: *Synoptic and Dynamic Climatology.* Routledge.

Basist, A. B., G.D., 1994: Statistical Relationships between Topography and Precipitation Patterns. *Journal of Climate,* **7**, 1305-1315.

Bates, B. C., P. Hope, B. Ryan, I. Smith, and S. Charles, 2008: Key findings from the Indian Ocean Climate Initiative and their impact on policy development in Australia. *Climatic Change*, **89**, 339-354.

Beesley, C. A., A. J. Frost, and J. Zajaczkowski, 2009: A comparison of the BAWAP and SILO spatially interpolated daily rainfall datasets. *18th World IMACS/MODSIM Congress, Cairns, Australia,* 3886-3892.

Beniston, M., 2003: Climatic change in mountain regions: A review of possible impacts. *Climatic Change*, **59**, 5-31.

Bettolli, M. L., O. C. Penalba, and W. M. Vargas, 2010: Synoptic weather types in the south of South America and their relationship to daily rainfall in the core crop-producing region in Argentina. *Australian Meteorological and Oceanographic Journal,* **60**, 37-48.

Bonsal, B. and Shabbar, A., 2013: Impacts of Large-scale Circulation Variability on Low Streamflows over Canada: A Review. *Canadian Water Resources Journal*, **33 (2)**, 137-154.

Brigode, P., Z. Micovic, P. Bernardara, E. Paquet, F. Garavaglia, J. Gailhard, and P. Ribstein, 2013: Linking ENSO and heavy rainfall events over coastal British Columbia through a weather pattern classification. *Hydrology and Earth System Sciences*, **17**, 1455-1473.

Browning, S. A. and I. D. Goodwin, 2013: Large-Scale Influences on the Evolution of Winter Subtropical Maritime Cyclones Affecting Australia's East Coast. *Monthly Weather Review*, **141**, 2416-2431.

Budin, G. R. 1985: Interannual variability of Australian snowfall. *Australian Meteorological Magazine*, **33,** 145-159.

Bureau of Meteorology, 2012: Exceptional heavy rainfall across southeast Australia. Special Climate Statement. 39, 1 pp.

Bureau of meteorology 2008b: http://www.bom.gov.au/climate/about/?bookmark=sam

Bureau of Meteorology 2013 http://www.bom.gov.au/climate/IOD/negative/

Cai, W. and Coauthors, 2014a: Increasing frequency of extreme El Nino events due to greenhouse warming. *Nature Climate Change*, **4**, 111-116.

Cai, W., A. Santoso, G. Wang, E. Weller, L. Wu, K. Ashok, Y. Masumoto, and T. Yamagata, 2014b: Increased frequency of extreme Indian Ocean Dipole events due to greenhouse warming. *Nature*, **510**, 254-260.

Cai, W., and T. Cowan, 2008: Evidence of impacts from rising temperature on inflows to the Murray-Darling Basin. *Geophysical Research Letters*, **35**.

Cai, W., and T. Cowan, 2013: Southeast Australia Autumn Rainfall reduction: A Climate-Change-Induced Poleward Shift of Ocean-Atmosphere Circulation. *Journal of Climate*, **26**, 189-205.

Cai, W., G. Shi, T. Cowan, D. Bi, and J. Ribbe, 2005: The response of the Southern Annular Mode, the East Australian Current, and the southern mid-latitude ocean circulation to global warming. *Geophysical Research Letters*, **32**.

Cai et al 2009: Recent unprecedented skewness towards positive Indian Ocean Dipole occurrences and its impact on Australian rainfall. *Geophysical Research Letters*, **36**.

Cai, W., P. van Rensch, T. Cowan, and A. Sullivan, 2010: Asymmetry in ENSO Teleconnection with Regional Rainfall, Its Multidecadal Variability, and Impact. *Journal of Climate*, **23**, 4944-4955.

Cai, W., X. Zheng, E. Weller, M. Collins, T. Cowan, M. Lengaigne, W. Yu, and T. Yamagata, 2013: Projected response of the Indian Ocean Dipole to greenhouse warming. *Nature Geoscience*, **6**, 999-1007.

Callow, N., H. McGowan, L. Warren, and J. Speirs, 2014: Drivers of precipitation stable isotope variability in an alpine setting, Snowy Mountains, Australia. *Journal of Geophysical Research: Atmospheres*, **119**, 3016-3031.

Caloiero, T., 2015: Analysis of rainfall trend in New Zealand. *Environmental Earth Sciences*, **73**, 6297-6310.

Cassano, E. N., and J. J. Cassano, 2010: Synoptic forcing of precipitation in the Mackenzie and Yukon River basins. *International Journal Climatology*, **30**, 658-674.

Catto, J. L., N. Nicholls, C. Jakob, and K. L. Shelton, 2014: Atmospheric fronts in Current and Future Climates. Geophysical Research Letters, **41(21)**, 7642-7650.

Champion, A. J., K. I. Hodges, L. O. Bengtsson, N. S. Keenlyside, and M. Esch, 2011: Impact of increasing resolution and a warmer climate on extreme weather from northern Hemisphere extratropical cyclones. *Tellus Series A: Dynamic Meteorology and Oceanography*, **63A**, 893-906.

Chappell, A., and C. T. Agnew, 2001: Geostatistical Analysis and Numerical Simulation of West African Sahel Rainfall. Land Degradation: Papers selected from Contributions to the Sixth Meeting of the International Geographical Union's Commission on Land Degradation and Desertification, Perth, Western Australia, 20-28 September 1999, A. J. Conacher ed., Kluwer Academic Publishers, Netherlands, 19-35.

Chiew, F. H. S., W. J. Young, and W. Cai, 2011: Current drought and future hydroclimate projections in southeast Australia and implications for water resources management. *Stochastic Environmental Research Risk Assessment*, **25**, 601-612.

Christensen, J. H. and Coauthors, 2013: Climate Phenomena and their Relevance for Future Regional Climate Change. Climate Change 2013: The Physical Science Basis. Contribution of Working Group I to the Fifth Assessment Report of the Intergovernmental Panel on Climate Change, T. F. Stocker, D. Qin, G.-K. Plattner, M. Tignor, S.K. Allen, J. Boschung, A. Nauels, Y. Xia, V. Bex and P.M. Midgley eds., Cambridge University Press, Cambridge, United Kingdom and New York, NY, USA., 1217-1308.

Christensen, J.H., B. Hewitson, A. Busuioc, A. Chen, X. Gao, I. Held, R. Jones, R.K. Kolli, W.-T. Kwon, R. Laprise, V. Magaña Rueda, L. Mearns, C.G. Menéndez, J. Räisänen, A. Rinke, A. Sarr and P. Whetton, 2007: Regional Climate Projections. In: Climate Change 2007: The Physical Science Basis. Contribution of Working Group I to the Fourth Assessment Report of the Intergovernmental Panel on Climate Change [Solomon, S., D. Qin, M. Manning, Z. Chen, M. Marquis, K.B. Averyt, M. Tignor and H.L. Miller (eds.)]. Climate Change 2007: Working Group I: The Physical Science Basis.

Chubb, T. H., S. T. Siems, and M. J. Manton, 2011: On the Decline of Wintertime Precipitation in the Snowy Mountains of Southeastern Australia. *Journal of Hydrometeorology*, **12**, 1483-1497.

Chubb, T., M. J. Manton, S. T. Siems, A. D. Peace and S. P. Bilish, 2015: Estimation of Wind-Induced Losses from a Precipitation Gauge Network in the Australian Snowy Mountains. *Journal of Hydrometeorology*, **16**, 2619-2638.

Cinco, T., R. G. de Guzman, F. D. Hilario, and D. M. Wilson, 2014: Long-term trends and extremes in observed daily precipitation and near surface air temperature in the Phillipines for the period 1951 - 2010. Atmospheric Research, **145-146**, 12-26.

Coleman, J. S. M. and J. C. Rogers, 2007: A Synoptic Climatology of the Central United States and Associations with Pacific Teleconnection Pattern Frequency. *Journal of Climate*, **20**, 3485-3497

Colquhoun, J. R., 1978: Snowfall on the New South Wales Snowy Mountains. Technical Report 25, Department of Science and the Environment, Bureau of Meteorology, Sydney, Australia.

Costin, A., M. Gray, C. Totterdell, and D. Wimbush, 2000: Kosciuszko alpine flora, CSIRO Publishing, Victoria, Australia pp 3-33.

Cravatte, S., T. Delcroix, D. Zhang, M. McPhaden, and J. Leloup, 2009: Observed freshening and warming of the western Pacific Warm Pool. Climate Dynamics, **33**, 565-589.

CSIRO, 2012: Climate and water availability in south-eastern Australia: A synthesis of findings from Phase 2 of the South eastern Australian Climate Initiative (SEACI), CSIRO, Australia, September 2012, 41 pp.

Dai, J., M. Manton, S. Siems, and E. Ebert, 2013: Estimation of Daily Winter Precipitation in the Snowy Mountains of South Eastern Australia. *Journal of Hydrometeorology*, **15**, 909-920.

Davis, C. J., 2013: Towards the development of long-term winter records for the Snowy Mountains. *Australian Meteorological and Oceanographic Journal*, **63**, 303-313.

Davis, R. E., and L. S. Kalkstein, 1990: Development of an Automated Spatial Synoptic Climatological Classification. *International Journal of Climatology*, **10**, 769-794.

De'Ath, G, 2007: Boosted trees for ecological modelling and prediction. *Ecology*, **88(1)**, 243-251.

Dee, D. P. and Coauthors, 2011: The ERA-Interim reanalysis: Configuration and performance of the data assimilation system. *Quarterly Journal of the Royal Meteorology Society*, **137**, 553-597.

Delworth, T. L., and F. Zeng, 2014: Regional rainfall decline in Australia attributed to anthropogenic greenhouse gases and ozone levels. *Nature Geoscience Letters*, **7**, 583-587.

Demiroglu, O. C., M. T. Turp, T. Ozturk, and M. L. Kurnaz, 2016: Impact of Climate Change on Natural Snow Reliability, Snowmaking capacities, and Wind Conditions of Ski Resorts in Northeast Turkey: A Dynamical Downscaling Approach. *Atmosphere*, **7(52)**, 12pp.

Ding, Q., E. Steig, D. S. Battisti, and J. M. Wallace, 2012: Influence of the Tropics on the Southern Annular Mode. *Journal of Climate*, **25**, 6330-6348.

Drosdowsky, W., 2005: The Latitude of The Subtropical Ridge over Eastern Australia: The L Index Revisited. *International Journal of Climatology*, **25**, 1291-1299.

Eder, B. K., J. M. Davis, and P. Bloomfield, 1994: An Automated Classification Scheme Designed to Better Elucidate the Dependence of Ozone on Meteorology. *Journal of Applied Meteorology*, **33**, 1182-1199.

Eichler, T. P., and J. Gottschalck, 2013: A Comparison of Southern Hemisphere Cyclone Track Climatology and Interannual Variability in Coarse-Gridded Reanalysis Datasets. *Advances in Meteorology*, **2013**, 1-16.

Elith, J., J. R. Leathwick, and T. Hastie, 2008: A working guide to boosted regression trees. *Journal of Animal Ecology*, **77**, 802-813.

England, M. H., and F. Huang, 2005: On the Interannual Variability of the Indonesian Throughflow and Its Linkage with ENSO. *Journal of Climate*, **18**, 1435-1444.

ESCCI 2015, NSW Government Environment and Heritage, Eastern Seaboard Climate Change Intiative. http://www.climatechange.environment.nsw.gov.au/Impacts-of-climate-change/East-Coast-Lows/Eastern-Seaboard-Climate-Change-Initiative, 2015

Evans, J., M. Ekstrom and F. Ji, 2012: Evaluating the performance of a WRF physics ensemble over South-East Australia. *Climate Dynamics*, **39**, 1242-58.

Feiccabrino, J., D. Gustafsson, and A. Lundberg, 2013: Surface-based precipitation phase determination methods in hydrological models. *Hydrology Research*, **44.1**, 44-57.

Fiddes, S., A. B. Pezza, and V. Barras, 2014: Synoptic climatology of extreme precipitation in alpine Australia. *International Journal of Climatology*, **35**, 172-188.

Fiddes, S. L. and A. B. Pezza, 2015: Current and future climate variability associated with wintertime precipitation in alpine Australia. *Climate Dynamics*, **44,** 2571-2587.

Fischer, A. M., D. E. Keller, M. A. Liniger, J. Rajczak, C. Schar, and C. Appenzeller, 2014: Projected changes in precipitation intensity and frequency in Switzerland: a multi-model perspective. *International Journal of Climatology,* **35 (11)**, 3204-3219.

Folland, C. 2008: Interdecadal Pacific Oscillation time series. ftp://wxmaps.org/pub/kinter/c20c/IPO.doc

Frei, C., and C. Schär, 1998: A precipitation climatology of the Alps from high-resolution rain-gauge observations. *International Journal of Climatology*, **18(8)**, 873-900.

Gallant, A. J. E., A. S. Kiem, D. C. Verdon-Kidd, R. C. Stone, and D. J. Karoly, 2012: Understanding hydroclimate processes in the Murray-Darling Basin for natural resources management. *Hydrology and Earth System Sciences,* **16**, 2049-2068.

Gallant, A. J. E., K. J. Hennessy, and J. Risbey, 2007: Trends in rainfall indices for six Australian regions: 1910-2005. *Australian Meteorological Magazine,* **56**, 223-239.

Gao, X., P. Schlosser, E. Monier, and D. Entekhabi, 2014: An Analogue Approach to Identify Heavy Precipitation Events: Evaluation and Application to CMIP5 Climate Models in the United States. *Journal of Climate,* **27**, 5941-5963.

Garreaud, R. D., and D. S. Battisti, 1999: Interannual (ENSO) and Interdecadal (ENSO-like) Variability in the Southern Hemisphere Tropospheric Circulation. *Journal of Climate*, **12**, 2113-2123.

Ghassemi, F., and I. White, 2007: *Inter-Basin Water Transfer: Case Studies from Australia, United States, Canada, China and India.* First ed. Cambridge University Press.

Gibson, P. B., S. E. Perkins-Kirkpatrick, and J. A. Renwick, 2016: Projected changes in synoptic weather patterns over New Zealand examined through self-organising maps. *International Journal of Climatology*, published online DOI: 10.1002/joc.4604

Gillies, R. R., S. Wang, and M. R. Booth, 2012: Observational and Synoptic Analyses of the Winter Precipitation Regime Change over Utah. *Journal of Climate*, **25**, 4679-4698.

Godfrey, J. S., 1996: The effect of the Indonesian throughflow on ocean circulation and heat exchange with the atmosphere: A review. *Journal of Geophysical Research*, **101(C5)**, 12217-12237.

Gong, D. and S. Wang, 1999: Definition of Antarctic oscillation index. *Geophysical Research Letters*, **26 (4)**, 459-462.

Gornall, J., R. Betts, E. Burke, R. Clark, J. Camp, K. Willett, and A. Wiltshire, 2010: Implications of climate change for agricultural productivity in the early twenty-first century. *Philosophical Transactions of the Royal Society B*, **365**, 2973-2989.

Graham, N. E., 1995: Simulation of Recent Global Temperature Trends. *Science,* **267,** 666-671.

Green, K., and C. M. Pickering, 2009: the Decline of Snowpatches in the Snowy Mountains of Australia: Importance of Climate Warming, Variable Snow, and Wind. *Arctic, Antarctic, and Alpine Research*, **41 (2)**, 212-218

Grieger, J., G. C. Leckebusch, M. G. Donat, M. Schuster, and U. Ulbrich, 2014: Southern Hemisphere winter cyclone activity under recent and future climate conditions in multi-model AOGCM simulations. *International Journal of Climatology*, **34**, 3400-3416.

Grinsted, A., J. C. Moore, and S. Jevrejeva, 2004: Application of the cross wavelet transform and wavelet coherence to geophysical time series. *Nonlinear Processes in Geophysics,* **11**, 561-566.

Gyakum, J. R., 2008: The Application of Fred Sanders' Teaching to Current Research on Extreme Cold-Season Precipitation Events in the Saint Lawrence River Valley Region. *Synoptic-Dynamic Meteorology and Weather Analysis and Forecasting Meteorological Monographs*, **33 (55)**, American Meteorological Society, 241 pp.

Harrison, D. E., and A. M. Chiodi, 2010: Trends in ENSO diagnosed with the Darwin sea level pressure record. *American Geophysical Union, Fall Meeting 2010, abstract #GC23F-0972*, San Francisco, AGU,

Hart, M., R. de Dear, and R. Hyde, 2006: A synoptic climatology of tropospheric ozone episodes in Sydney, Australia. *International Journal of Climatology,* **26**, 1635-1649.

Hendon, H., E-P. Lim, H. Nguyen, 2014: Seasonal Variations of Subtropical Precipitation Associated with the Southern Annular Mode. *Journal of Climate*, **27**, 3446-3460.

Hendrikx, J., C. Zammit, E. Ö. Hreinsson , and S. Becken, 2013: A comparative assessment of the potential impact of climate change on the ski industry in New Zealand and Australia. *Climatic Change*, **119**, 965-978.

Hennessy, K. J., P. H. Whetton, K. Walsh, I. N. Smith, J. M. Bathols, M. Hutchinson, and J. Sharples, 2008: Climate change effects on snow conditions in mainland Australia and adaptation at ski resorts through snowmaking. *Climate Research,* **35**, 255-270.

Hennessy, K. J., P. H. Whetton, J. Bathols, M. Hutchinson, and J. Sharples, 2003: The impact of climate change on snow conditions in Australia. Consultancy report for the Victorian Dept. of Sustainability and Environment, NSW National Parks and Wildlife Service, Australian Greenhouse Office and the Australian Ski Areas Association.

Hennessy, K. J., R. Suppiah, and C. M. Page, 1999: Australian rainfall changes, 1910-1995. *Australian Meteorological Magazine*, **48**, 1-13.

Hennessy, K., P. Whetton, I. Smith, J. Bathols, M. Hutchinson, and J. Sharples, 2003: The impact of climate change on snow conditions in mainland Australia. CSIRO Atmospheric Research, Aspendale, Victoria, Australia.

Hess, N. P., and H. Brezowsky, 1969: Katalog der Grosswetterlagen Europas. *Berichte des Deutschen Wetterdienstes,* **113,** Offenbach.

Hewitson, B. C., and R. G. Crane, 2002: Self-organising maps: applications to synoptic climatology. *Climate Research*, **22,** 13-26.

Ho, M., A. S. Kiem, and D. C. Verdon-Kidd, 2012: The Southern Annular Mode: A comparison of indices. *Hydrology and Earth System Sciences*, **16**, 967-982.

Hope, P., 2006: Projected future changes in synoptic systems influencing southwest Western Australia. *Climate Dynamics*, **26,** 765-780.

Hoskins, B. J., and K. I. Hodges, 2005: A New Perspective on Southern Hemisphere Storm Tracks. *Journal of Climate*, **18**, 4108-4129.

Hoy, A., A. Schucknecht, M. Sepp, and J. Matschullat, 2014: Large-scale synoptic types and their impact on European precipitation. *Theoretical and Applied Climatology,* **116**, 19-35.

MDBA 2016 http://www.mdba.gov.au/discover-basin/people/economy-basin.

IPCC 1995: The Science of Climate Change: Contribution of Working Group I to the Second Assessment Report of the Intergovernmental Panel on Climate Change. Eds. J. T. houghton, L. G. Meira Filho, B. A Callander, N. Harris, A. Kattenberg, and K. Maskell. Cambridge University Press.

IPCC 2014: Climate Change 2014 Synthesis report, Summary for Policymakers.

Izumo, T. J. Vialard, M. Lengaigne, C. de Boyer Montegut, S. K. Behara, J-J. Luo, S. Cravatte, S. Masson, and T. Yamagata, 2010: Influence of the state of the Indian Ocean Dipole on the following year's El Nino. *Nature Geoscience*, **3**, 168-172.

Izumo, T., M. Lengaigne, J. Vialard, J. Luo, T. Yamagata, and G. Madec, 2013: Influence of Indian Ocean Dipole and Pacific recharge on following year's El Nino: interdecadal robustness. *Climate Dynamics,* **42 (1)**, 291-310.

Jeffrey, S. J., J. O. Carter, K. B. Moodie, and A. R. Beswick, 2001: Using spatial interpolation to construct a comprehensive archive of Australian climate data. *Environmental Modelling and Software*, **16**, 309-330.

Jiang, N., 2011: A new objective procedure for classifying New Zealand synoptic weather types during 1958-2008. *International Journal of Climatology,* **31**, 863-879.

Jiang, N., K. Cheung, K. Luo, P. J. Beggs, and W. Zhou, 2012: On two different objective procedures for classifying synoptic weather types over east Australia. *International Journal of Climatology,* **32**, 1475-1494.

Jouffray, J., M. Nystrom, A. V. Norstrom, I. D. Williams, L. M. Wedding, J. N. Kittinger, and G. J. Williams, 2015: Identifying multiple coral reef regimes and their drivers across the Hawaiian archipelago. *Philosophical Transactions of the Royal Society B,* **370**, 20130268.

Kalkstein, L. S., G. Tan, and J. A. Skindlov, 1987: An Evaluation of Three Clustering Procedures for Use in Synoptic Climatological Classification. *Journal of Climate and Applied Meteorology,* **26**, 717-730.

Karoly, D. J., 1989: Southern Hemisphere Circulation Features Associated with El-Niño-Southern Oscillation Events. *Journal of Climate*, **2**, 1239-1252.

Keener, V. W., G. W. Feyereisen, U. Lall, J. W. Jones, D. D. Bosch, and R. Lowrance, 2010: El-Nino/Southern Oscillation (ENSO) influences on monthly NO3 load and concentration, stream flow and precipitation in the Little River Watershed, Tifton, Georgia (GA). *Journal of Hydrology,* **381**, 352-363.

Kidson, J. W., 1999: Principal Modes of Southern Hemisphere Low-Frequency Variability Obtained from NCEP-NCAR Reanalyses. *Journal of Climate*, **12**, 2808-2830.

Kidson, J. W., 2000: An analysis of New Zealand synoptic types and their use in defining weather regimes. *International Journal of Climatology,* **20**, 299-316.

Kiem, A. S., and D. C. Verdon-Kidd, 2009a: Climatic drivers of Victorian streamflow: Is ENSO the dominant influence? *Australian Journal of Water Resources*, **13(1)**, 17-30.

Kiem and Verdon-Kidd 2009b: Towards understanding hydroclimatic change in Victoria, Australia – why was the last decade so dry? *Hydrology and Earth System Sciences*, **6**, 6181-6206.

Kiem, A. S., and D. C. Verdon-Kidd, 2011: Steps toward "useful" hydroclimatic scenarios for water resource management in the Murray-Darling Basin. *Water Resources Research,* **47**, 1-14.

Kiem, A. S., S. W. Franks, and G. Kuczera, 2003: Multi-decadal variability of flood risk. *Geophysical Research Letters*, **30 (2)**.

Kingston, D. G., C. S. Webster, and P. Sirguey, 2015: Atmospheric circulation drivers of lake inflow for the Waitaki River, New Zealand. *International Journal of Climatology*, online version.

Kirtman, B., S.B. Power, J.A. Adedoyin, G.J. Boer, R. Bojariu, I. Camilloni, F.J. Doblas-Reyes, A.M. Fiore, M. Kimoto, G.A. Meehl, M. Prather, A. Sarr, C. Schär, R. Sutton, G.J. van Oldenborgh, G. Vecchi and H.J. Wang, 2013: Near-term Climate Change: Projections and Predictability. In: Climate Change 2013: The Physical Science Basis. Contribution of Working Group I to the Fifth Assessment Report of the Intergovernmental Panel on Climate Change [Stocker, T.F., D. Qin, G.-K. Plattner, M. Tignor, S.K. Allen, J. Boschung, A. Nauels, Y. Xia, V. Bex and P.M. Midgley (eds.)]. Cambridge University Press, Cambridge, United Kingdom and New York, NY, USA.

Kirono, D. G. C., F. H. S. Chiew, and D. M. Kent, 2010: Identification of best predictors for forecasting seasonal rainfall and runoff in Australia. *Hydrological Processes*, **24**, 1237-1247.

Knight, D. B., R. E. Davis, S. C. Sheridan, D. M. Hondula, L. J. Sitka, M. Deaton, T. R. Lee, S. D. Gawtry, P. J. Stenger, F. Mazzei, B. P. Kenny, 2008: Increasing frequencies of warm and humid air masses over the conterminous United States from 1948 to 2005. *Geophysical Research Letters*, **35**.

Lamb, H. H., 1950: Types and spells of weather around the year in the British Isles: Annual trends, seasonal structure of the year, singularities. *Quarterly Journal of the Royal Meteorological Society*, **76 (330)**, 393-429.

Landvogt, P. K., J. A. T. Bye, and T. P. Lane, 2008: An investigation of recent orographic precipitation events in northeast Victoria. *Australian Meteorological Magazine*, **57**, 235-247.

Lim, E-P., H. H. Hendon, J. M. Arblaster, F. Delage, H. Nguyen, S-K. Min, and M. Wheeler, 2016: The impact of the Southern Annular Mode on future changes in Southern Hemisphere rainfall. *Geophysical Research Letters*, **43(13)**, 7160-7167.

Lobell, D.B., W. Schlenker, and J. Costa-Roberts, 2011: Climate Trends and Global Crop Production Since 1980. *Science*, **333**, 616-620.

Lorenzo, M. N., J. J. Taboada, and L. Gimeno, 2008: Links between circulation weather types and teleconnection patterns and their influence on precipitation patterns in Galicia (NW Spain). *International Journal of Climatology*, **28**, 1493-1505.

Maher, P., and S. C. Sherwood, 2014: Disentangling the Multiple Sources of Large-Scale Variability in Australian Wintertime Precipitation. *Journal of Climate*, **27**, 6377-6392.

Maheras, P., K. Tolika, C. Anagnostopoulou, M. Vafiadis, I. Patrikas and H. Flocas, 2004: On the relationships between circulation types and changes in rainfall variability in Greece. *International Journal of Climatology*, **24**, 1695-1712.

Mantua, N. J., and S. R. Hare, 2002: The Pacific Decadal Oscillation. *Journal of Oceanography*, **58**, 35-44.

Marshall, A. G., D. Hudson, M. C. Wheeler, H. H. Hendon and O. Alves, 2012: Simulation and prediction of the Southern Annular Mode and its influence on Australian intra-seasonal climate in POAMA. *Climate Dynamics*, **38 (11-12)**, 2483-2502.

Marshall, G. J., 2003: Trends in the Southern Annular Mode from Observations and Reanalyses. *Journal of Climate*, **16**, 4134-4143.

Martin, E. and Durand, Y. 1998, 'Precipitation and snow cover variability in the French Alps', in Beniston, M and Innes, J. L. (ed.), The impacts of climate variability on forests, Springer-Verlag, Heidelberg/New York, pp. 81-92.

McGowan, H. A., S. K. Marx, J. Denholm, J. Soderholm, and B. S. Kamber, 2009: Reconstructing annual inflows to the headwater catchments of the Murray River, Australia, using the Pacific Decadal Oscillation. *Geophysical Research Letters*, **36**.

McIntosh, P. C., M. J. Pook, J. S. Risbey, S. N. Lisson, and M. Rebbeck, 2007: Seasonal climate forecasts for agriculture: Towards better understanding and value. Field Crops Research, **104**, 130-138.

McKerchar, A. I., J. A. Renwick, and J. Schmidt, 2010: Diminishing streamflows on the east coast of the South Island New Zealand and linkage to climate variability and change. Journal of Hydrology (NZ), **49 (1)**, 1-14.

MDBA 2016 http://www.mdba.gov.au/discover-basin/people/economy-basin

MDBA, 2014: Running the River Murray. http://www.mdba.gov.au/river-information/running-river-murray 2014

Meehl, G. A., J. M. Arblaster, and C. Tebaldi, 2005: Understanding future patterns of increased precipitation intensity in climate model simulations. *Geophysical Research Letters,* **32**.

Meneghini, B., I. Simmonds, and I. N. Smith, 2007: Association between Australian rainfall and the Southern Annular Mode. *International Journal of Climatology,* **27**, 109-121.

Meyers, G., P. McIntosh, L. Pigot, and M. Pook, 2007: The Years of El Nino, La Nina, and Interactions with the Tropical Indian Ocean. *Journal of Climate,* **20**, 2872-2880.

Milrad, S. M., E. H. Atallah, J. G. Gyakum, and G. Dookhie, 2014: Synoptic Typing and Precursors of Heavy Warm-Season Precipitation Events at Montreal, Quebec. *Weather Forecasting.* **29**, 419-444.

Mo, K. C., 2000: Relationships between Low-Frequency Variability in the Southern Hemisphere and Sea Surface Temperature Anomalies. *Journal of Climate,* **13**, 3599-3610.

Moore, B. J., L. F. Bosart, D. Keyser, and M. L. Jurewicz, 2013: Synoptic-Scale Environments of Predecessor Rain Events Occurring East of the Rocky Mountains in Association with Atlantic Basin Tropical Cyclones. *Monthly Weather Review,* **141**, 1022-1047.

Moron, V., A. W. Robertson, M. N. Ward, and O. Ndiaye, 2008: Weather types and rainfall over Senegal. Part I: Observational analysis. *Journal of Climate,* **21**, 266-287.

Murphy, B. F., and B. Timbal, 2008: A review of recent climate variability and climate change in Southeastern Australia. *International Journal of Climatology,* **28**, 859-879.

Nathan, R. J., and T. A. McMahon, 1990: Evaluation of automated techniques for baseflow and recession analyses. *Water Resources Research,* **26**, 1465-1473.

Newman, M., M. Alexander, T. Ault, K. Cobb, C. Deser, E. Di Lorenzo, N. Mantua, A. Miller, S. Minobe, H. Nakamura, N. Schneider, D. Vimont, A. Phillips, J. Scott, and C. Smith, 2016: The Pacific Decadal Oscillation, Revisited. *Journal of Climate*. doi:10.1175/JCLI-D-15-0508.1, in press.

Newton, B. W., T. D. Prowse, and B. R. Bonsal, 2014a: Evaluating the distribution of water resources in western Canada using synoptic climatology and selected teleconnections. Part 1: winter season. *Hydrological Processes,* **28**, 4219-4234.

Newton, B. W., T. D. Prowse, and B. R. Bonsal, 2014b: Evaluating the distribution of water resources in western Canada using synoptic climatology and selected teleconnections. Part 2: summer season. *Hydrological Processes,* **28**, 4235-4249.

Nicholls, N., 2005: Climate variability, climate change and the Australian snow season. *Australian Meteorological Magazine,* **54**, 177-185.

Nicholls, N., 2010: Local and remote causes of the southern Australian autumn-winter rainfall decline, 1958-2007. *Climate Dynamics,* **34**, 835-845.
Nicholls, N., and B. Lavery, 1992: Australian rainfall trends during the twentieth century. *International Journal of Climatology,* **12**, 153-163.

O'Donnell, A. J., E. R. Cook, J. G. Palmer, C. S. M. Turney, G. F. M. Page, and P. F. Grierson, 2015: Tree Rings Show Recent High Summer-Autumn Precipitation in Northwest Australia Is Unprecedented within the Last Two Centuries. *PLoS ONE,* **10 (6)**.

Oliver, E. C. J., T. J. O'Kane, and N. J. Holbrook, 2015: Projected changes to Tasman Sea eddies in a future climate. *Journal of Geophysical Research: Oceans,* **online version**.

Pepler, A. S., B. Trewin, and C. Ganter, 2015: The influences of climate drivers on the Australian snow season. *Australian Meteorological and Oceanographic Journal*, **65 (2)**, 195-205.

Pepler, A.S., A. Di Luca, F. Ji, L. V. Alexander, J. P. Evans, and S. C. Sherwood, 2016: Projected changes in east Australian midlatitude cyclones during the 21st century. *Geophysical Research Letters,* **43**, 334-340.

Pezza, A. B., I. Simmonds, and J. A. Renwick, 2007: Southern Hemisphere cyclones and anticyclones: Recent trends and links with decadal variability in the Pacific Ocean. *International Journal of Climatology*, **27**, 1403-1419.

Pezza, A. B., T. Durrant, and I. Simmonds, 2008: Southern Hemisphere Synoptic Behaviour in Extreme Phases of SAM, ENSO, Sea Ice Extent, and Southern Australian Rainfall. *Journal of Climate*, **21**, 5566-5584.

Plavcova, E., J. Kysely, and P. Stepanek, 2014: Links between circulation types and precipitation in Central Europe in the observed data and regional climate model simulations. *International Journal of Climatology,* **34**, 2885-2898.

Poli, P. H. Hersbach, D. Tan, D. Dee, J. N. Thepaut, A. Simmons, C. Peubey, P. Laloyaux, T. Komori, P. Berrisford, and R. Dragani, 2013: The data assimilation system and initial performance evaluation of the ECMWF pilot reanalysis of the 20th-century assimilating surface observations only (ERA-20C), ECMWF ERA Rep. 14, 59 pp.

Pook, M. J., J. S. Risbey, and P. C. Mcintosh, 2012: The synoptic climatology of cool-season rainfall in the Central Wheatbelt of Western Australia. *Monthly Weather Review*, **140**, 28-43.

Pook, M. J., J. S. Risbey, and P. C. McIntosh, 2014: A comparative synoptic climatology of cool-season rainfall in major grain-growing regions of southern Australia. *Theoretical and Applied Climatology*, **117**, 521-533.

Pook, M. J., P. C. McIntosh, and G. A. Meyers, 2006: The synoptic decomposition of cool-season rainfall in the southeastern Australian cropping region. *Journal of Applied Meteorology and Climatology*, **45**, 1156-1170.

Pook, M., J. Risbey, and P. McIntosh, 2010: East coast lows, atmospheric blocking and rainfall: a Tasmanian perspective. *IOP Conf. Series: Earth and Environmental Science 012011,* **11**, 1-6.

Pook, M., S. Lisson, J. Risbey, C. C. Ummenhofer, P. McIntosh, and M. Rebbeck, 2009: The autumn break for cropping in southeast Australia: Trends, synoptic influences and impacts on wheat yield. *International Journal of Climatology,* **29**, 2012-2026.

Post, D. A., F. H. S. Chiew, J. Teng, B. Wang, and S. Marvanek, 2012: Projected changes in climate and runoff for south-eastern Australia under 1°C and 2°C global warming, *CSIRO, Australia*. A SEACI Phase 2 special report.

Power, S., T. Casey, C. Folland, A. Colman, and V. Mehta, 1999: Inter-decadal modulation of the impact of ENSO on Australia. *Climate Dynamics*, **15,** 319-324

Praskievicz, S., and H. Chang, 2009: Winter precipitation intensity and ENSO/PDO variability in the Willamette Valley of Oregon. *International Journal of Climatology,* **29**, 2033-2039.

Rasmussen, R., C. Liu, K. Ikeda, D. Gochis, D. Yates, F. Chen, M. Tewari, M. Barlage, J. dudhia, W. Yu, and K. Miller, 2011: High-resolution coupled climate runoff simulations of seasonal snowfall over Colorado: A process study of current and warmer climate. *Journal of Climate*, **24**, 3015-3048.

Rasmussen, R., B. Baker, J. Kochendorfer, T. Meyers, S. Landolt, A. P. Fischer, J. Black, J. M Theriault, P. Kucera, D. Gochis, C. Smith, R. Nitu, M. Hall, K. Ikeda, and E. Gutmann, 2012: How well are we measuring snow? The NOAA/FAA/NCAR winter Precipitation Test Bed. *Bulletin of the American Meteorological Society*, **June 2012**, 811-829.

Reisinger, A., R.L. Kitching, F. Chiew, L. Hughes, P.C.D. Newton, S.S. Schuster, A. Tait, and P. Whetton, 2014: Australasia. *Climate Change 2014: Impacts, Adaptation, and Vulnerability. Part B: Regional Aspects.*

Renwick, J. A., 2011: Kidson's Synoptic Weather Types and Surface Climate Variability over New Zealand. *Weather and Climate*, **31**, 3-23.

Risbey, J. S., M. J. Pook, and P. C. McIntosh, 2013: Spatial trends in synoptic rainfall in southern Australia. *Geophysical Research Letters*, **40**, 3781-3785.

Risbey, J. S., M. J. Pook, P. C. Mcintosh, C. C. Ummenhofer, and G. Meyers, 2009a: Characteristics and variability of synoptic features associated with cool season rainfall in southeastern Australia. *International Journal of Climatology,* **29**, 1595-1613.

Risbey, J. S., M. J. Pook, P. C. McIntosh, M. C. Wheeler, and H. H. Hendon, 2009b: On the remote drivers of rainfall variability in Australia. *Monthly Weather Review,* **137**, 3233-3253.

Romero, R., G. Sumner, C. Ramis, and A. Genoves, 1999: A classification of the atmospheric circulation patterns producing significant daily rainfall in the Spanish Mediterranean area. *International Journal of Climatology*, **19**, 765-785.

Saji, N. H., and T. Yamagata, 2003: Possible impacts of Indian Ocean Dipole mode events on global climate. *Climate Research,* **25**, 151-169.

Saji, N. H., B. H. Goswami, P. N. Vinayachandran, and T. Yamagata, 1999: A dipole mode in the tropical Indian Ocean. *Nature,* **401**, 360-363.

Schepen, A., Q. J. Wang, and D. Robertson, 2012: Evidence for using lagged climate indices to forecast Australian seasonal rainfall. *Journal of Climate,* **25**, 1230-1246.

Schnur, R. and D. P. Lettenmaier, 1998: A case study of statistical downscaling in Australia using weather classification by recursive partitioning. *Journal of Hydrology*, **212-213**, 362-379.
Sheridan, S. 2003: North American weather-type frequency and teleconnection indices. *International Journal of Climatology*, **23,** 27-45.

Sheridan, S. and C. C. Lee, 2012: Synoptic climatology and the analysis of atmospheric teleconnections, *Progress in Physical Geography*, **36 (4)**, 548-557.

Shi, G., J. Ribbe, W. Cai, and T. Cowan, 2008: An interpretation of Australian rainfall projections. *Geophysical Research Letters,* **35**.

Simmonds, I. and P. Hope, 1997: Persistence characteristics of Australian rainfall anomalies. *International Journal of Climatology*, **17,** 597-613.

Snowy Hydro Limited, 2003: *Engineering Features of the Snowy Mountains Scheme.* Fourth ed. Snowy Hydro Ltd.

Snowy Hydro Limited, Snowy Mountains Scheme. **2014** http://www.snowyhydro.com.au/energy/hydro/snowy-mountains-scheme

Speer, M. S., P. Wiles, and A. Pepler, 2009: Low pressure systems off the New South Wales coast and associated hazardous weather: establishment of a database. *Australian Meteorological and Oceanographic Journal*, **58,** 29-39.

Speer, M. S., L. M. Leslie, and A. O. Fierro, 2011: Australian east coast rainfall decline related to large scale climate drivers. *Climate Dynamics*, **36**, 1419-1429.

Sprintall, J., and A. Revelard, 2014: The Indonesian Throughflow response to Indo-Pacific climate variability. *Journal of Geophysical Research: Oceans,* **119**, 1161-1175.

Stahl, K., R. D. Moore, and I. G. McKendry, 2006: The role of synoptic-scale circulation in the linkage between large-scale ocean-atmosphere indices and winter surface climate in British Columbia, Canada. *International Journal of Climatology,* **26**, 541-560.

Stocker, T. F. and Coauthors, 2013: IPCC, 2013: Climate Change 2013: The Physical Science Basis. Contribution of Working Group 1 to the Fifth Assessment Report of the Intergovernmental Panel on Climate Change.

Stone, R. C., 1989: weather types at Brisbane, Queensland: An example of the use of principal components and cluster analysis. *International Journal of Climatology*, **9**, 3-32.

Sturman, A. P., and N. J. Tapper, 2006: *The Weather and Climate of Australia and New Zealand.* Second Ed. Oxford University Press.

Suppiah, R. H., and K.J. Hennessey, 1998: Trends in total rainfall, heavy rain events and number of dry days in Australia. *International Journal of Climatology,* **10**, 1141-1164.

Tan, P., M. Steinbach, and V. Kumar, 2006: Chapter 8: Cluster Analysis: Basic Concepts and Algorithms. *Introduction to Data-Mining*, Pearson Addison-Wesley, 487-568.

Tapp, R. G., and S. L. Barrell, 1984: The north-west Australian cloud band: climatology, characteristics and factors associated with development. *Journal of Climatology,* **4**, 411-424.

The National Oceanography Centre, 2015: Cross wavelet and wavelet coherence. http://noc.ac.uk/using-science/crosswavelet-wavelet-coherence, 2015.

Therneau, T., E. Atkinson, 2013: An introduction to recursive partitioning using the RPART routines. http://www2.uaem.mx/r-mirror/web/packages/rpart/vignettes/longintro.pdf

Timbal, B., and R. Fawcett, 2013: A Historical Perspective on Southeastern Australian Rainfall since 1865 Using the Instrumental Record. *Journal of Climate,* **26**, 1112-1129.

Timbal, B., and W. Drosdowsky, 2013: The relationship between the decline of Southeastern Australian rainfall and the strengthening of the subtropical ridge. *International Journal of. Climatology,* **33**, 1021-1034.

Timbal, B. and H. H. Hendon, 2011: The role of tropical modes of variability in recent rainfall deficits across the Murray-Darling Basin. *Water Resources Research*, **47(9)**, 1-16.

Torrence, C., and G. P. Compo, 1998: A Practical Guide to Wavelet Analysis. *Bulletin of the American Meteorological Society,* **79(1)**, 61-78.

Tozer, C. R., A. S. Kiem, and D. C. Verdon-Kidd, 2012: On the uncertainties associated with using gridded rainfall data as a proxy for observed. *Hydrology and Earth System Sciences,* **16**, 1481-1499.

Trauth, M., 2007: *MATLAB Recipes for Earth Sciences.* Third ed. Springer-Verlag.

Trenberth, K. E., 1997: The Definition of El Niño. *Bulletin of the American Meteorological Society,* **78**, 2771-2777.

Trenberth, K. E., 1998: Atmospheric moisture residence times and cycling: Implications for rainfall rates and climate change. *Climatic Change*, **39**, 667-694.

Trenberth, K. E., and T. J. Hoar, 1996: The 1990-1995 El Nino-Southern Oscillation event: Longest on record. *Geophysical Research Letters,* **23 (1)**, 57-60.

Ummenhofer, C. C. and Coauthors, 2011: Indian and Pacific Ocean Influences on Southeast Australian Drought and Soil Moisture. *Journal of Climate,* **24**, 1313-1336.

Ummenhofer, C. C., A. S. Gupta, A. S. Taschetto, and M. H. England, 2009a: Modulation of Australian precipitation by meridional gradients in east Indian Ocean sea surface temperature. *Journal of Climate,* **22**, 5597-5610.

Ummenhofer, C. C., M. H. England, P. C. Mclntosh, G. A. Meyers, M. J. Pook, J. S. Risbey, A. S. Gupta, and A. S. Taschetto, 2009b: What causes southeast Australia's worst droughts? *Geophysical Research Letters,* **36**.

Vallebona, C., E. Pellegrino, P. Frumento, and E. Bonari, 2014: Temporal trends in extreme rainfall intensity and erosivity in the mediterranean region: a case study in southern Tuscany, Italy. *Climatic Change,* **128**, 139-151.

van Dijk, A. I. J. M., H. E. Beck, R. S. Crosbie, R. A. M. de Jeu, Y. Y. Liu, G. M. Podger, B. Timbal, and N. R. Viney, 2013: The Millennium Drought in southeast Australia (2001–2009): Natural and human causes and implications for water resources, ecosystems, economy, and society, *Water Resources Research*, **49**, 1040-1057.

van Sebille, E., J. Sprintall, F. U. Schwarzkopf, A. Sen Gupta, A. Santoso, M. H. England, A. Biastoch, and C. W. Boning, 2014: Pacific-to-Indian Ocean connectivity: Tasman leakage,

Indonesian Throughflow, and the role of ENSO. *Journal of Geophysical Research: Oceans,* **119**, 1365-1382.

Verdon-Kidd, D. C., A. S. Kiem, and R. Moran, 2013: Links between the Big Dry in Australia and hemispheric multi-decadal climate variability – implications for water resource management. *Hydrology and Earth System Sciences,* **10**, 13539-13593.

Verdon-Kidd, D. C., and A. S. Kiem, 2009a: On the relationship between large-scale climate modes and regional synoptic patterns that drive Victorian rainfall. *Hydrology and Earth System Sciences,* **13**, 467-479.

Verdon-Kidd, D. C., and A. S. Kiem, 2009b: Nature and causes of protracted droughts in southeast Australia: Comparison between the Federation, WWII, and Big Dry droughts. *Geophysical Research Letters,* **36**, 1-6.

Visbeck, M., 2009: A station-based southern annular mode index from 1884 to 2005. *Journal of Climate,* **22**, 940-950.

Viviroli, D., D. R. Archer, W. Buytaert, H. J. Fowler, G. B. Greenwood, A. F. Hamlet, Y. huang, G. Koboltschnig, M. I. Litaor, J. I. Lopez-Moreno, S. Lorentz, B. Schadler, H. Schreier, K. Schwaiger, M. Vuille, and R. Woods, 2011: Climate change and mountain water resources: Overview and recommendations for research, management and policy. *Hydrology and Earth System Sciences,* **15**, 471-504.

Wang, G., S. B. Power, and S. McGree, 2016: Unambiguous warming in the western tropical Pacific primarily caused by anthropogenic forcing. *International Journal of Climatology*, **36,** 933-944.

Wang, X. L. and Y. Feng, published online July 2013: RHtestsV4 User Manual. *Climate Research Division, Atmospheric Science and Technology Directorate, Science and Technology Branch, Environment Canada. 28 pp. [Available online at http://etccdi.pacificclimate.org/software.shtml]"*

Wang, X. L., 2008a: Accounting for Autocorrelation in Detecting Mean Shifts in Climate data Series Using the Penalized Maximal *t* or *F* Test. *Journal of Applied Meteorology and Climatology*, **47**, 2423-2444.

Wang, X. L., 2008b: Penalized maximal F-test for detecting undocumented mean-shifts without trend-change. *Journal of Atmospheric and Oceanic Technology*, **25 (No.3)**, 368-384.

Whan, K., B. Timbal, and J. Lindesay, 2014: Linear and nonlinear statistical analysis of the impact of sub-tropical ridge intensity and position on south-east Australian rainfall. *International Journal of Climatology,* **34**, 326-342.

Whetton, P. H., 1988: A synoptic climatological analysis of rainfall variability in south-eastern Australia. *Journal of Climatology*, **8**, 155-177.

Whetton, P., K. Hennessy, J. Clarke, K. Mcinness, and D. Kent, 2012: Use of *Representative Climate Futures* in impact and adaptation assessment. *Climatic Change*, **115,** 433-442.

Whitfield, P. H., R. D. Moore, S. W. Fleming, and A. Zawadzki, 2010: Pacific Decadal Oscillation and the Hydroclimatology of Western Canada - Review and Prospects. *Canadian Water Resources Journal,* **35(1)**.

Widmann, M., and C. Schar, 1997: A principal component and long-term trend analysis of daily precipitation in Switzerland. *International Journal of Climatology,* **17**, 1333-1356.
Wilks, D. S., 2006: *Statistical Methods in the Atmospheric Sciences.* Second ed. Academic Press, United States of America.

Wilson, L, Manton, MJ, Siems, ST, 2013: Relationship between rainfall and weather regimes in south-eastern Queensland, Australia. *International Journal of Climatology,* **33**, 979-991.

Wise, E. K., M. L. Wrzesien, M. P. dannenberg, and D. L. McGinnis, 2015: Cool-Season Precipitation Patterns Associated with Teleconnection Interactions in the United States. *Journal of Applied Meteorology and Climatology*, **54**, 494-505.

WMO, 2011: Guide to Climatological Practices Third Edition. WMO-No. 100.

Wright, W. J., 1989: A synoptic climatological classification of winter precipitation in Victoria. *Australian Meteorological Magazine,* **37**, 217-229.

Yarnal, B., 1993: Synoptic Climatology in Environmental Analysis: A Primer. First ed. Wiley.

Ye, H., D. J. Leathers, and L. S. Kalkstein, 1993: Classification of upper level circulation patterns in the polar region and their relationship to surface air temperature. *Middle States Geographer,* **26**, 1-6.

Yuter, S. E., D. E. Kingsmill, L. B. Nance, and M. Loffler-Mang, 2006: Observations of Precipitation Size and Fall Speed Characteristics within Coexisting Rain and Wet Snow. *Journal of Applied Meteorology and Climatology*, **45**, 1450-1464.

Zappa, G., L. C. Shaffrey, K. I. Hodges, P. G. Sansom, and D. B. Stephenson, 2013: A multimodel assessment of future projections of North Atlantic and European extratropical cyclones in the CMIP5 climate models. *Journal of Climate*, **26 (16)**, 5846-5862.